USING SEAFLOOR CHARACTERISTICS AS INDICATORS FOR PAST, MODERN AND FUTURE MARINE ENVIRONMENTS IN POTTER COVE, KING GEORGE ISLAND, ANTARCTICA

Dissertation zur Erlangung des Doktorgrades

an der Fakultät für Mathematik, Informatik und Naturwissenschaften

Fachbereich Geowissenschaften

der Universität Hamburg

vorgelegt von

Anne-Cathrin Wölfl

Hamburg

2015

Tag der Disputation: 22.05.2015

Folgende Gutachter empfehlen die Annahme der Dissertation:

Prof. Dr. Christian Betzler

Dr. H. Christian Hass

Declaration on oath

I hereby declare, on oath, that I have written the present dissertation by my own and have not used other than the acknowledged resources and aids.

Eidesstattliche Versicherung

Hiermit erkläre ich an Eides statt, dass ich die vorliegende Dissertationsschrift selbst verfasst und keine anderen als die angegebenen Quellen und Hilfsmittel benutzt habe.

_____ _____

Ort/Datum Unterschrift

SUMMARY

The Western Antarctic Peninsula belongs to the fastest warming regions worldwide. The consequences of this climatic trend include significant impacts on terrestrial and marine systems. Environmental reconstruction and continuous observation of these environments is the key to a deeper understanding of potential impacts and a sound basis for the prediction of future trends.

The objective of this PhD thesis is to delineate past, modern and future environments in Potter Cove, a small tributary embayment on King George Island, South Shetland Islands, Antarctica. It is aimed to assess past and modern impacts of climate change on this representative coastal system and to suggest future developments under the recent climatic trend. Seafloor characteristics have been investigated using hydroacoustics, underwater video recordings and sediment samples. Multivariate analyses were applied to faciliate and improve the data processing and the objective interpretation of the data sets. The majority of the data was acquired during two field campaigns within the international research programme IMCOAST during the austral summer season of 2010/2011 and 2011/2012.

The deglaciation history of King George Island is still debated and subject of numerous scientific studies. In this thesis, high-resolution swath bathymetry, shallow seismics and one sediment core allowed the delineation of submarine landforms and sub-bottom characteristics in Potter Cove that are instrumental to reconstruct glacial dynamics during the Late Holocene. Furthermore, ancient and modern environmental processes are described and interpreted. The results reveal the occurrence of moraine deposits and glacial lineations in the inner part of the cove. The seafloor is made up of glacial debris that has been deposited underneath or in direct vicinity of grounded ice. This deposit is covered by a thin layer of meltwater-derived sediments. The moraine ridges evidence the occurrence of glacial stillstands and potential readvances since 2.6 cal kyr BP. Landforms on the slope in the outer cove include channel structures, ice plough marks and pockmarks. The seafloor consists of gravity flow deposits that result from sediment disturbance by deep-keeled icebergs and from sediment overload. The latter was most likely caused by the accumulation of glacial debris on top of the slope, when the glacier was situated in direct proximity. Furthermore, submarine channel structures that were eroded by meltwater discharge or turbidity currents, transport until today large amounts of sediments onto the slope.

The modern habitat distribution in Potter Cove was assessed with an acoustic seabed discrimination system that was validated by underwater video images using a linear discriminant approach. Due to the absence of wave and current measurements

in the study area, bed shear stress estimates were calculated to delineate zones prone to sediment erosion. On the basis of the investigations, two habitat classes were identified in Potter Cove. The soft-sediment habitat consists of fine sediments with a scattered occurrence of echinodermata, ascidians and pennatulids. The stone habitat is instead characterised by the occurrence of stone and boulder fields with occasional sediment patches and various abundances of different macroalgae species. The habitat distribution is mainly controlled by erosion processes besides sediment supply and coastal morphology. Furthermore, seafloor characteristics in the soft-sediment habitat have been assessed in detail and subsequently attributed to environmental processes present in the study area. Sediment cores were used to identify depositional trends. A fuzzy cluster analysis was applied to classify this habitat into different marine deposition zones, including *the central depressions*, *the transitional environment*, *the shallow water environment* and *the glacier-proximal setting*.

Predictions for the future development of Potter Cove have been made based on global climate scenarios. Rapid glacial retreat has caused the establishment of the Fourcade Glacier at the land-sea interface. The predicted warming trend will sooner or later result in a complete retreat on land and change the glacier-proximal cove environment into a glacier-distal setting. Enhanced precipitation rates and stronger south-westerly winds will additionally relocate and enhance terrestrial discharge and furthermore result in changes within the water circulation system. A rather calm seafloor environment is assumed for the deeper innermost part of the cove, whereas energy conditions will be increased in the outer part and along the shallow rims of the cove. The seafloor in the outer cove will be subject to enhanced mass flow events and disturbance by ice. Regarding the habitat distribution, an expansion of the stone habitat into the cove and into deeper waters is predicted with long-term effects on the marine ecosystems in Potter Cove. The marine zonation in the soft-sediment habitat will experience a change in sediment characteristics and will shift according to new meltwater pathways and the relocation of the erosion-prone areas.

ZUSAMMENFASSUNG

Die Westantarktische Halbinsel gehört zu den sich am schnellsten erwärmenden Gebieten der Erde. Konsequenzen dieser Entwicklung beinhalten beträchtliche Auswirkungen auf terrestrische und marine Ökosysteme. Umweltrekonstruktion und fortlaufende Überwachung dieser Gebiete sind der Schlüssel zu einem tieferen Verständnis möglicher Auswirkungen und eine solide Grundlage um zukünftige Entwicklungen vorauszusagen.

Ziel dieser Doktorarbeit ist die Analyse vergangener, rezenter und zukünftiger Lebensräume in Potter Cove, einer kleinen Nebenbucht auf King George Island, Süd-Shetland Inseln, Antarktis. Bisherige und anhaltende Auswirkungen des Klimawandels auf dieses repräsentative Küstensystem sollen bewertet, sowie zukünftige Entwicklungen unter Fortsetzung der heutigen klimatischen Entwicklung vorhergesagt werden. Hydroakustische Daten, Unterwasseraufnahmen und Sedimentproben wurden ausgewertet, um die Eigenschaften des Meeresbodens zu beschreiben. Mittels multivariater Datenanalyse wurde die Datenverarbeitung, sowie die objektive Interpretation verschiedener Datensätze ergänzt und vereinfacht. Der Großteil der Daten wurde auf Feldkampagen im Rahmen des IMCOAST Programms während der südlichen Sommersaison 2010/2011 und 2011/2012 aufgenommen.

Die Enteisungsgeschichte auf King George Island, die vor ungefähr 15.000 cal yr BP begann, wird immer noch kontrovers diskutiert und ist Gegenstand zahlreicher wissenschaftlicher Studien. Auf der Grundlage von Fächerecholotdaten, Flachwasserseismik und Sedimentkerndaten wurden submarine Landformen und der Aufbau des Meeresbodens beschrieben, die von entscheidender Bedeutung bei der Rekonstruktion glazialer Dynamiken im späten Holozän sind. Desweiteren wurden vergangene und rezente Prozesse im Untersuchungsgebiet aufgedeckt und interpretiert. Die Ergebnisse belegen das Vorkommen von Moränenablagerungen und glazialer Lineation im inneren Teil der Bucht. Der Meeresboden besteht aus glazialem Schutt, der unterhalb oder in unmittelbarer Nähe der Gletschersohle abgelagert wurde. Bedeckt sind diese Ablagerungen von einer dünnen Sedimentschicht, die durch Schmelzwasserzuflüsse eingetragen wurde. Die Moränenrücken belegen Gletscherstagnationen, sowie mögliche Gletschervorstöße innerhalb der letzten 2.6 cal kyr BP. Landformen auf dem Hang in der äußeren Bucht beinhalten Rinnenstrukturen, Eisbergkratzer und Pockennarben ähnliche Strukturen. Die Analyse des Meeresbodenaufbaus lässt Ablagerungen von massiven Rutschungen erkennen, die durch Eisbergkiele oder erhöhte Sedimentlast ausgelöst wurden. Letztere hat ihren Ursprung in der vermehrten Akkumulation von glazialem Material, als der Gletscher sich in unmittelbarer Nähe befunden hat. Zusätzlich

transportieren die untermeerischen Rinnenstrukturen, die durch Schmelzwasserabfluss oder Trübeströme entstanden sind, große Mengen an Sedimenten auf den Hang.

Die heutige Verbreitung mariner Lebensräume in Potter Cove wurde mithilfe eines akustischen Meeresboden-Klassifikationssystems kartiert, welches durch Unterwasseraufnahmen und eine lineare Diskriminanzanalyse validiert wurde. Aufgrund fehlender Wellen- und Strömungsdaten im Untersuchungsgebiet wurden Scherspannungen am Meeresboden berechnet und Zonen erhöhter Erosionsanfälligkeit ausgewiesen. Die Ergebnisse zeigen zwei Habitatklassen in Potter Cove. Das Lockersediment-Habitat besteht aus feinen Sedimenten mit sporadisch vorkommenden Ansammlungen von Echinodermen, Ascidien und Pennatuliden. Das Gesteinshabitat ist dagegen charakterisiert durch Stein- und Blockfelder mit vereinzelten Sedimentflecken und Makroalgenbewuchs. Die Habitatverbreitung wird hauptsächlich durch Erosionsprozesse, aber auch durch Sedimentverfügbarkeit und Küstenmorphologie bestimmt. Darüber hinaus wurden weitere Meeresbodeneigenschaften im Lockersediment-Habitat untersucht und Prozessen im Untersuchungsgebiet zugeordnet. Mithilfe von Sedimentkernen wurden Ablagerungstrends identifiziert. Eine Fuzzy Clusteranalyse wurde angewandt um dieses Habitat in marine Ablagerungszonen zu unterteilen, einschließlich *der zentralen Becken*, *der Übergangszone*, *dem Flachwasserbereich und der gletschernahen Zone.*

Einschätzungen zukünftiger Entwicklungen in Potter Cove wurden aus globalen Klimaszenarien abgeleitet. Schneller Eisrückzug in der Bucht führte zu einer Positionierung des Fourcade Gletschers an der Schnittstelle zwischen Land und Ozean. Die prognostizierte Erwärmung der Klimaszenarien wird früher oder später den Rückzug des Gletschers aufs Land zur Folge haben und die gletscherdominierte Bucht in ein gletscherfernes Milieu verwandeln. Erhöhte Niederschlagsraten und verstärkte Westwinde im südlichen Ozean werden eine Verlagerung der Schmelzwasserflüsse sowie eine Zunahme der Abflussraten zur Folge haben und auch ozeanografische Prozesse beeinflussen. Eher ruhigere Bedingungen am Meeresboden abseits von Wellen und Strömungen werden für die tieferen Bereiche der inneren Bucht angenommen, wohingegen die Energie durch Brandungseinwirkung in der äußeren Bucht und entlang der Ränder noch zunehmen wird. Desweiteren wird der Meeresboden in diesem Bereich vermehrt Massenbewegungen und Eisbergaktivität ausgesetzt sein. Hinsichtlich der Habitatverteilung wird eine Ausdehnung des Gesteinshabitats in die innere Bucht und in höhere Wassertiefen angenommen mit Langzeitfolgen für das marine Ökosystem. Die marine Zonierung im Lockergestein-Habitat wird eine Änderung der Sedimenteigenschaften erfahren und sich gemäß neuen Schmelzwasserabflüssen und der Verschiebung der Zonen mit erhöhter Erosionsanfälligkeit verlagern.

TABLE OF CONTENTS

LIST OF FIGURES

LIST OF TABLES

1. INTRODUCTION

The Western Antarctic Peninsula region is recently experiencing rapid regional warming beyond the range of natural variability (Vaughan et al., 2003). Temperature reconstructions between 1957 and 2006 demonstrate a West Antarctic warming at a rate of approximately 0.11°C per decade (Steig et al., 2009). Observations from the northern tip of the Antarctic Peninsula instead indicate warming equivalent to ~3.5°C per century (Mulvaney et al., 2012). Global climate change scenarios point out the exceptional sensitivity of polar regions towards atmospheric temperature changes (Moline et al., 2008). Manifold consequences of this warming trend include serious impacts on the marine and terrestrial environments (Vaughan et al., 2001). Ice shelves retreated dramatically along the northern Antarctic Peninsula since the 1950s (Vaughan and Doake, 1996), a consequence that has long been predicted (Mercer, 1978). Pritchard et al. (2012) reported ice shelf retreat up to 7 m/year along the west coast of Antarctica. Cook et al. (2005) find glacier retreat associated with the atmospheric warming trend, but further suggest that also the loss of ice shelves might cause acceleration of inland glaciers. They state that 87 % of 244 marine glacier fronts on the peninsula have retreated between 1940 and 2001. Furthermore, a reduced duration of sea ice cover (1-2 days/year) has been reported by Vaughan et al. (2003 and references therein), while the ice-free season in the summer becomes longer (Martinson et al., 2008). Kruss et al. (2006) have shown that glacier retreat can lead to rapidly progressing changes in the biotic environment. As a result, valuable habitats may shift, dissect or even disappear. In this significant state of change, it is fundamental to continuously observe these environments in flux, if potential impacts and future trends in the light of global warming are to be predicted.

This PhD thesis was part of the international research programme IMCOAST that intended to assess the impact of climate induced glacial melting on marine coastal systems in the Western Antarctic Peninsula region. The study area Potter Cove is a small tributary embayment on King George Island, South Shetland Islands. King George Island has several scientific stations with increased scientific activity that can be seen as a consequence of competing political interests between Great Britain, Argentina and Chile since the end of the Second World War (Kraus, 2005). Ease of access as well as long time series that document climatic variations make this region a valuable study site. Furthermore, the small ice cap and its tidewater glaciers respond rapidly to environmental change. Besides local knowledge acquisition,

seafloor characteristics and dynamics of an area such as Potter Cove can contribute to our general understanding of glacier-influenced bays in higher latitudes under climatic pressure. It is assumed that Potter Cove stands representative for other coastal systems located on the Antarctic Peninsula. Therefore, the overall aim of this thesis is to assess the impact of climatic change in Potter Cove by providing profound knowledge about the past and modern seafloor environments. Furthermore, potential future developments under the ongoing warming trend are predicted. The specific objectives of this thesis by chapter are:

Chapter 2. Glacier-retreat related submarine landforms in Potter Cove

This chapter presents a comprehensive investigation of the seafloor morphology and associated sub-bottom characteristics in Potter Cove. Submarine landforms and deposition trends are then discussed in the context of the Last Glacial Maximum and the deglaciation history. The aims are to reveal the origin of ancient and modern landforms and to evaluate Late Holocene retreat behaviour of the Fourcade Glacier in Potter Cove.

Chapter 3. Distribution and characteristics of marine habitats in Potter Cove based on hydroacoustics and bed shear stress estimates

The aims of this chapter are to provide an up-to-date seafloor habitat map based on hydroacoustic data and to define how environmental parameters control the habitat distribution. Additionally, the recent distribution pattern is compared to former habitat studies. The results were then to be used to predict the future development of the habitats in the cove.

Chapter 4. Evaluation of seafloor characteristics and fuzzy clustering of the marine environment in Potter Cove

This chapter aims to assess the distribution of certain seafloor characteristics, including mean grain size, mud content, organic carbon content and bathymetry and to relate them to environmental processes present in the study area. A transect of sediment cores is used to identify depositional trends. Furthermore, Potter Cove is classified into marine deposition zones using a fuzzy cluster approach.

1.1. Regional Setting

The study area Potter Cove (58°40'W, 62°13'S) is located in the southwest of King George Island, South Shetland Islands (Fig. 1.1A). The South Shetland Islands are a 550 km long island chain that lies approximately 120 km northwest of the Antarctic Peninsula. The total land area sums up to 3,687 km^2 and is divided into nine main islands and several smaller ones. Most of the area is capped with ice, only 10 % are ice-free, including peninsulas, capes, points and narrow coastal fringes (López-Martinez et al., 2012). Towards the south, the Bransfield Strait separates the islands from the Antarctic Peninsula. Here, water depths increase to more than 1000 m about 10 km off the coast. The northern coastlines are exposed to the Drake Passage, where a broad shelf descends towards the South Shetland Trench.

King George Island, the largest island of the South Shetland Islands, is characterised by a cold maritime climate with mean annual precipitation rates of 438 mm (Lee et al., 2004). Annual air temperatures between 1947 and 1995 were -2.8°C on average (Ferron et al., 2004). Furthermore, a warming trend of 1.1°C was observed during this period with the strongest augmentation during winter months. More recent investigations report that the mean annual air temperature increased by 1.2°C between 1991 and 2005 (Schloss et al., 2008). However, Carrasco (2013) reports a lower warming rate for the last decade (2001-2010), compared to the last quarter of the 20^{th} century. Most of the island is occupied by a thin ice cap that has been described as partly temperate consisting of cold and temperate parts (Rückamp et al., 2010). The ice cap is approximately 100 km long and 25 km wide, with a maximum elevation of around 700 m above sea level (Osmanoğlu et al., 2013). The average thickness is approximately 250 m (Blindow et al., 2010). Smaller ice fields are dispersed along the coast and expose bedrock or gravel beaches in between (Griffith and Anderson, 1989). Geological investigations revealed that the island is composed of igneous rocks of pyroclastic, volcanic or plutonic origin that rest on a basement complex of schist, gneiss and sedimentary rocks (Yeo et al., 2004). Glaciers flow down to the coastline or directly into the surrounding waters, where they are grounded between 20 and 80 m on average (John and Sudgen, 1971). Icebergs containing debris layers are a common feature near the glacier termini. Large discharges of glacial meltwater are common, resulting in sediment-laden surface plumes in the bays. Sediment fallout from these surface plumes and deposition of coarser materials mobilized by heavy rains, as well as exceptional discharges via meltwater creeks, form the principal sediment sources in this region (Griffith and Anderson, 1989; Yoon et al., 1992). The importance of meltwater as transporting agent for lithogenic particles from the coastal drainage during summer months was shown by Khim et al. (2007). This study revealed that the particle influx

is controlled by the amount of snow-meltwater influx from land. Potter Cove is a small tributary inlet to Maxwell Bay, which is a large fjord system located between King George Island and Nelson Island. The Argentinean research station Carlini Base (formerly Jubany Base) is located on the southern coast of Potter Cove (Fig. 1.1B). The cove is about 4 km long and 2.5 km wide and is divided into an inner and an outer part by a shallow submarine sill that is located 30 m below sea level. Whereas water depths in the outer cove are generally below 100 m, water depths in the inner cove hardly reach below 50 m. The eastern and northern coast of the cove are characterised by steep slopes partly occupied by the Fourcade Glacier. The glacier drains the King George Island ice cap through the Warzawa ice field. Surface iceflow velocities at the glacier terminus reach up to approximately 25 cm per day (Moll and Braun, 2006). The southern coast of the cove has a flat topography dissected by the meltwater streams Matías and Potter Creek, which discharge suspended sediments into the cove (Varela, 1998). The coastal area in the southwest of Potter Peninsula is characterised by a flat terrain with occasional steep surfaces and outcropping bedrock both on land and below sea level. Lindhorst and Schutter (2014) describe the area along the coast as a prograding strand plain with gravel-beach ridges on top that developed during storm events. The marine environment is characterised by an average sedimentation rate of 3-4 mm per year (Monien, pers.comm.). This is in accordance with a study from Yoon et al. (2010) that reports a rate of 3 mm per year (308.1 cm/kyear) from Collins Harbor, another inlet to Maxwell Bay. Fine sediments can be found in protected locations, whereas more exposed areas are dominated by coarser material according to Veit-Köhler (1998). She has performed early sedimentological investigations in Potter Cove, but without assessing spatial variability and sediment parameters in detail. The circulation pattern in Potter Cove is mainly driven by wind, tides, waves and density gradients. The wind field is bidirectional (Klöser et al., 1994) and shows most frequent intensities between 8 and 12 m/s (Schloss and Ferreyra, 2002). The tidal range in the study area is around 1.5 m (Schöne et al., 1998). Roese and Drabble (1998) describe two different circulation systems that result from the east-west bidirectional wind field. One is a cyclonic gyre, where water renewal commences along the northern coast with clear water entering from Maxwell Bay and leaving the cove on the southern side. In response to the wind direction, the associated vertical circulation results in either downwelling or upwelling. Furthermore, strong westerly winds enhance water pile-up in the inner cove, thereby expanding the subsurface layer that flows out of the cove. Sea ice normally covers the cove from July until late October (Khim and Yoon, 2003).

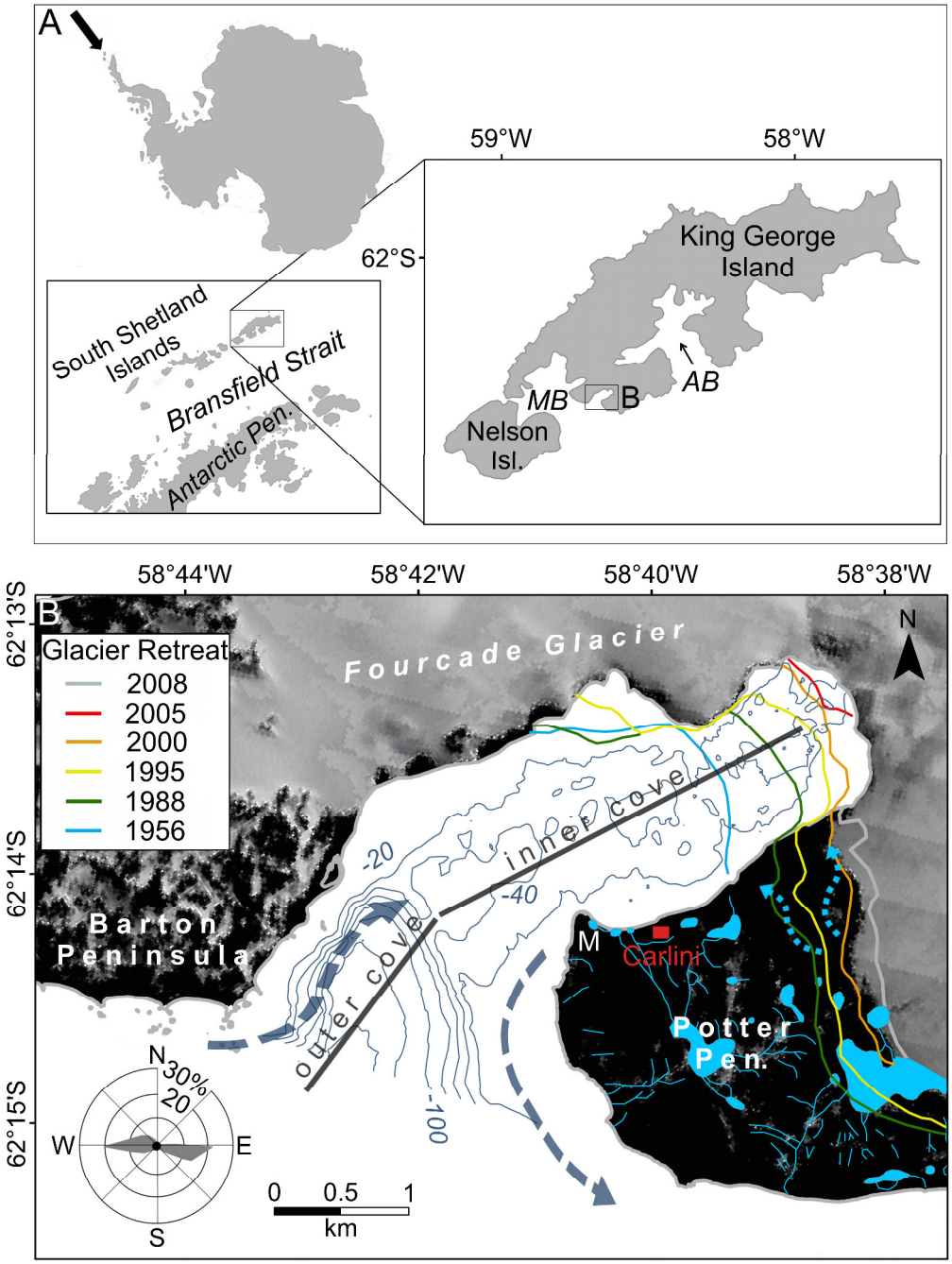

Fig. 1.1. Overview of the study area. A. Map showing the location of King George Island and Potter Cove, MB = Maxwell Bay, AB = Admiralty Bay. B. Map of the study area Potter Cove. Blue lines illustrate 20-m contour lines. Dashed arrows (dark blue) indicate the general water circulation. Wind rose plot indicates wind direction distribution from Roese and Drabble (1998). M = Mirounga Point. Landsat satellite image data are from the Antarctic Digital Database. Meltwater systems have been digitized from Kraus and del Valle (2008). Meltwater channels that developed after 2008 are indicated by dashed arrows (light blue). Coastline and glacier fronts from Rückamp et al. (2011).

1.2. Last Glacial Maximum and Deglaciation of the South Shetland Islands

During the Pleistocene, the Antarctic Peninsula region has undergone several glacial episodes. The Last Glacial Maximum (LGM) took place around 18 cal kyr BP (calibrated kiloyears before present), when the Antarctic Peninsula was covered by a large ice sheet that reached the continental shelf according to studies from e.g. Cowan et al. (2008), Bentley et al. (2010) and Simms et al. (2011). A study from Heroy and Anderson (2005) proposed that grounding ice even advanced as far as to the shelf edge. Fast-flowing ice streams filled the troughs that intersected the shelf and deposited trough-mouth fans at their termini (Davies et al., 2012 and references therein). Furthermore, a study from Heroy et al. (2008) found evidence that an ice shelf covered Bransfield Strait during the LGM.

The timing of deglaciation in this region is still a subject under debate. Milliken et al. (2009) analysed a high resolution marine sediment core at the entrance of Maxwell Bay that indicates deposition proximal to a former ice grounding line at its base. The associated seismic record shows that this till deposit rests on bedrock. Above the till deposit, fine-grained glacimarine sediments are found. This transition most likely represents the onset of deglaciation associated with decoupling of the ice sheet from the seafloor and was radiocarbon-dated to approximately 14 cal kyr BP. Terrestrial records from King George Island reveal an earlier ice recession already around 15.5 cal kyr BP (e.g. Seong et al., 2009). At ~10.1 ka, sediment characteristics indicate an environmental change from a glacial- to a meltwater-influenced setting. Open marine conditions were established in Maxwell Bay, while the ice kept on retreating towards the shallow margins of the fjord system during the Mid-Holocene Climatic Optimum (MHCO) that occurred between 8.2 and 5.9 cal kyr BP, according to Milliken et al. (2009). A study from the South Orkney Islands, located more than 700 km east of King George Island, identified a similar time span for the MHCO between 8.2 and 4.8 cal kyr BP (Lee et al., 2010). Evidence from Bransfield Strait reveals a much shorter period instead (6.8 to 5.9 cal kyr BP) (Heroy et al., 2008). Afterwards, sea surface temperatures decreased, while sea ice cover increased until 2.6 cal kyr BP (Milliken et al., 2009). According to Simms et al. (2011), this neoglacial advance ended around 1.7 cal kyr BP. Furthermore, they assume that either the adjacent coves in Maxwell Bay remained filled with grounded ice during the MHCO until 1.7 cal kyr BP or that the ice readvanced from the inner coves before that as suggested by Ingólfsson et al. (1998). A gradual warming after 1.7 cal kyr BP is also evidenced by increased sea surface temperatures between 1.6 and 0.5 cal kyr BP reported from Palmer Deep, a basin located on the West Antarctic Peninsula Shelf (Shevenell et al., 2011). Furthermore, Das and Alley (2008) reported maximum meltlayer frequencies around

0.8 cal kyr BP from the West Antarctic Ice Sheet. In general, little is known about climate fluctuations after ~1.7 cal kyr BP such as the Little Ice Age (LIA, 500-100 cal yr BP/1450-1850 AD; IPCC, 2013), a period of cooling that is mainly described from the Northern Hemisphere. Bertler et al. (2011) proposed that the LIA took place over entire Antarctica and further evidence is provided by several studies from the South. Ice advances during the LIA have been reported from glaciers in southern South America (Masiokas et al., 2009; Dowdeswell and Vásquez, 2013). Yoo et al. (2009) reports an increase in sea-ice extent during the time of the LIA (330 cal yr BP) along the continental shelf north of the South Shetland Islands. A sediment core study from Hass et al. (2010) places the LIA between 550 and 50 cal yr BP in Maxwell Bay. Also Monien et al. (2011) identified a main climate event in Maxwell Bay that is equivalent to the timing of the LIA. A novel approach using optically-stimulated luminescence was used by Simms et al. (2012), where they report a neoglacial advance on King George Island between 450-250 cal yr BP. However, Milliken et al. (2009) found little evidence for a LIA advance in Maxwell Bay and report even low variation in glacier grounding lines after 2.6 cal kyr BP.

1.3. Overview of selected methods used in this thesis

1.3.1. Acoustic ground discrimination system RoxAnn

The RoxAnn system is manufactured by Sonavision Ltd. of Aberdeen, Scotland. According to Chivers et al. (1990), it was the first commercial acoustic classification system on the market. This single beam acoustic bottom classifier uses the first and the second echosounder returns to analyse seafloor characteristics. The hardware includes a head amplifier that is connected to an echosounder and to a transducer. A parallel receiver receives the echos from the head amplifier and processes them (Hardie, 2008) (Fig. 1.2). Furthermore, the signals are spatially referenced by a Global Positioning System. The logging software RoxMap, specifically written for RoxAnn applications is used to log and display the data. This program illustrates the RoxAnn parameters in a 2D feature space, in which user defined coloured squares are supposed to represent different seafloor classes (Burns et al., 1989).

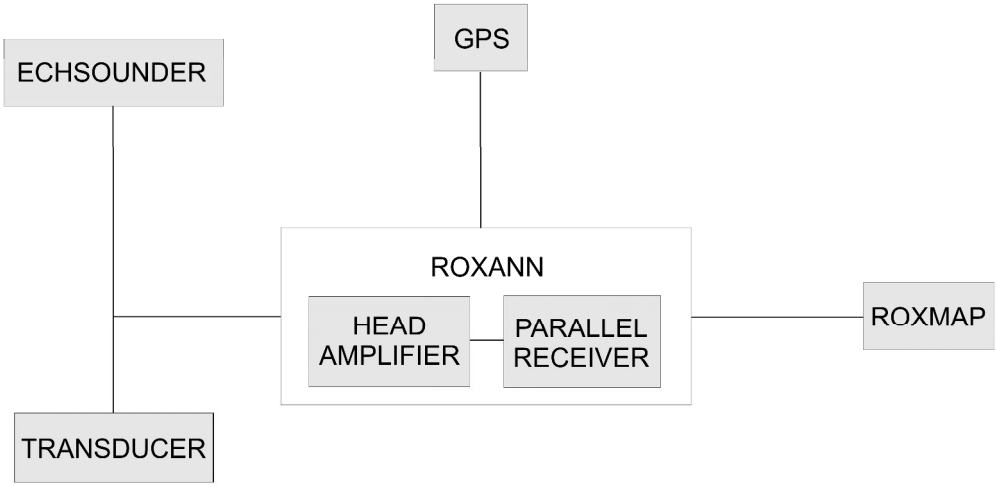

Fig. 1.2. RoxAnn system configuration (modified after Penrose et al., 2005).

The RoxAnn system applies an echo-integration methodology in order to obtain two parameters that reflect certain seafloor conditions. The first parameter E1 is derived from the first returning echo of the emitted pulse and includes only the tail part of the amplitude (Kenny et al., 2003) (Fig. 1.3). A perfectly smooth seafloor returns the energy from the initial reflection directly beneath the transducer, where the emitted pulse impinges on the surface at a perpendicular angle. A rougher seafloor instead scatters the emitted pulse and reflects energy also from other angles back to the transducer (Penrose et al., 2005). This backscattered energy appears only in the second part of the first echo that is used for the calculation, since the first part or the peak of the echo results from the specular return of the pulse (Hamilton et al., 1999). Therefore, the E1 parameter is a bottom backscatter index that reflects the acoustic roughness of the seafloor. The second parameter E2, reflected twice on the seafloor and once at the sea surface is included as a whole (Kenny et al., 2003) (Fig. 1.3). The acoustic impedance between seawater and seafloor influences the amount of energy that is reflected back to the transducer (Chivers et al., 1990). E2 is commonly used as an indicator of bottom hardness, whereas it is more related to acoustic reflectivity (Penrose et al., 2005). Agglomerations of E1 and E2 pairings in a 2D feature space are related to certain seafloor characteristics (Penrose et al., 2005). The relationship between them can be defined by calibrating the signals by direct observation, underwater photographs, video recordings or seafloor samples.

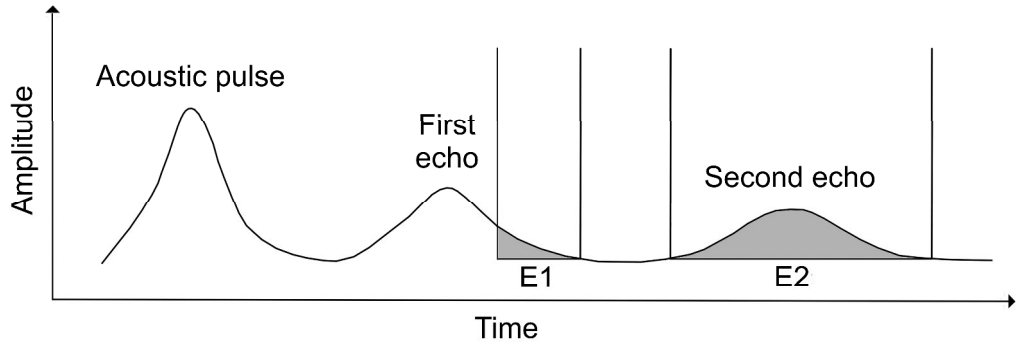

Fig. 1.3. Voltage trace of typical echosounder output for a single ping.

Seafloor habitat maps based on surveys using the RoxAnn system have been produced by several authors (Sotheran et al., 1997; Cholwek et al., 2000; Brown et al., 2005; Mielck et al., 2014). However, Humborstad et al. (2004) have stressed the importance of applying independent observations to avoid misinterpretations. Hamilton et al. (1999) evaluated the performance of the RoxAnn system and found major drawbacks depending on the survey conditions. The authors generally criticize the multi-echo approach and rather recommend using only the first echo. Depth and slope changes, rough terrain as well as vessel speed and engine noise were found to have an impact on the amount of energy that is received with the second echo. Kloser et al. (2001) also detected depth dependence during a RoxAnn survey. However, it was stated by the manufacturer that bathymetric changes are compensated by a pulse integration constant that adjusts the E1 and E2 gate areas. Signal variation due to increasing water depths are compensated by means of time varying gain (Chandu, SonaVision, pers. comm., 2014). Furthermore, the interpretation of the data using the concept of RoxAnn squares does not appear as an optimal classification method, since the RoxAnn parameters are not orthogonal to each other and squares cut across the data trend (Hamilton et al., 1999).

1.3.2. Multivariate analyses

Linear Discriminant Analysis

A linear discriminant analysis analyses group structures by uncovering the relation between one nonmetric dependent variable (the group designation) and one or more metric independent variables. Linear discriminant functions that separate groups, ideally minimize the variance of the data within the group and maximize the variance between the groups (Hair et al., 2009). A classification of unallocated observations can then be predicted, by calculating a distance measure between an observation

and the group centres in the multivariate feature space. This measurement is then used to assign the observation to a certain group (Burrough and McDonnell, 1998). Examples of hydroacoustic data processing using this method can be found in Lucieer (2005).

Fuzzy Cluster Analysis

The term cluster analysis refers to a variety of unsupervised cluster algorithms, which assign a set of observations to a certain amount of clusters. The perfect cluster will join observations with similar attributes and will be well separated from the other clusters in the multivariate feature space. The fuzzy c-means algorithm that is applied in this study is an extension of the k-means algorithm introduced by MacQueen (1967), with the advantage to characterise each observation's similarity to every cluster (Bezdek et al., 1984). The similarities are quantified using membership values that range between 0 and 1, indicating low similarity between an observation and a cluster close to 0 and high similarity close to 1 (Zadeh, 1965). The information delivered by the membership values is reflected by the confusion index after Burrough et al. (1997). This index approaches 0, when the confusion is low, implying low uncertainty, whereas a value close to 1 indicates high confusion and therefore high uncertainty in class attribution. The hard classification is achieved by assigning the cluster with the highest membership value to the observation (Defuzzification). Different kinds of cluster algorithms for classifying marine environments have been successfully applied (e.g. Kostylev et al., 2001; Kruss et al., 2008; Greenstreet et al., 2010). The study from Lucieer and Lucieer (2009) were among the first ones that applied and recommended the fuzzy algorithms for spatial marine data sets, since it enables the quantification of uncertainty and the identification of transition zones that are characteristic for natural classes. The application of the fuzzy cluster analysis in this study follows their approach with some modifications.

1.3.3. The use of a geographic information system for data preparation

Central to parts of this study was the objective evaluation and classification of multi-layered data sets obtained in Potter Cove by using multivariate statistics. The integration of abiotic variables and subsequent classification of seabed features can be performed using Geographic Information Systems (GIS). Classification procedures are increasingly supported by GIS (Verfaillie et al., 2009 and references therein). Two separate analyses are involved, including 1) interpolation of data from individual sampling points into a continuous layer, and 2) classification of multivariate variables into seafloor categories (Lucieer and Lucieer, 2009).

The data input into the multivariate analyses requires extensive pre-processing of the data sets. The first step was to transform point data from the field into spatial data by using interpolation algorithms, since a pixel-based classification was intended as final output. All raster data sets were subsequently transformed into vectors for the final data set that fulfilled the requirements for the analyses. The transformation of rasters into vectors using the software ArcGIS (10.0, ESRI) and associated analysis tools provided by the software are described in subchapter 3.1.4 and 4.1.2.

1.4. Statement of contribution from author and co-authors

The PhD candidate Anne-Cathrin Wölfl was responsible for the study design, most of the data acquisition and analysis, interpretation of results, literature review and manuscript preparation. All steps were conducted with support from the supervisors. Three scientific manuscripts have been prepared that are presented in chapter 2-4.

Contributions to chapter 1/Wölfl*, A.-C., Wittenberg*, N., Feldens, P., Hass, H.C., Betzler, C., Kuhn, G. (submitted to Antarctic Science). Glacier-retreat related submarine landforms in a shallow Antarctic fjord (Potter Cove, King George Island)
*These authors contributed equally to this work

Wittenberg, N. prepared the manuscript together with the PhD candidate. She mostly collected, analysed and interpreted the seismic and sediment core data. Furthermore, Figure 2.3, 2.4, 2.5, and 2.6 were solely designed by her and are included in the thesis with some modifications. Feldens, P. helped processing the multibeam data set and reviewed the manuscript. Hass, H.C. reviewed and edited the manuscript. He also recorded the seismic profiles. Betzler, C. and Kuhn, G. reviewed the manuscript. Kuhn, G. also measured the geochemical proxies of the core and provided helpful comments concerning the interpretation of seismic records. The multibeam data set was provided by the United Kingdom Hydrographic Office (United Kingdom Hydrographic Office data © Crown copyright and database right).

Contributions to chapter 2/Wölfl, A.-C., Lim, C.H., Hass, H.C., Lindhorst, S., Tosonotto, G., Lettmann, K., Kuhn, G., Wolff, J.O., Abele, D., (2014). Distribution and characteristics of marine habitats in a subpolar bay based on hydroacoustics and bed shear stress estimates - Potter Cove, King George Island, Antarctica. Geo-Marine Letters, 34(5), 435-446. DOI 10.1007/s00367-014-0375-1

Lim, C.H., Lettmann, K.A., Wolff, J.O. conducted the bed shear stress estimates and reviewed the manuscript. Hass, H.C. reviewed and edited the manuscript and gave advice on structure and design. Further, he recorded the single-beam profiles together with the PhD candidate. Tosonotto, G. provided single-beam bathymetric data. Kuhn, G. and Abele, D. reviewed the manuscript.

Contributions to chapter 3/Wölfl, A.-C., Hass, H.C., Monien, P., Wittenberg, N., Kuhn, G. (in prep.). Evaluation of seafloor characteristics and fuzzy clustering of the marine environment in Potter Cove, King George Island, Antarctica.

Hass, H.C., Kuhn, G., reviewed and edited the manuscript. Hass, H.C., Wittenberg, N. obtained the sediment samples together with the PhD candidate. Kuhn, G. also measured the organic carbon content of the seafloor sediment samples. Monien, P. obtained and prepared the sediment cores.

2. GLACIER-RETREAT RELATED SUBMARINE LANDFORMS IN POTTER COVE

King George Island and especially Potter Cove have been in the focus of numerous investigations over the past decades. The glacial retreat history covering the previous century is mainly derived from high-resolution satellite images. A study from Simões et al. (1999) showed that glacier fronts on King George Island retreated from hundreds of meters up to 1 km between 1956 and 1995. Rückamp et al. (2011) have demonstrated that since 1956 ice loss in Potter Cove mainly occurs through the tidewater glacier, rather than through the ice lobe that is grounded on Potter Peninsula. The deglaciation history following the Last Glacial Maximum (LGM) has been documented by several recent studies focusing on the large fjord systems on King George Island using high-resolution marine sediment records (Milliken et al., 2009; Simms et al., 2011; Majewski et al., 2012). During deglaciation, ice has retreated through the fjords of King George Island, leaving a valuable record of Holocene submarine landforms behind.

In this chapter, high resolution hydroacoustic data from Potter Cove, including multibeam bathymetry and seismic data are evaluated. Additionally, a sediment core from the outer cove is examined that covers the latest deglacial record. Submarine landforms and sub-bottom characteristics are mapped and interpreted with the intention to delineate ancient and modern environmental processes and to investigate the Late Holocene retreat behaviour of the Fourcade Glacier.

2.1. Methods

2.1.1. Multibeam bathymetry

Swath bathymetry of the seafloor in Potter Cove was collected between January and February 2012 by the United Kingdom Hydrographic Office using a Kongsberg Maritime EM 3002 multibeam echosounder. This system uses frequencies in the 300 kHz band and has an electronic pitch compensation system as well as roll stabilized beams. The total survey area sums up to approximately 7 km^2. Data were processed using Fledermaus 7.3 (QPS) to remove erroneous depth values and subsequently gridded to a horizontal resolution of 5 m. Visualisation was performed using ArcGIS 10.1 (ESRI). Multibeam data was further complemented in the shallow areas by a single-beam data set provided by Gabriela Tosonotto from the IAA (Instituto Antártico Argentino, Buenos Aires, Argentina) for illustrative purposes (Fig. 2.1).

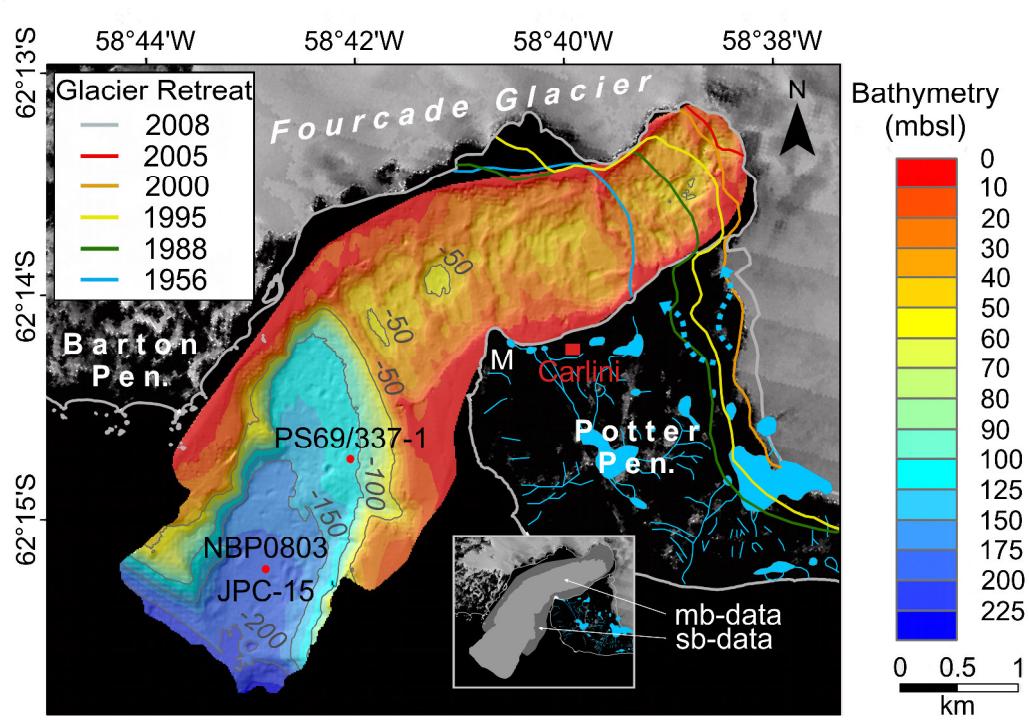

Fig. 2.1. Swath-bathymetry of the seafloor in Potter Cove including an overview showing where multibeam (mb) and single-beam (sb) data was processed. Contour lines (grey) are displayed in a 50 m interval. Sediment core positions are indicated. M = Mirounga Point. Landsat satellite image data are from the Antarctic Digital Database. Meltwater systems have been digitized from Kraus and del Valle (2008). Meltwater channels that developed after 2008 are indicated by dashed arrows (light blue). Coastline and glacier fronts from Rückamp et al. (2011).

2.1.2. Sub-bottom profiling

High resolution seismic data were obtained during the IMCOAST field campaign in December 2010 using a parametric sub-bottom profiler SES light (Innomar). The survey was performed from a Zodiac Mk4 inflatable dinghy during calm sea state with the transducer mounted on a specially designed floater. This floater was towed several meters behind and at least one meter beside the track of the air bubbles produced by the engine of the zodiac. A GPS antenna was also deployed on the floater. During recording, the frequencies were switched between 4 kHz and 15 kHz depending on the need for deeper penetration or higher resolution. The emitted frequency is indicated in Figure 2.4. The frequency variation is assumed to have a negligible effect on the categorization in this study. Data processing was performed using the ISE (Innomar) software. A sound velocity of 1500 m/s was used to convert the two-way travel time into water depth. Acoustic facies types were visually determined and classified. Additionally, Parasound profiles from the mouth of Potter Cove were incorporated that were recorded with 4 kHz during Polarstern cruise ANT-XXIII/4 in 2006 (Gohl, 2007).

2.1.3. Sediment core

During Polarstern cruise ANT-XXIII/4 in 2006 (Gohl, 2007), sediment core PS69/337-1 was recovered with a 10 m gravity corer at 62°14’46.32’’S, 58°42’08.28’’W (Fig. 2.1). Two times the gravity corer was deployed at the core station and bended at approximately 2 m. The core was obtained in 115 meters below sea level (mbsl) and has a length of 1.26 m. Internal structures were identified using radiographs (not shown in this study). Sediment samples were taken in 1-cm intervals and grain size analyses performed. Prior to the measurements, carbonate and organic matter were removed by treatment with acetic acid and hydrogen peroxide. Sodium polyphosphate was subsequently added to disaggregate and prevent new aggregation of particles before shaking the samples overnight by means of an orbital shaker. Before and during grain size analysis, the samples were kept dispersed by ultrasonic treatment. Grain size analyses were performed using a Cilas 1180L particle-size analyser, which measures particles in 100 size classes between 0.04 and 2,500 µm. The data output is expressed in volume percent (vol.%). Grain size statistics were calculated using the GRADISTAT program of Blott and Pye (2001). For the purpose of this study, the percentile statistics of Folk and Ward (1957) were used for further applications.

Furthermore, the total organic carbon content (TOC) was determined for the sediment samples by combustion using an Eltra CS2000 Carbon and Sulfur Determinator. The samples were freeze-dried, pulverized and decalcified using

hydrochloride acid. Iron cuttings and wolfram were added as catalysts. The total carbon contents (TC) were determined by a CNS elemental analyzer Vario EL III, in order to obtain the carbonate content ($CaCO_3$). The following formula after Stein et al. (1994) was used: $CaCO_3$ = (TC-TOC) * 8.333. The results are given in weight percent dry sediment (wt.%).

AMS radiocarbon dating was performed on a mixture of benthic and planktonic foraminiferas (1.2 mg) that was taken in 1.22 - 1.23 m core depth. The analysis was carried out at the Leibniz-Laboratory for Radiometric Dating and Isotope Research at the University of Kiel. A total reservoir effect of 1300 years for this region is suggested by Berkman and Forman (1996), but deviating corrections exist for dating marine carbonate shells (e.g. Davies et al., 2012). In this study, a total of 1100 years was chosen according to recent sediment core studies from Maxwell Bay (Milliken et al., 2009; Simms et al., 2011; Majewski et al., 2012). The radiocarbon age was calibrated using the program Calib 6.1.1. (marine09, Reimer et al., 2009) and a local reservoir effect (δR) of 700 years added to the 400 years that are already implemented in the programme. The resulting age is 318.5 ± 42 cal yr BP. It is presented as the 1-sigma mean and rounded to the next decade (Tab. 2.1).

Tab. 2.1. Radiocarbon age for core PS69/ 337-1. Calibrated with Calib 6.1.1. and dataset "marine09", corrected with δR=700.

Lab Code	Core Depth [m]	Radiocarbon Age [BP]	Cal. Age [BP] (1-σ)	Cal Age [BP] (rounded)
KIA 43473	1.22 -1.23	1375+/-30	318.5	320

2.2. Results

2.2.1. Morphology of Potter Cove

The inner part of Potter Cove can be described as a submarine hanging valley that enters the main trough of Maxwell Bay through a steep slope located in the outer part of the cove (Fig. 2.1). The slope starts with a rather steep gradient of approximately

30 % and flattens out towards the seafloor of Maxwell Bay. The flanks of the slope are slightly steeper in the west of the cove than in the east.

Distinct ridges and ridge assemblages hereinafter referred to as moraine complexes occur in the inner part of the cove (Fig. 2.2). These complexes (M_{1-4}) divide the inner cove into four different basins (B_{1-4}). The outermost of the moraine complexes (M_4) is the submarine sill that separates the cove into an inner and an outer part. It has an approximate width of 80 m and is characterised by a very regular shape compared to the other complexes that are rather sinuous. The seafloor on the south-western side of M_4 declines in a steep slope that widens towards Maxwell Bay. Two moraine complexes are found in the central inner cove (M_2, M_3). M_2 is comprised of a number of unequally spaced large ridges that are mainly located along the southern side of the cove. The youngest moraine complex (M_1) lies close to the glacier terminus and is relatively broad (~200-300 m) and irregular in its shape. Towards the north, another moraine complex is laterally attached (M_{lat}) and runs parallel to the cove axis in east-west direction. The central parts of the complexes reveal outlets that are V-shaped, but exhibit different incision depths (Fig. 2.2A). The outlets of the innermost moraine complex M_1 are less incised and show a more jagged morphology when compared to the other outlets. Within all four basins occur small ridges that stretch transverse to the cove axis (Fig. 2.2). These ridges are much smaller in their extent than the moraine complexes. They are 1-3 m high, gently curved and reveal an unequal spacing between ~50 and ~180 m. Transverse small ridges are not very pronounced proximal to the seaward dipping side of the M_1. The most irregular seafloor topography is found in B_1 compared to the more distal areas. Streamlined landforms occur in this basin that have an almost parallel orientation to the inner cove axis and are approximately between 50 and 150 m long. It appears that these landforms are overprinted by small ridges.

The seafloor surface of the slope in the outer cove is rough and characterised by depressions (Fig. 2.2). Small sinuous depressions occur mainly on the upper slope, whereas large depressions, almost circular in shape, occur in water depths between 100 and 200 m. Large depressions at the base of the slope are approximately 70 m in diameter and between 2 and 6 m deep. They reveal a raised rim and occur close to the flanks of the bay. Two large depressions occur further upslope. They are similar in shape, but slightly smaller in diameter and reveal depth values up to 10 m. In the southeast of the study area, a large incisive channel structure cuts in northwest-southeast direction (Fig. 2.2). The observed part of this structure is < 400 m long, 20 m wide and 10 m deep and inclines with a gradient of approximately 12 % towards the northwest. The topography of Potter Peninsula (Fig. 2.2B) reveals valley structures close to a 90 m high plateau where the largest proglacial lake is situated and continues towards this channel. Further small-scale channel structures are found further downfjord.

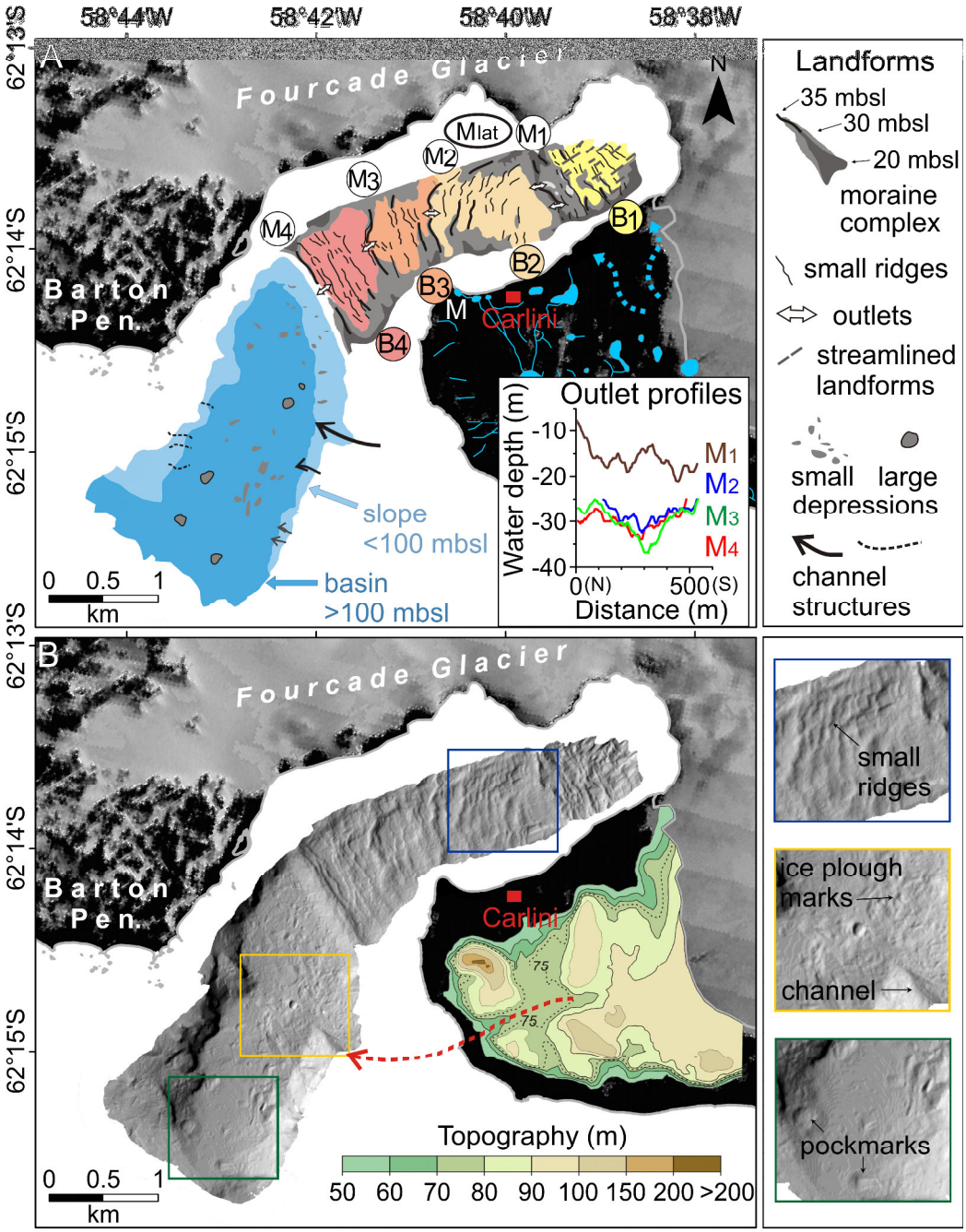

Fig. 2.2. Maps illustrating the seafloor morphology in Potter Cove. A. Geomorphic sketch of submarine landforms observed in Potter Cove, Bx= Basin x, Mx= Moraine complex x. Outlet profiles of moraine complexes are shown. B. Bathymetric hillshade from Potter Cove and topographic hillshade from Potter Peninsula (Braun et al., 2001). The dashed arrow (red) indicates the inferred meltwater pathway towards the largest submarine channel structure. Landsat satellite image data are from the Antarctic Digital Database. Meltwater systems have been digitized from Kraus and del Valle (2008). Meltwater channels that developed after 2008 are indicated by dashed arrows (light blue). The coastline has been extracted from Rückamp et al. (2011).

2.2.2. Sub-bottom characteristics

Four sub-bottom profiles were selected to present the sub-bottom characteristics of Potter Cove that were classified into different acoustic facies (Fig. 2.3). Profile A-B recorded in the inner part of the cove shows that the acoustic penetration is rather low (< 10 m) (Fig. 2.4A). Furthermore, it is characterised by a strong surface reflection and an acoustically chaotic sub-bottom with abundant point-source (hyperbolic) reflections that fade out towards greater depth. Occasionally, a thin acoustically transparent layer (< 3 m thick) drapes the chaotic structure. Together, these characteristics form the *chaotic facies*.

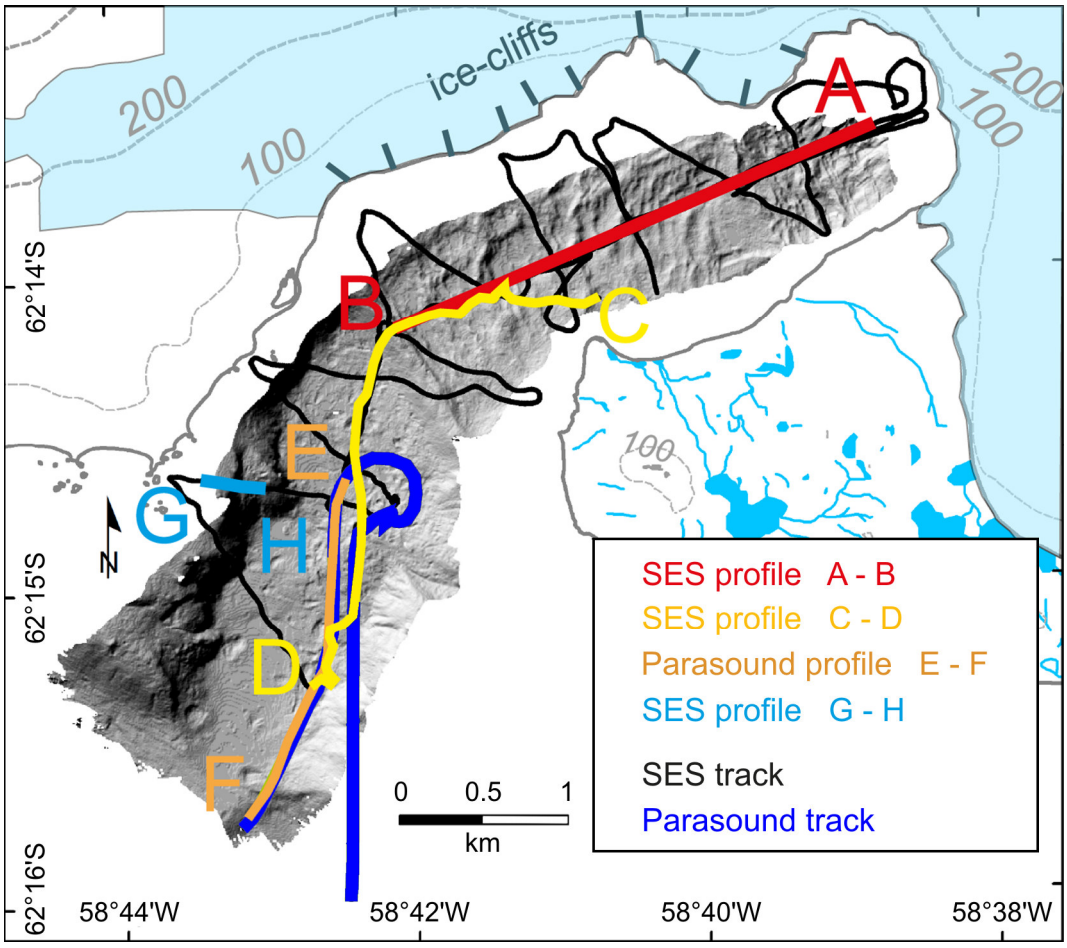

Fig. 2.3. Overview of the sub-bottom tracks and profile lines. Bathymetric hillshade in the background (modified after Wittenberg).

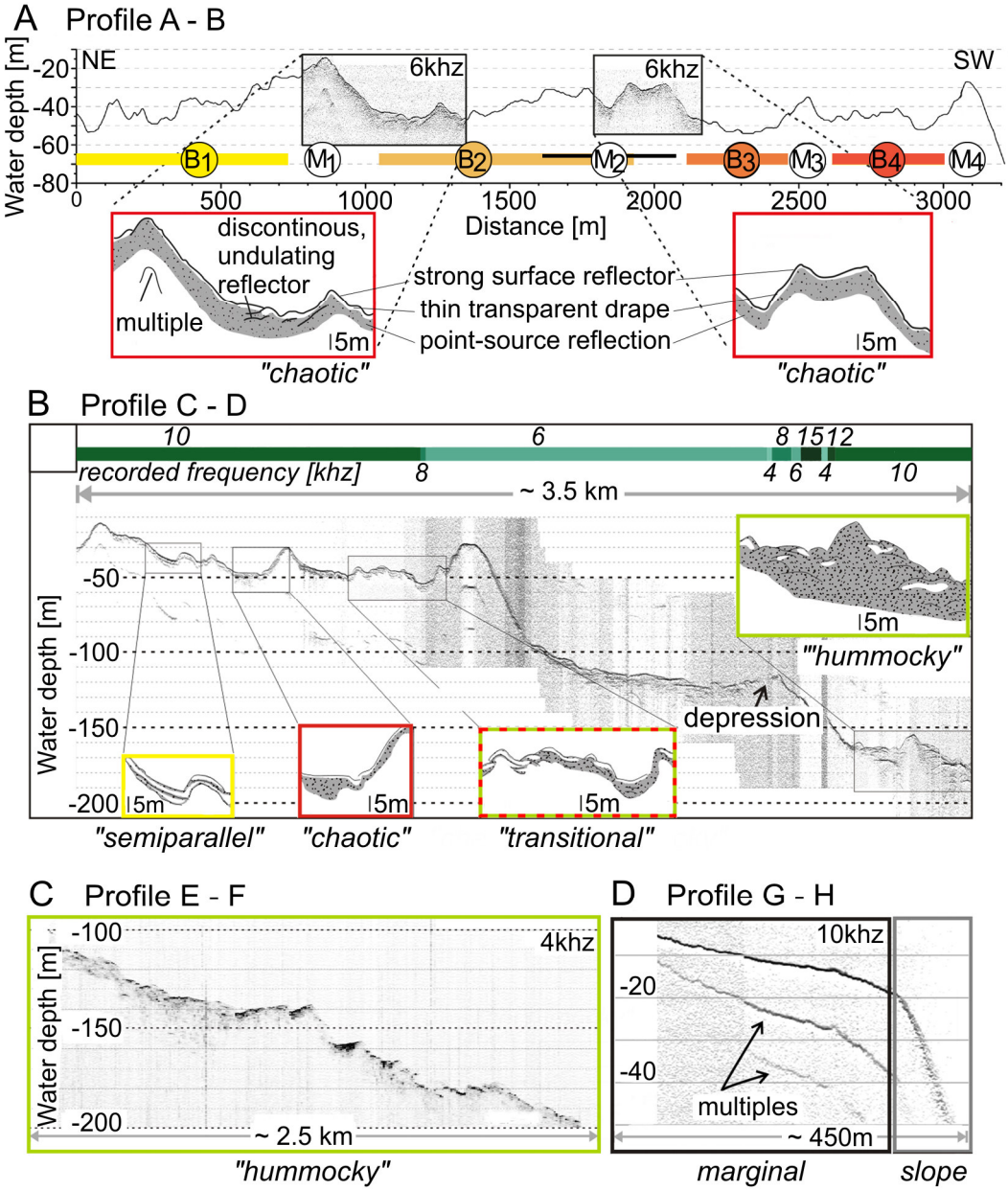

Fig. 2.4. Sub-bottom profiles in Potter Cove and associated acoustic classification. For profile location see Figure 2.3. A. Profile A-B shows a cross section (generated by multibeam depth soundings) along the inner cove axis. Parts of the SES profile and sketches with acoustic characteristics are shown. Bx= Basin x, Mx= Moraine complex x. Vertical exaggeration (V.E.): ~6.6. B. SES profile C-D. Sketches with acoustic characteristics are shown. Furthermore, sub-bottom characteristics of a depression are indicated. Frequency variations are illustrated in green. V.E.: ~6.6. C. Parasound profile E-F. V.E.: ~10. D. SES profile G-H showing no acoustic penetration (modified after Wittenberg).

Profile C-D (Fig. 2.4B) shows almost parallel subsurface reflections at short intervals in a confined area near the southern coast that are referred to as the *semi-parallel facies*. The sub-bottom classified as *hummocky-facies* is characterised by deeper sound penetration and strong, undulating reflectors in several meters below the seafloor. Furthermore, a transition from a chaotic to a hummocky sub-bottom is recognised. This sub-bottom structure is therefore characterised as *transitional facies*. In the outer cove in approximately 120 m water depth, a depression was crossed with almost no recorded reflections.

The Parasound profile was included to compare it with the SES profile (Fig. 2.4C). It appears that both profiles are similar in penetration as well as resolution. This might be considered as a proof of quality for the sediment echosounding applied from a zodiac. The profile shows the *hummocky facies* with a strong reflection pattern in some sediment filled depressions in the outer cove.

In areas marginal to the coast in less than 25 m water depths, the profiles show no sound penetration (Fig. 2.4D). Associated with this are diffuse seafloor reflections with also limited acoustic penetration across steep slopes (Fig. 2.4E). These two characteristics are not included in the classification since they provide no information about the sub-bottom characteristics.

The spatial distribution of the acoustic characteristics shows the dominance of the the *chaotic facies* in the inner cove, whereas the *hummocky facies* dominates in the outer cove (Fig. 2.5). The *semi-parallel facies* was only detected in a small area northwest of the coast of Potter Peninsula. The *transitional facies* that marks the transition between the *chaotic facies* and the *hummocky facies* occurs in the outermost basin of the inner cove (B_4).

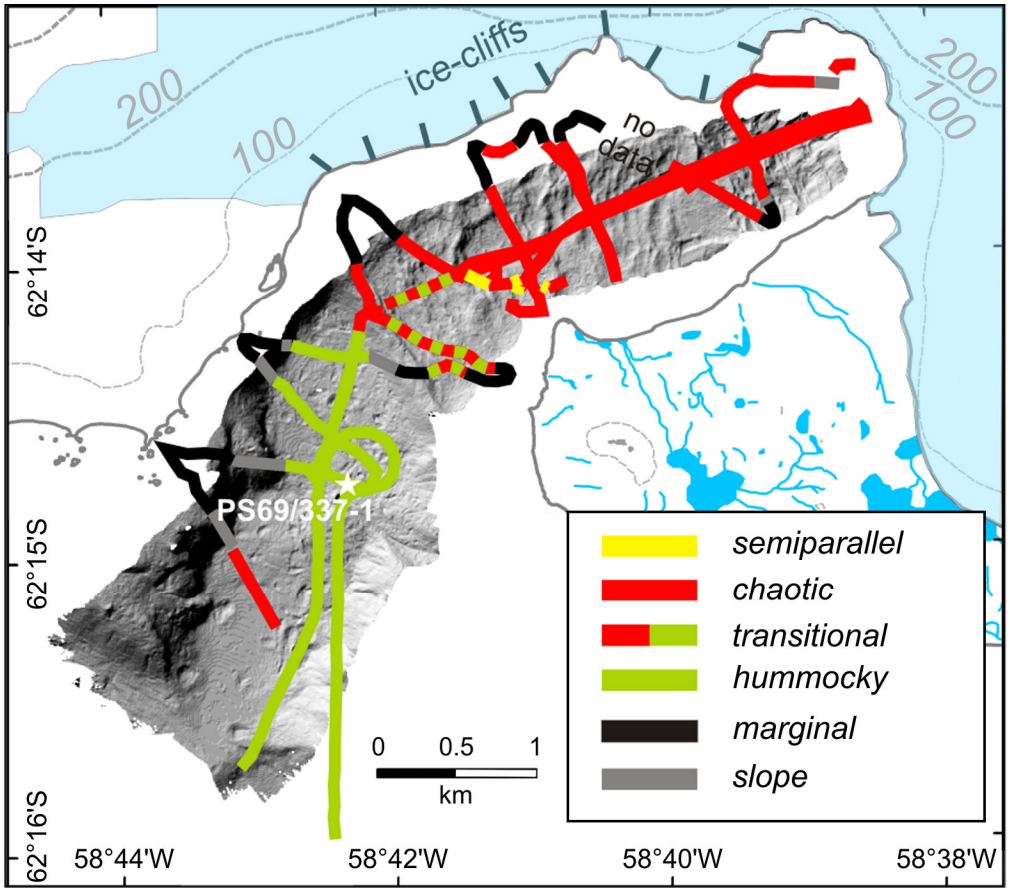

Fig. 2.5. Sub-bottom classification of Potter Cove. Bathymetric hillshade in the background (modified after Wittenberg).

The grain size analyses of sediment core PS69/337-1 revealed an average composition of ~45 vol.% sand, ~45 vol.% silt and ~10 vol.% clay (Fig. 2.6). Frequently, scattered dropstones occur. Bioturbation seems to be limited to minor disturbances in the upper 0.5 m of the core. At 1.2 m core depth, a sand layer is present with an erosional base. The amount of sand slightly decreases towards the core top until 0.35 m despite some minor fluctuations. At 0.35 m another sand layer occurs. The sediments mainly consist of terrigenous grain components, but also siliceous and carbonate shells, shell fragments and sponge spicules are found. TOC contents show on average 0.3 wt.% with an increasing trend towards the core top. $CaCO_3$ contents are ~1.8 wt.% on average. Both records show little variations in the lower part and increased variation in the upper part of the core. Maximum concentrations of $CaCO_3$ occur in the sand layer at 1.2 m (2.8 wt.%), where a suitable amount of foraminifera shells could be extracted for AMS radiocarbon dating. The dating result provides a calibrated and reservoir-corrected age of ~320 cal yr BP /~1630 AD (Tab. 2.1).

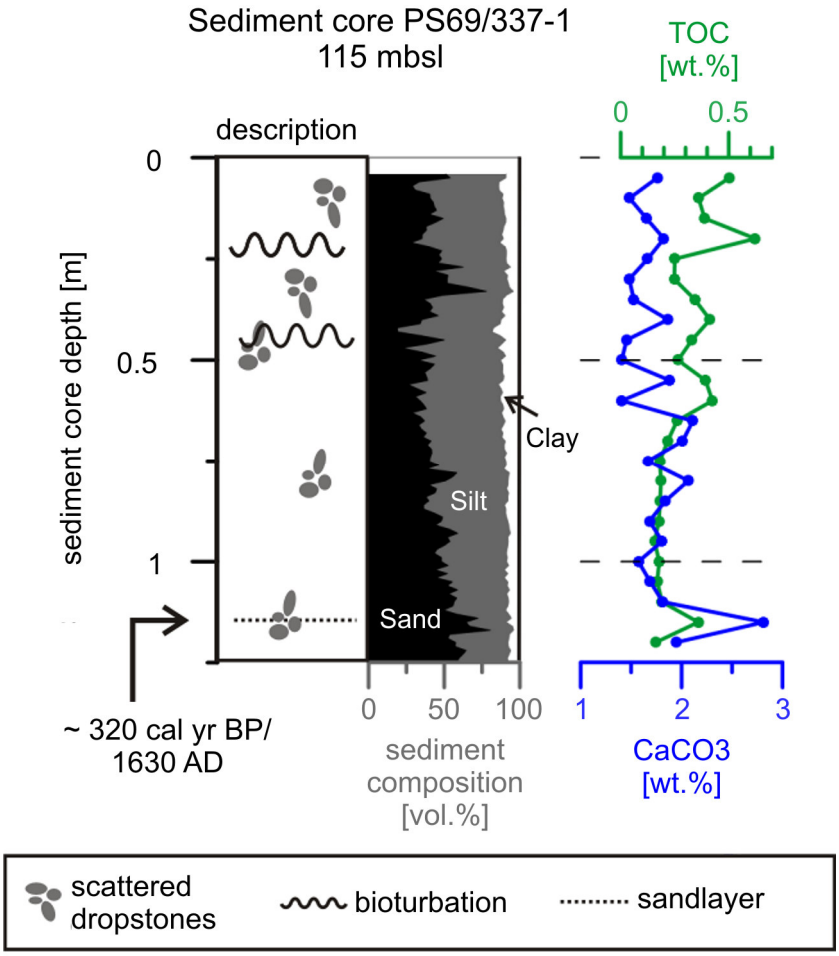

Fig. 2.6. Sediment core PS69/337-1 including lithology, sediment composition, total organic carbon (TOC) and carbonate ($CaCO_3$) content (modified after Wittenberg).

2.3. Discussion

The outermost moraine complex (M_4) that rims the inner Potter Cove is interpreted to be transverse to the direction of former ice flow and most likely represents a terminal moraine that captured the last maximum expansion of grounded ice in the inner cove (Fig. 2.2). The vertical drop in elevation of approximately 50 m might have prevented further advances of the grounding line downfjord. Formation of a calving front associated with accumulation of glacial debris at this position shaped this distinct moraine. Generally, the other moraine complexes in the inner cove are interpreted to

be either moraines that developed during a period of glacial readvances or recessional moraine ridges resulting from glacial stillstands during deglaciation (Ottesen and Dowdeswell, 2006). The youngest moraine complex (M_1) at the head of the cove might also originate from a readvance or a prolonged stillstand of the glacier front at this location. The latter might be attributed to climatic forcing, but could also be caused by the narrowing of the cove that might have confined the groundling line to this location. The longitudinal part of this moraine complex ($M_{lateral}$) was most likely formed parallel to the flowing ice. This feature is interpreted as a lateral moraine that rimmed the Fourcade Glacier or as a medial moraine where ice streams or glaciers have merged. Blindow et al. (2010) concluded that the ice cap of King George Island is temperate, since percolation of meltwater and a water table were recognised in ground-penetrating radar profiles on the ice cap. It is assumed that the outlets found within the moraine complexes result from subglacial meltwater drainage. The V-shaped character of the incision might furthermore be an indication of high-energy flow according to Dowdeswell and Fugelli (2012). The different shape of the incision in the innermost moraine complex M_1 can most likely be attributed to the relatively younger age of this feature that has not been exposed to long-term meltwater activity. The formation of the small ridges in the inner cove cannot be resolved based on the available data. It may be assumed that they are associated with glacial advance or glacial retreat and have formed during minor advances or stillstands of the Fourcade Glacier grounding line. Sea ice that is present in Potter Cove in winter (Khim and Yoon, 2003) could potentially inhibit calving events at the glacier front and the small ridges might therefore represent push moraines that originate from winter readvances of the ice (Ottesen and Dowdeswell, 2006). It is unlikely that the small ridges represent crevasse fillings that stayed in situ when the glacier melted (Christoffersen et al., 2005), since the glaciers on the South Shetland Islands are very clean and only slight bands of debris occur occasionally (Griffith and Anderson, 1989). Furthermore, it must be taken into consideration that the small ridges represent corrugation ridges (Jakobsson et al., 2011). They form where glacial ice breaks of at the grounding line and rhythmically settles on the seafloor according to the tides, squeezing the sediment into ridges. The absence of small ridges west of M_1 might be attributed to sediment deposits that drape the morphologic structures underneath, either derived from high sediment discharge at the glacier front or enhanced fluvial sediment input from the nearby meltwater streams. The streamlined landforms in B_1 close to the glacier front are interpreted as glacial lineations that indicate the direction of former ice flow. They are assumed to be generated at the ice-sediment or ice-bedrock interface beneath actively flowing ice during an ice advance, when the glacier was grounded in the cove (Ottesen and Dowdeswell, 2006). It can be assumed that they also occur further downfjord, but sediments have draped the seafloor for a longer period of time and smoothed its morphology underneath (Ottesen and Dowdeswell, 2009). The sub-bottom character of B_1 does not reveal any specific characteristics when compared to the other basins.

The small depressions occur mainly on the upper slope in the outer cove (Fig. 2.2). Their sinuous shape is similar to a type of iceberg plough marks described by Pudsey et al. (1994) from the Antarctic continental shelf. They do not resemble well-developed furrows that result from ice scouring over the seafloor, but are rather irregularly distributed curvy deepenings that result from deep-keeled grounded icebergs that are set in motion by wave and tidal activity. Icebergs are a common feature in the Peninsula region and have also been observed in Maxwell Bay. The larger, almost circular depressions that occur between 100 and 200 m water depth are instead attributed to another origin. Dowdeswell and Vásquez (2013) observed numerous crater-like features in fjords from southern Chile that they interpret as pockmarks. In their study, they calculated crater depth and diameter of over 80 pockmarks. They were found in water depths less than 160 m with median crater depths between 3 and 5 m and median diameters between 40 and 60 m. The depressions from this study reveal similar water and crater depths as well as diameters compared to those reported from Chile and are also interpreted as pockmarks. Their formation might result from groundwater seepage, pore water escape or gas venting (Paull et al., 1999 and references therein). Potential sources for natural gases are petroleum occurrences, organic-rich sedimentary deposits and methane hydrates (Rogers et al., 2006). Römer et al. (2014) reported microbial methane formation in fjords and troughs surrounding South Georgia that is located ~1,500 km northeast of King George Island in the Southern Atlantic Ocean. They suggest that methane seepage is far more widespread in polar and sub-polar regions than presumed. Pockmarks reported from settings comparable to Potter Cove were formed mainly by escaping pore water and venting of gas. A recent study suggests that pockmarks discovered in two Spitsbergen fjords represent dewatering structures that reflect sediment displacement by upwelling pore water, due to loading of water-saturated sediments by debris flows (Ottesen et al., 2008). Another study from Spitsbergen fjords found seepage of thermogenic gases and migration of pore water responsible for the formation of pockmarks (Forwick et al., 2009). For the study area, these two mechanisms are also considered as possible. The steep slope in the outer cove as well as the hummocky acoustic facies type are indications for the occurrence of sediment gravity flows (e.g. debris flows and turbidity currents) in this area. Where the load on the water-saturated sediments exceeded a critical threshold, pore water might have escaped from the sediments underneath and pockmarks were formed. Furthermore, thermogenic gases must be considered as a possible origin of the pockmarks, since hydrothermal venting has also been reported from Bransfield Strait, where recent volcanic activity causes heating and boiling of pore fluids in gas-charged sediments, expressed as sediment volcanism and seeps on the seafloor surface (Somoza et al., 2004). The reason for the absence of bottom and sub-bottom reflections below one pockmark might also be ascribed to the presence of gas that decreases the sound velocity and increases the attenuation which prevents penetration and results in an acoustic blanking. However, it can as well be attributed

to the raised rim that can scatter the acoustic energy and prevent reflection. Furthermore, it might appear that this is either a rather recent phenomenon or a continuous process, because otherwise an infilling of the pockmarks might have taken place. The definition and formation of the incised channel structures in the outer cove is difficult to reconstruct, since the shallow areas of Potter Cove were not surveyed and hence the bathymetric data only reveals small segments of probably much larger features. According to the topography of Potter Peninsula, the largest submarine channel structure most likely represents an extension of a meltwater stream system that drained the Warzawa Icefield and its proglacial lakes on Potter Peninsula. An erosional pathway is detected that starts near the largest proglacial lake on the 90 m high plateau on Potter Peninsula and is assumed to end as the submarine channel structure near the west coast. The origin of this channel might be ascribed to erosion processes such as gravity flows or subglacial meltwater drainage proximal to a former ice margin. Similar features in a much larger extent were identified by Dowdeswell and Vásquez (2013) from the seafloor of glacier-influenced fjords in Patagonia. They have been formed by turbidity currents either triggered by glacifluvial meltwater flow and the transport of coarser sediments from the river plain or through slope failures. Since the results of this study hold evidence for the existence of subglacial meltwater discharge and the occurrence of gravity flows, it is assumed that the channel was initially formed by these processes, either constantly or during flood events, where large amounts of meltwater were transported from the ice cap to the seafloor (Lowe and Anderson, 2003).

Four different acoustic facies types were classified according to the sub-bottom characteristics in Potter Cove and their spatial distribution illustrated (Fig. 2.5). The *chaotic facies* discovered in the inner cove is assumed to represent till deposits that have formed underneath or in direct vicinity of grounded ice. Seismic facies analysis in glacigenic sequences is usually difficult when till is present (Stewart and Stocker, 1990). Acoustic energy is scattered in a chaotic manner and the high acoustic impedance of till deposits typically limits transmission of sound energy. The thin reflection-free layer that is observed on top of the till deposits most likely represents a fine sediment drape (< 3 m) that settled out of meltwater plumes. A reason for the rather thin drape might be the geologically short period of time since the glacier retreated and exposed the seafloor in the inner cove. The thickness of this drape increases downfjord, most likely due to longer exposure time with increasing distance to the glacier front. However, export of suspended sediment out of the cove might also limit the accumulation. Characteristic for the rare *semi-parallel facies* near the southern coast in B_3 is the limited penetration depth similar to the till deposits, but also the occurrence of more subsurface reflections that may indicate a stacked deposition of sediments of different origin. This is most certainly owed to permanent or periodic sediment input via meltwater streams from the adjacent Potter Peninsula. Furthermore, it might also be related to a longer exposure time of B_3 compared to

basins B_{1-2} that made episodic sediment rainout from meltwater plumes visible in the sub-bottom profiles. The profiles recorded on the slope in the outer cove reveal the *hummocky facies*, indicating material or density changes with depth. It can be assumed that this facies results from deposition and stacking of sediment gravity flows that are likely to occur in this area. The *transitional facies* between chaotic and hummocky is observed in B_4, where till and stacked deposits occur side by side, indicating formation beneath grounded ice, but also deposition of resedimented material, such as debris flows or turbidites. The profiles recorded in areas close to the coastline, referred to as *marginal* are interpreted as exposed bedrock or rockfall deposits.

The low recovery of sediment core PS69/337-1 in Potter Cove can be ascribed to the bending of the coring device at approximately 2 m below the seafloor, what might indicate the presence of coarser or stiffer material underneath. Linear interpolation from the age of 320 cal yr BP at 1.2 m to the core top yields a sedimentation rate of 0.43 cm/yr, similar to the rates reported from the inner Potter Cove (Monien, pers.comm.). Majewski et al. (2012) investigated a sediment core from Maxwell Bay (NBP0703-JPC-15) that lies approximately 1.2 km downfjord from the core site of PS69/337-1 (Fig. 2.1). No age model was set up for NBP0703-JPC-15, but the core base yields an age of 805 cal yr BP that was also derived from foraminifera samples. Taking only this age into account, the sedimentation rate would have been 0.37 cm/year comparable to the one from this study. NBP0703-JPC-15 shows also only minor changes in sediment composition throughout the core, suggesting no significant change in deposition. The sediment characteristics found in PS96/337-1 from this study indicate predominately rain out from dispersed meltwater plumes derived from the terminus of the Fourcade Glacier. But also glaciofluvial meltwater input from the Warzawa Icefield through proglacial drainage on Potter Peninsula is assumed to be a potential source area. Furthermore, sediment gravity flows could have also reached the core site through the submarine channel structures. The similar grain size characteristics of PS69/337-1 from this study and NBP0703-JPC-15 are rather atypical for ice-proximal deposits, reflecting deposition at some distance from a glacier grounding line since ~ 320 cal yr BP for core site PS69/337-1 and since 805 cal yr BP for core site NBP0703-JPC-15. The existence of a floating ice tongue instead is conceivable. Therefore, it is carefully suggested that the Fourcade Glacier was situated somewhere behind the outermost terminal moraine (M_1) during the last 805 cal yr BP. That implies also that during the LIA (500-100 cal yr BP/1450-1850 AD, IPCC 2013), the Fourcade Glacier remained inside the inner cove.

Glacier Retreat:

During the LGM, the Fourcade Glacier in Potter Cove merged into the ice stream that occupied Maxwell Bay. The seafloor morphology in the cove provides information about the retreat behaviour of the glacier following the LGM. The maximum preserved position of the glacier front is delineated by the outermost moraine complex (M_4) that is located between the inner and outer cove. Its formation is assumed to have taken place during the last neoglacial period between 2.6 and 1.7 cal kyr BP and during subsequent initial retreat. Seafloor morphology in addition to climate forcing might have controlled the stability of the grounding line at this position. A renewed advance up to this point during the last ~ 800 cal yr BP/at least ~300 cal kyr BP is ruled out according to the findings from the sediment cores. In addition, no other major cooling period is recognised after 1.7 cal kyr BP, except for the LIA. However, increased ice rafting has been reported prior to 1.0, 0.85 and 0.14 cal kyr BP that indicates further smaller cooling events according to Milliken et al. (2009). As the glacier was situated at the location of M_4, subglacial debris piled up in front of the grounding line. Downslope transport of this material over time through turbidity or gravity flows is assumed to be one reason for the formation of pockmarks beside sediments delivered by the channel structures. Channel formation might have also initiated during this time, even though it cannot be ruled out that these structures were predesigned. After the Fourcade Glacier decoupled from M_4, further moraine complexes were formed in the inner cove due to short-term stillstands or potential readvances. In general, the retreat of the Fourcade Glacier is assumed to be associated with enhanced subglacial meltwater discharge that incised outlets into the moraine ridges. The highly fringed morphology of M_2 might indicate stacking of several moraines. One may speculate that these features are the result of glacial readvances that took place during the LIA, but this cannot be completely solved at this stage of analysis. M_1 seems to be the result of a prolonged stillstand of the Fourcade Glacier at this location sometime around the 1950s. Satellite images from 1956 evidence the position of the glacier front just behind this moraine complex. Reliable temperature records from the Antarctic Peninsula began only in the 1950s, but it is suggested that warming began earlier and therefore glacial retreat (Vaughan et al., 2001). As a consequence, the glacier front must have been situated beyond the location of M_1 before. It can be assumed that the ice limit never reached further eastwards into B_1 or that the glacier readvanced during a cooling event. An assignment of M_1 to the LIA is therefore not very likely. Behind M_1 in the youngest ice-free basin, fast glacial retreat took place within approximately 50 years.

2.4. Conclusions

Landforms and sub-bottom characteristics found in Potter Cove hold evidence of ancient and modern processes instrumental to reconstruct glacial dynamics during the Late Holocene and their impact on the cove environment. The inner and the outer cove represent two different settings regarding their formation, topography and environmental processes. Glacial deposits are not observed in the outer cove, whereas they are quite common in the inner cove, permitting assumptions about the retreat history of the Fourcade Glacier.

Moraine complexes, originating from glacial advances or glacial stillstands divide the inner cove into four different basins. The outermost moraine complex (M_4) is a relict of the neoglacial period between 2.6 and 1.7 cal kyr BP and represents the latest preserved maximum position of grounded ice in the cove. The subsequent retreat of the Fourcade Glacier was interrupted by several stillstands and readvances evidenced by further moraine complexes as well as small moraines. Around the 1950s, the glacier reached the location of the innermost and last moraine complex (M_1). Since then, the glacier uncovered the basin at the head of the cove (B_1) within only 50 years. Outlets within the moraine complexes were most likely formed by subglacial meltwater flow during or shortly after the deposition of the associated complex. The seafloor in the inner cove consists of till deposits covered with fine sediments that originate from deposition of meltwater plumes. Glacial lineations that were formed parallel to the ice flow underneath the advancing glacier are still visible under this thin drape at the head of the cove. Furthermore, an area is identified along the southern coast, reflecting an enhanced and probably periodic sediment input from meltwater streams on Potter Peninsula.
Turbulent sediment-laden meltwater discharge is also evidenced in the outer cove by channel structures. The largest feature most likely represents the submarine extension of an observed braided drainage system on Potter Peninsula. Irregularly distributed ice plough marks nearby on the upper slope are the result of grounded icebergs that enter the outer cove from Maxwell Bay. This process might as well destabilize the seafloor sediments and result in the initiation of gravity flows, besides sediment supply through the channel structures. The additional sediment load is assumed to release the escape of pore water that results in the formation of pockmarks downfjord. However, also venting of gas must be considered, since hydrothermal activity has been observed in Bransfield Strait.

3. DISTRIBUTION AND CHARACTERISTICS OF MARINE HABITATS IN POTTER COVE BASED ON HYDROACOUSTICS AND BED SHEAR STRESS ESTIMATES

During the last few decades, hydroacoustic devices have increasingly been used for detailed seafloor mapping applications (Hobbs, 1985; Magorrian et al., 1995; Kostylev et al., 2001), since they represent fast and low-budget alternatives to conventional mapping techniques such as grab sampling or direct observation by diving (Chivers et al., 1990). Numerous studies have demonstrated the capability of hydroacoustics to detect changes in seafloor habitats and benthic communities (McRea et al., 1999; Bartholomä, 2006; Jerosch et al., 2007; Ierodiaconou et al., 2011).

Several studies have provided crucial information regarding the ecosystem structure in Potter Cove (e.g. Sahade et al., 1998; Quartino et al., 2005; Schloss et al., 2012), whereas investigations including the spatial distribution of seafloor habitats and their characterisation are still needed. Benthic associations have been shown to be closely linked to oceanographic processes, e.g. bed shear stress (Warwick and Uncles, 1980), but direct measurements of waves and currents are also still missing in Potter Cove. General oceanographic processes have been reconstructed in the area on the basis of the regional wind field (e.g. Roese and Drabble, 1998). The availability of such data, however, is deemed important. In earlier years, the influence of these processes on marine environments was mostly determined by direct observations (e.g. Aller, 1989). More recently, hydrodynamic models have been applied to compute bed shear stresses that are found capable of altering the distribution of sediments and benthic organisms (e.g. Hemer, 2006).

Therefore, the objectives of this study are to delineate seafloor habitats in Potter Cove based on hydroacoustics and to define how environmental parameters control the habitat distribution in this particular environment. Due to the absence of wave and current measurements, field observations are combined with results from current and wave models, since the distribution of habitats is closely linked to current and wave exposure. Furthermore, the results are to be compared to former studies and a prospect is carefully given concerning the future development of the study area

representative for other coastal ecosystems that experience similar environmental pressures.

3.1. Methods

3.1.1. Acoustic ground discrimination

The RoxAnn GD-X device was equipped with a Furuno LS 4100 echo-sounder using an operational frequency of 200 kHz, a beam width with an opening angle of 10° and a depth range of 50 m. The system was set up according to the specifications provided by the manufacturer. Prior to actual surveys, RoxAnn was run for about 20 minutes to stabilize the system. Surveys were performed at a vessel speed of approximately four knots using a Zodiac Mk4 inflatable dinghy. Acoustic transect lines were run at 200 m intervals during calm and stable sea states in November 2011 (Fig. 3.1). The water depth in the study area varied between 1 and 55 m. Data recorded at water depths greater than 50 m, as well as blank and erroneous values caused by slow vessel speed, sharp movements, air bubbles, shoals or technical failures (Foster-Smith and Sotheran, 2003), were subsequently removed. Slope effects are assumed to be minor because of a mean slope of only 4°. This is being confirmed by the comparison of along-slope profiles (not shown in this thesis) and cross-slope profiles (as suggested by Hamilton et al., 1999), the two showing only minor differences at intersections.

3.1.2. Underwater video images

An underwater video survey for calibration purposes was performed at a vessel speed of approximately one knot using the same Zodiac Mk4 inflatable dinghy. A Kongsberg colour zoom camera (oe1366/67 Mk II) fitted with a miniature underwater lamp was used for real-time recordings of the seafloor. The resolution was set at 352 x 288 pixels. Time and GPS positions were tracked by a logging device and displayed on a monitor. Following the RoxAnn surveys, 29 short video profiles were obtained during slight sea conditions from the end of December 2011 until the end of January 2012 (Fig. 3.1). The profiles were evaluated for usable images, which were then assigned to several seafloor classes that have been defined by the observer.

3.1.3. Sediment samples

During the field campaign in the austral summer season of 2010/2011, 136 sampling stations were occupied using a small van Veen grab sampler from a Zodiac Mk3 inflatable dinghy (Fig. 3.1). At 121 of these, surficial sediments were successfully recovered. At the remaining 15 stations sediment recovery failure is assumed to have been due to either operational difficulties or the presence of boulders at the seabed. For calibration purposes, sampling stations located on or in direct proximity of the hydroacoustic survey lines were selected and grain size analyses performed. For a detailed description on the performance of the grain size analyses, see chapter 2.1.3.

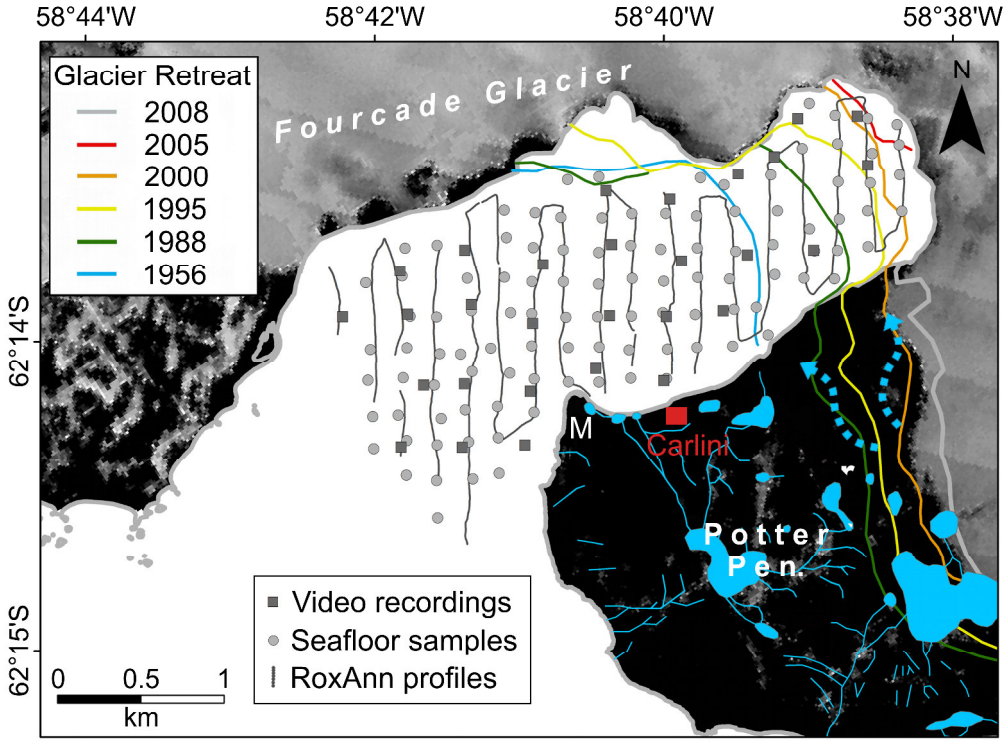

Fig. 3.1. Map of the study area showing the RoxAnn profiles and the positions of video recordings and seafloor samples. M = Mirounga Point. Landsat satellite image data are from the Antarctic Digital Database. Meltwater systems have been digitized from Kraus and del Valle (2008). Meltwater channels that developed after 2008 are indicated by dashed arrows (light blue). Coastline and glacier fronts from Rückamp et al. (2011).

3.1.4. Statistical analyses

In this chapter, a supervised method is used for seafloor classification, even though the use of an unsupervised classification method was recommended by

Schlagintweit (1993). Also Greenstreet et al. (1997; 2010) applied an unsupervised method by clustering false colour composite images (FCCI) that were based on the two RoxAnn parameters as well as on water depth. In the course of unsupervised classification algorithms, the classes are not selected by the analyst but by the analytical routine itself. The advantage is that the number of clusters as well as the boundaries between the clusters are chosen according to the data structure. Problems appear when there is no distinct clustering of the data, what can be caused by gradual changes between classes or the existence of transition zones. Furthermore, interpretation of the classes must take place subsequent to the analysis. In Potter Cove, gradual changes between different sea floor habitats occur and validation material is sparse, since only little seafloor information could be obtained, due to bad weather conditions during field campaigns. Limited knowledge about the nature of the seafloor also complicates interpretation of clusters. Furthermore, the geomorphology of the seafloor in Potter Cove (depth and slope changes) as well as the conditions during the survey (swell, different vessel speeds) are enhancing the susceptibility to errors of the second RoxAnn parameter. Therefore, a linear discriminant analysis, belonging to the supervised methods is used in this chapter for evaluating the RoxAnn data set (see chapter 1.3.2). This analysis distinguishes predefined groups on the basis of validated data. The advantage is that validation and therefore characterisation of the groups takes place before the analysis, so that there are no difficulties interpreting groups after the analysis, especially when lacking validation material.

For calibration purposes, the relationships between the hydroacoustic signals, the video classes and the grain size parameters were investigated. The evaluation of the video images resulted in the differentiation of several habitat classes, which were subsequently assigned to the nearest hydroacoustic data points. By plotting these points in a scatter diagram and displaying them according to their class assignment, it became apparent that two classes were clearly separated by the hydroacoustic signals and are therefore suitable for calibrating the hydroacoustic signals (Fig. 3.2A). To assess the relationship between the hydroacoustic data and the grain size parameters, Pearson's Correlation Coefficients between E1, E2, their ratio and several grain size parameters, including mean, mode and percentage sand, silt and clay were calculated. The coefficients show no strong correlation between the grain size parameters and the hydroacoustic variables. This is also visible in the scatter plots of mean grain size (in phi) against the hydroacoustic variables E1 and E2 (Fig. 3.2B, C). Therefore, the grain size parameters are not adequate to validate the RoxAnn data set in this approach. It is therefore assumed that the hydroacoustic device is either not able to detect small-scale changes in grain size or that other seafloor properties influence the hydroacoustic signal, e.g. that epibenthos present in the study area alters the acoustic signal and has consequently little informative value concerning sediment classes. Even though the sediment distribution in Potter Cove is

assumed to be more or less stable from one year to the next, small shifts in sediment composition may occur between seasons and thereby reduce the correlation between parameters.

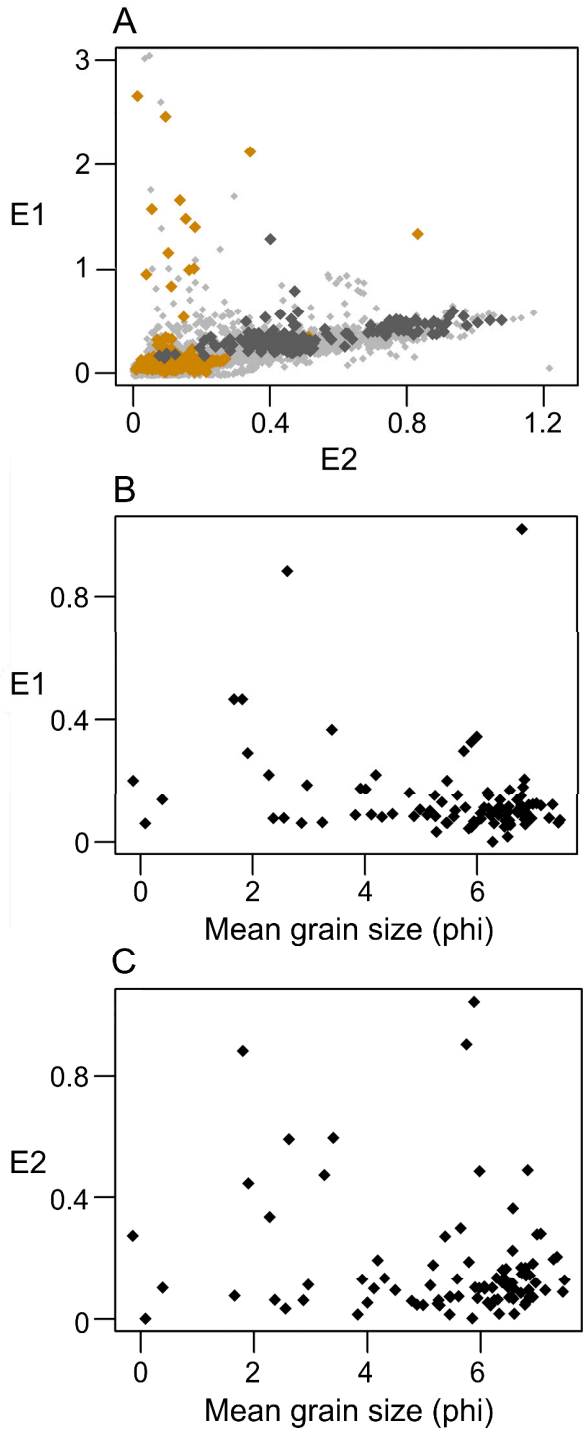

Fig. 3.2. A comparison between the hydroacoustic parameters with each other and with the mean grain size parameter (in phi units). A. Scatter plot showing the separation of the validated hydroacoustic data points into two classes (illustrated in yellow and dark grey) with non-validated measurements in the background (light grey). B. Scatter plot of mean grain size (in phi) versus E1. C. Scatter plot of mean grain size (in phi) versus E2.

Based on these findings, the video classes were used to validate the RoxAnn data set in order to perform the linear discriminant analysis. The performance of the analysis is illustrated in Figure 3.3. As a first step, a GIS was used to transform the hydroacoustic parameters E1 and E2 retrieved from the RoxAnn system as point information into two raster data sets. The interpolation method ordinary kriging with a grid cell size of 50 m was applied, in order to obtain a spatial habitat map of the study area after the analysis. Subsequently, a point layer was generated in the GIS, based on the positions of the evaluated video observations that holds the information of the associated video classes. For validation purposes, every single point from this layer was joined to the RoxAnn data that is found in a search radius of 50 m and the respective video class assigned to the hydroacoustic signals. The linear discriminant model was built on this validated RoxAnn data set and subsequently used to predict the class membership of the study area by the two RoxAnn raster data sets. The model was trained with a random subset containing 70 % of all validated RoxAnn positions. The predictive capability of the model was tested with the remaining 30 % of the data using 1,000 iterations and the mean calculated. The class assignment of the spatial hydroacoustic data through the linear discriminant model resulted in a gapless seafloor habitat map with a grid cell size of 50 m. Again, 1,000 iterations were used to obtain a probability map to evaluate spatial uncertainty and to point out zones of uncertain classification. Statistical analyses and illustrations were performed using the software R (version 2.15.1, package MASS; Venables and Ripley, 2002) and ArcGIS (version 10.0).

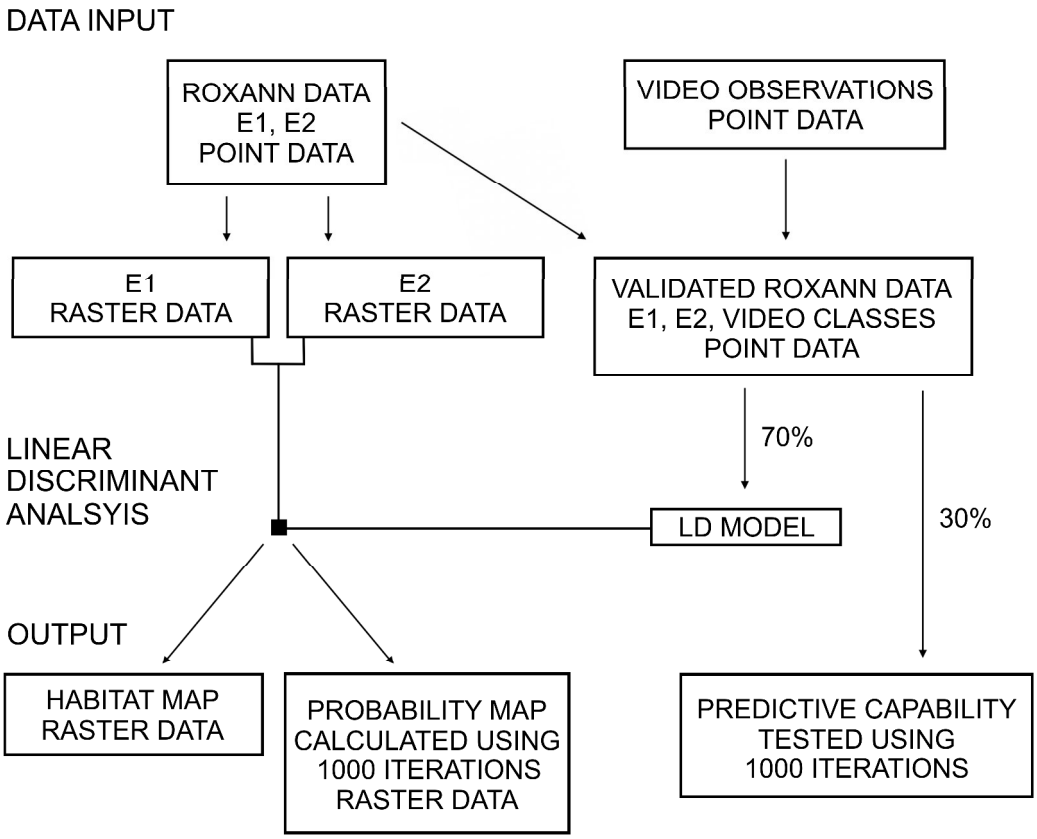

Fig. 3.3. Workflow diagram showing the performance of the linear discriminant analysis, including data input, data transformation and data output.

3.1.5 Numerical modelling

Results from current and wave models were used to estimate the skin friction bed shear stress distribution in Potter Cove. Lim (2014) used the finite volume coastal ocean model FVCOM-SWAVE (Chen et al., 2003; Qi et al., 2009) for the simulation of wave-current interactions to compute the current velocity close to the seafloor and to calculate the current skin friction bed shear stress. In addition, the two-dimensional structured-grid wave model SWAN (Booij et al., 1999, version 40.85) was applied to simulate wind-generated surface waves and to compute wave parameters such as significant wave height, peak wave period, wavelength and near-bed orbital velocity, from which the wave skin friction bed shear stress was calculated (Lim et al., 2013). The equations used to compute wind-generated waves represent all physical processes involved in wave growth by wind, nonlinear transfer of wave energy through triad and quadruplet wave-wave interactions, wave dissipation due to whitecapping, bottom friction and depth-induced wave breaking.

The total skin friction bed shear stress was taken as the sum of the magnitudes of the skin friction bed shear stress components of both current- and wave-induced bed shear stresses. Calculations were performed following Soulsby (1998) with a median grain diameter (d_{50}) set to 63 µm, which is the boundary between coarse- and fine-grained sediments.

The incipient motion of a sediment grain occurs when the forces exerted by the total skin friction bed shear stress acting on a grain exceed the submerged weight of the grain counteracting them (Soulsby, 1997). The sediment density in Potter Cove was set to 2,650 kg/m^3. The critical bed shear stress was calculated to be 0.13 N/m^2, i.e. the sediment grains begin to move when the calculated total skin friction bed shear stress reaches or exceeds this value.

3.2. Results

3.2.1. Bed shear stress estimates

Model results such as tide-, wind- and wave-driven current speed in the lowest water layer, wave orbital velocity near the seabed and wave parameters were extracted from the FVCOM-SWAVE and SWAN models for the total bed shear stress calculation (Lim, 2014). A comparison of bed shear stresses induced by currents and waves shows that the latter significantly exceeds the critical value in the northern part of Potter Cove, as well as in the western and southern coastal zones along Potter Peninsula, whereas current-induced bed shear stress is generally very low and only becomes more significant during rough sea conditions, especially in shallow water (Lim, 2014).

The terms ‘mild’, ‘moderate’ and ‘rough’ are used to describe the modelled sea states in Potter Cove. Significant wave heights near the mouth of the cove and in the inner cove are summarized in Table 3.1. The total skin friction bed shear stress calculations for the three different sea states provide a general picture of the areas where the critical bed shear stress value is reached (Fig. 3.4) (Lim, 2014). The colour denoting the upper bed shear stress limit represents areas where the bed shear stress is equal to or exceeds the critical value of 0.13 N/m^2. They are hereinafter referred to as erosion prone areas. The spatial variability of the bed shear stress shows a clear trend from higher values in shallow water to lower ones in deeper water. During mild sea states, where significant wave heights are typically below 0.5 m, areas with critical bed shear stresses are restricted to shallow water around the

western entrance of Potter Cove, along the northern coast of the inner cove, and along the western and southern coast of Potter Peninsula. As the sea state increases from mild through moderate to rough conditions, these areas expand towards greater water depths.

Tab. 3.1. Wave conditions during different sea states in the outer and inner cove.

Sea State	Significant wave height in the outer cove (m)	Significant wave height in the inner cove (m)
Mild	0.43	0.17
Moderate	0.87	0.33
Rough	1.69	0.71

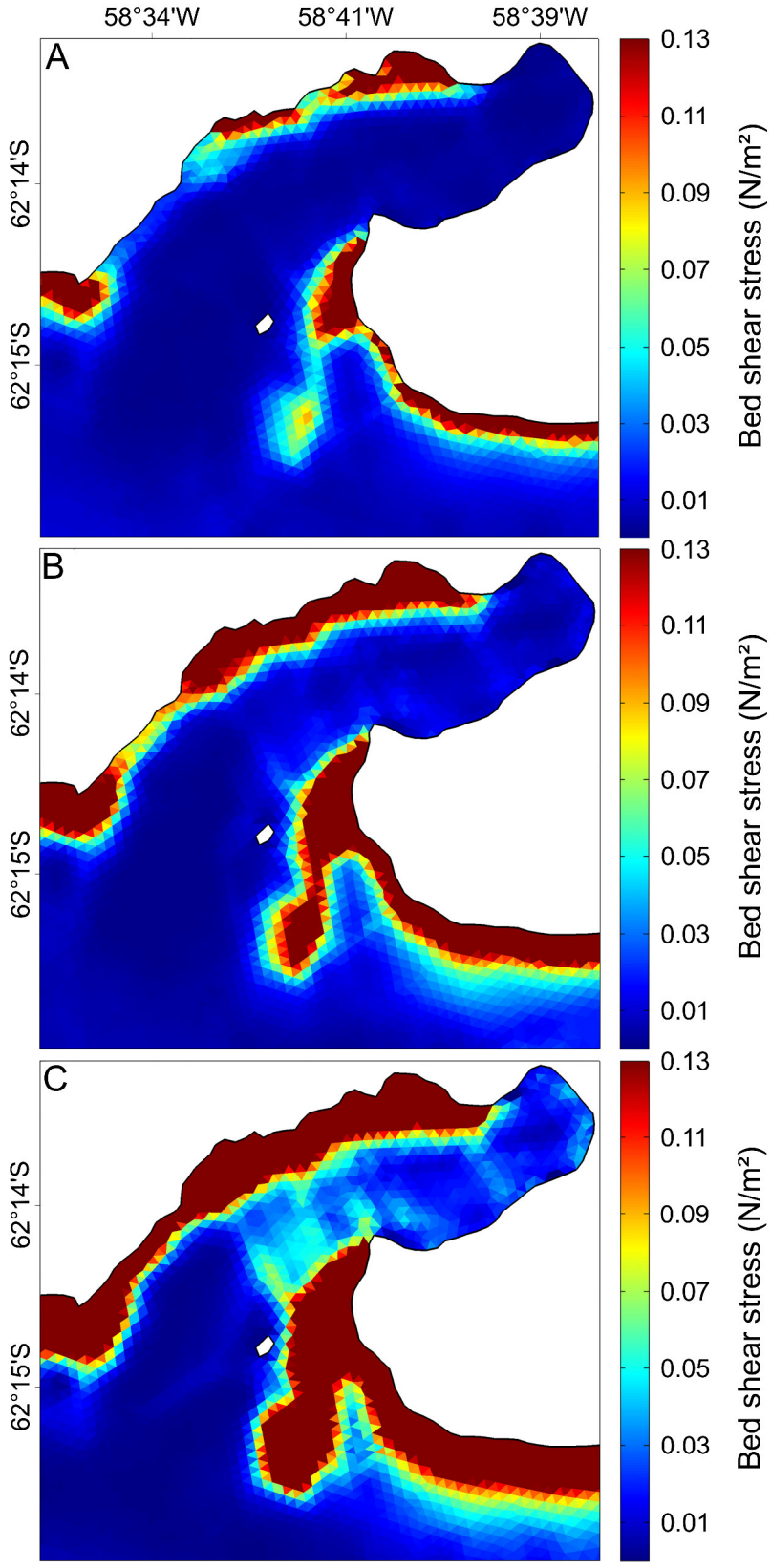

Fig. 3.4. Total skin friction bed shear stress. A. During mild sea state. B. During moderate sea state. C. During rough sea state (modified after Lim, 2014).

3.2.2. Validation of the acoustic data by underwater video images

The video evaluation resulted in the differentiation of two habitats i) soft-sediment habitats, and ii) stone habitats. The typical seafloor of the soft-sediment habitat consists of fine sediment with a scattered occurrence of echinodermata, ascidians and pennatulids (Fig. 3.5A). The stone habitat is characterised by the occurrence of stone and boulder fields with sporadic sediment sinks and various abundances of different macroalgae species such as *Himantothallus grandifolius*, *Desmarestia anceps* and *Desmarestia menziesii* (Fig. 3.5B).

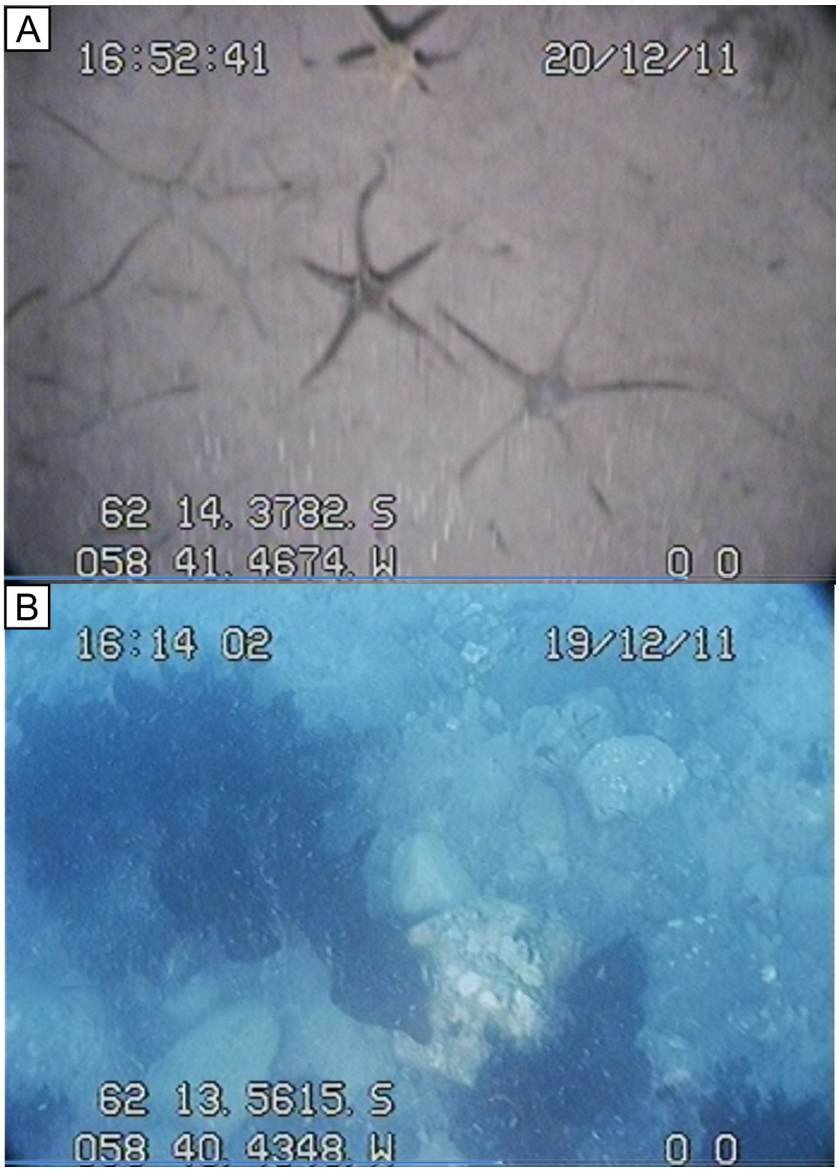

Fig. 3.5. Typical seabed environments as imaged during the video survey. A. Soft-sediment habitat recorded in 29 m water depth. B. Stone habitat recorded in 7 m water depth.

In toto, 4,671 hydroacoustic data points were assigned to either one of the two video classes, resulting in 3,134 points belonging to soft-sediment habitat and 1,537 points to stone habitats. A linear discriminant analysis was applied to the hydroacoustic data points that were validated by the video recordings and the model subsequently used to predict the class assignment of the unclassified hydroacoustic spatial data. Based on these results, a seafloor habitat map was compiled in which each pixel is assigned to one class (Fig. 3.6). The predictive capability of the model averages at 87 %.

The total area mapped in this way corresponds to approximately 4,500,000 m^2. Of this, 82 % belong to the soft-sediment habitat and 18 % to the stone habitat. The mean water depth in the former is about 28 m, in the latter 19 m. The zones representing critical bed shear stress values sum up to 7 % in the soft-sediment habitat and 60 % in the stone habitat.

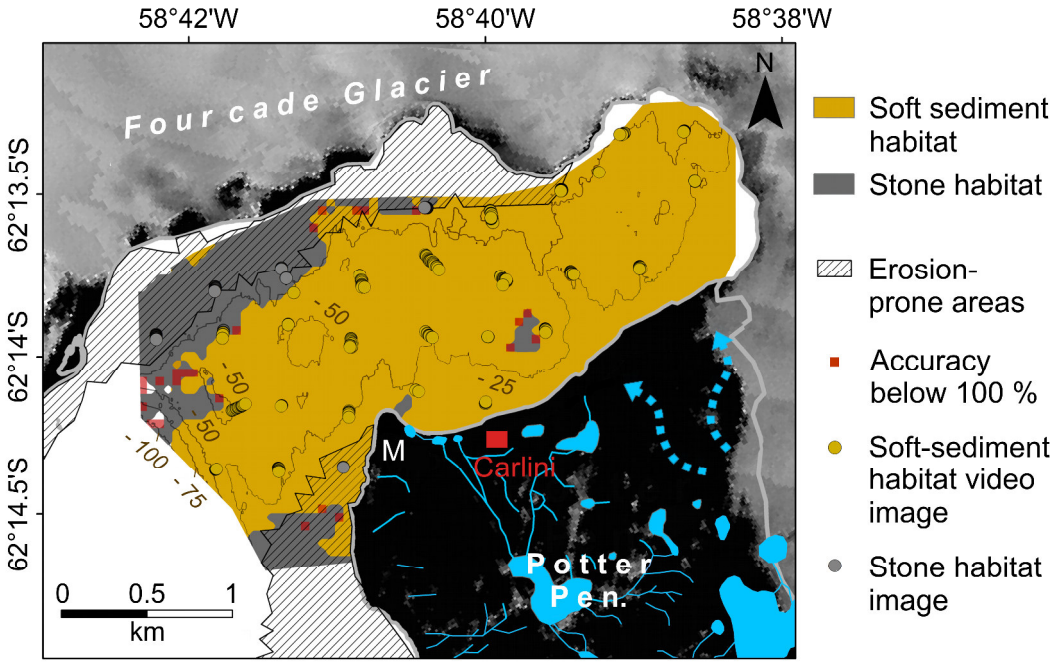

Fig. 3.6. Map of the study area showing the habitat distribution and erosion prone areas. Locations with classification accuracy below 100 % and results of the video evaluation are also shown. Contour lines refer to 25 m isobaths. M = Mirounga Point. Landsat satellite image data are from the Antarctic Digital Database. Meltwater systems have been digitized from Kraus and del Valle (2008). Meltwater channels that developed after 2008 are indicated by dashed arrows (light blue). The coastline has been extracted from Rückamp et al. (2011).

3.3. Discussion

In this chapter, a hydroacoustic data set was evaluated and validated by statistical means and underwater video images in order to distinguish different habitats in Potter Cove, King George Island. Interpretation of the data is mainly based on bed shear stress estimates due to the absence of wave and current measurements.

Combining the hydroacoustic data set with the video evaluation resulted in the differentiation of two major habitats in the study area, a soft-sediment and a stone habitat. The habitats are well separated by the hydroacoustic variables E1 and E2, which turned out to be applicable descriptors for their discrimination. The soft-sediment habitat is represented by low E1 and E2 values (0–0.2), indicating planar and soft substrata, whereas for the stone habitat class the corresponding values are higher, indicating rather hard and rough bottom conditions. Both are in agreement with the findings derived from the underwater video evaluation. Despite the distinct hydroacoustic separation between the two habitats, a common feature is the existence of transition zones between the identified classes (Lucieer and Lucieer, 2009). Furthermore, in the present approach, classification accuracies below 100 % were found at the boundaries between the habitats. As only one video recording detected the boundary between the two habitats in Potter Cove, it was not possible to define the transition zone as a separate class. This may have been achieved with a larger number of video recordings explicitly covering the transition zone. Consequently, predictions with lower accuracies may simply represent a transition zone between the detected habitats. It should also be taken into consideration that additional habitats may exist that were not detected by the acoustic ground discrimination system or the underwater video recordings. The broad scattering of hydroacoustic signals in the stone habitat suggests some variability in seafloor conditions, but it was not possible to identify any additional habitats.

The bed shear stress estimates have revealed areas prone to sediment erosion in Potter Cove. Waves generated by strong winds are typical for this region (Schloss and Ferreyra, 2002; Schloss et al., 2012) and have an enormous impact on the bed shear stress, especially in shallow water. This is in contrast to current-induced bed shear stresses which are much weaker (Lim et al., 2013). Lim (2014) also shows that the areas prone to sediment erosion expand into deeper water as sea states become rougher, such fluctuations being episodic rather than continuous in nature. This indicates the importance of considering oceanographic processes when characterising seafloor habitats, even if direct measurements are missing.

In the present chapter, model results were not only used to explain the spatial distribution of the two habitats, but also provided information about the conditions

during which habitat formation takes place. The estimated bed shear stress in the centre of the cove and near the eastern and southern coast of the inner cove is markedly lower than in the other areas, which is attributed to a decreasing influence of wave action on the seabed in deeper waters and smaller wave heights in the inner cove. In addition, the coast in the southern inner cove is partially sheltered by Mirounga Point (Fig. 3.6). According to the model results, the distribution of the stone habitat is in good agreement with areas shown to be prone to sediment erosion. Stony or hard bottoms are indicative of areas potentially subject to high bed sediment movement, any finer-grained sediment being evidently removed when bed shear stresses exceed critical values. Sedimentation rates are, in any case, expected to be rather low because the clear water masses entering the cove from Maxwell Bay do not carry substantial quantities of sediment with them (Roese and Drabble, 1998), and large meltwater streams are absent along the north coast of Potter Cove. The stones and boulders building up this habitat appear to have either been derived from the adjacent slopes over time or represent the remnants of moraines deposited by the Fourcade Glacier. The same applies to the stone habitat in the southern part of the cove, where bed shear stresses reach critical values along the entire coast.

The soft-sediment habitat occurs throughout the central and southern cove, where the availability of stones and boulders is limited, but large amounts of fine material are supplied by the Fourcade Glacier and meltwater streams. Here, low bed shear stresses associated with low wave action and small wave heights impair the movement of sediment. A similar habitat is found in the shallow waters at the head of the cove, where large amounts of fine sediment are deposited from sediment-laden surface plumes generated by glacial discharge and meltwater streams draining the Potter Peninsula. As before, low bed shear stresses in this part of the cove prevent sediment erosion. West of Mirounga Point, by contrast, a soft-sediment habitat occurs in an area prone to sediment erosion indicating higher energetic conditions.

The reason for the occurrence of two isolated stone habitat spots near the southern coast of the cove remains unclear, the locations being rather unfavourable for the formation of stone habitats. Due to their sheltered location and greater water depth, the areas exhibit low bed shear stresses. Low accuracy values might indicate an undetected habitat class or simply a misclassification due to erroneous hydroacoustic data points.

Quartino and Boraso de Zaixso (2008) reported the distribution of habitats above the 30 meter isobath in Potter Cove. The soft bottoms identified above the 30 m isobaths in their study are relatively congruent with the soft-sediment habitat and macroalgal assemblages on rocky substrate with the stone habitat. The only difference is that the macroalgal assemblages were not as extensive and did not extend as far to the northeast along the southern coast as the stone habitat identified in the present chapter. In an older study (Klöser et al., 1996) this limit is located even further to the

west than in the 2008 study, the investigation having been carried out by scuba diving from the waterline down to about 35 m. This could be an indication that erosion since 1996 has progressively exhumed a boulder field that was subsequently occupied by macroalgae.

Quartino et al. (2013) postulated that macroalgae assemblages would expand into the inner part of Potter Cove. The future development of these habitats, remains speculative, however, an expansion of the stone habitat into all erosion prone areas, and therefore also into the inner part of the cove, is assumed. At present, such a development is not yet evident in the northern and southeastern cove, even though the conditions seem favourable for the establishment of stone habitats. In the past, the Fourcade Glacier was located further downfjord, covering the area prone to erosion today. During glacier retreat, large amounts of fine material were released and deposited at the glacier front. It can therefore not be excluded that remnants of this material can still be found in the eastern erosion prone areas today, erosion having simply not been active long enough to remove all the fine material to expose the rocky bottom beneath. Alternatively, deposition may have outpaced erosion and/or the bed shear stress may have been different at that time. Clearly, these issues require further investigations.

With respect to future developments, potential changes in the wind field associated with global warming may affect the distribution of habitats in Potter Cove. Thus, a general poleward strengthening of south-westerly winds has been reported (e.g. Thompson and Solomon, 2002). Furthermore, Montes-Hugo et al. (2009) found an increase in wind intensity by up to 60 % along the Western Antarctic Peninsula since the 1970s, with monthly mean wind speeds up to 8 m/s. Stronger winds will probably extend the areas with higher bed shear stress into deeper waters, which would favour an expansion of the stone habitat. However, stronger winds can also modify the circulation systems in Potter Cove, especially the vertical circulation which is directly influenced by the wind field. Further consequences of global warming may also include an increased turbidity in the water column, as postulated by Schloss et al. (2002) which would affect the habitats and their benthic assemblages. Whichever the case, an expansion of the stone habitat, and therefore macroalgae coverage, would have a substantial impact on all those benthic communities that rely on macroalgal carbon production as a direct or indirect food source (e.g. Iken et al., 1998).

3.4. Conclusions

In this study, an up-to-date habitat distribution map of Potter Cove, defined on the basis of hydroacoustic data is presented. The controlling environmental processes are represented by estimates of bed shear stresses based on currents and waves as forcing agents. The critical bed shear stress for fine-grained sediment serves as criterion for potential bed erosion. It is shown that habitat formation is not continuous, but rather the result of storms that cause moderate to rough sea state conditions. Two major habitats have been identified, namely soft-sediment and stone habitats. The soft-sediment habitat is mainly composed of fine sediments with a scattered occurrence of a variety of marine benthic organisms. This habitat occupies the head of the cove, most of the southern cove and greater water depths in the central cove. The stone habitat exhibits stone and boulder fields that are partly covered by macroalgae. These are interrupted by occasional fine sediment deposits. This habitat principally occurs at shallow water depths in the northwest and southeast of Potter Cove, distinctly correlating with areas prone to sediment erosion. It is located near slopes and bedrock outcrops, and remote from fine sediment sources. Under the recent environmental conditions, an eastward advance of the stone habitat following the retreating glacier front is postulated. This implies an exposure of suitable substrates for macroalgal colonization with long-term effects on the biomass and species composition in the cove. It is expected that these findings can be applied to other polar coastal ecosystems similarly affected by climate warming and associated glacier retreat.

4. EVALUATION OF SEAFLOOR CHARACTERISTICS AND FUZZY CLUSTERING OF THE MARINE ENVIRONMENT IN POTTER COVE

Seafloor characteristics can provide information about marine systems, including the origin of sediments, oceanographic processes and depositional regimes. Seafloor classification techniques have recently gained more and more importance, as they summarize spatial variations in seafloor characteristics and enable a rapid and comprising characterisation of marine environments for a wide variety of applications.

The aim of this chapter is to assess the spatial distribution of sediment characteristics in Potter Cove and to link them to environmental processes of deposition. Therefore, depositional trends are revealed by the grain size distribution of short sediment cores obtained from the central Potter Cove. In addition, a fuzzy cluster algorithm is applied in order to classify the study area into marine deposition zones. The results include a map showing the distribution of marine deposition zones as well as a confusion map, illustrating the classification accuracy. Since clustering belongs to the unsupervised classification methods, the zones are interpreted subsequent to the analysis by evaluating the variable distributions.

4.1. Methods

4.1.1. Seafloor variables and sediment cores

Different types of analyses were performed on 97 sediment samples that have been recovered from the seafloor surface in Potter Cove (Fig. 4.1; for details on the sampling procedure, see chapter 3.1.3.). The results are used to designate marine

deposition zones in the soft-sediment habitat. Since only occasional sediment patches occur in the stone habitat, these areas do not represent the overall picture (see chapter 3).

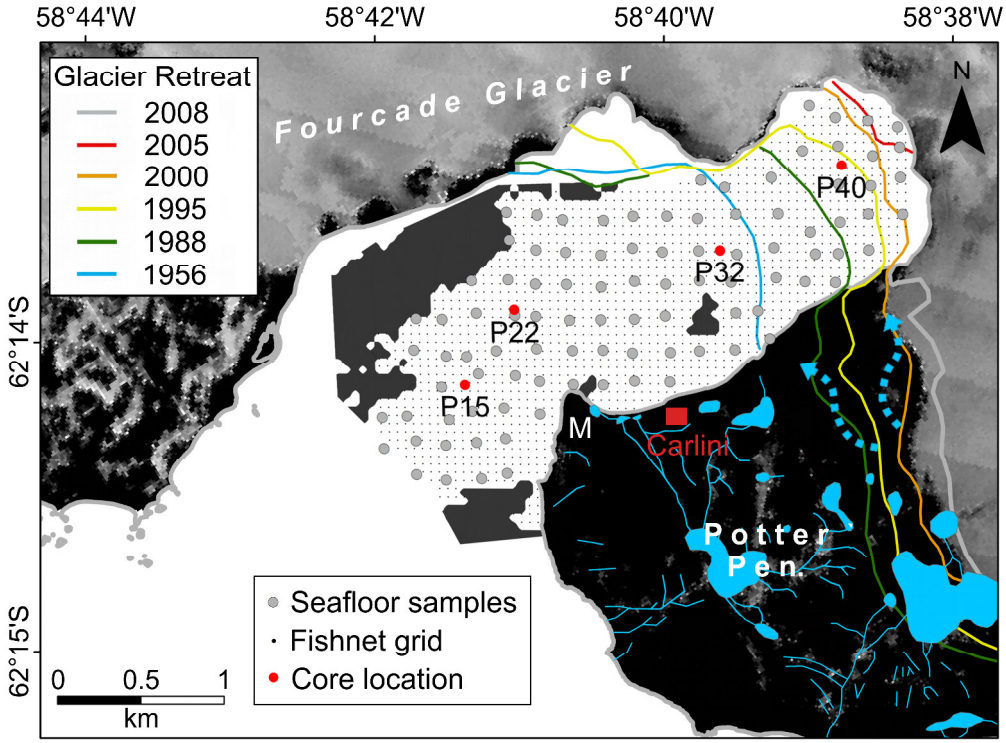

Fig. 4.1. Map of the study area showing positions of seafloor samples and sediment cores as well as a fishnet grid of rectangular cells. The grey area represents the stone habitat. M = Mirounga Point. Landsat satellite image data are from the Antarctic Digital Database. Meltwater systems have been digitized from Kraus and del Valle (2008). Meltwater channels that developed after 2008 are indicated by dashed arrows (light blue). Coastline and glacier fronts from Rückamp et al. (2011).

In addition, four sediment cores arranged in a transect line and located in the deeper basins have been recovered in Potter Cove during the austral summer season of 2009/2010 (Fig. 4.1, Tab. 4.1). A modified UWITEC gravity corer system with 60 cm clear PVC tubes (5.5 cm diameter) was used. Immediately after recovery, the cores were sampled at 1-cm intervals before they were directly lyophilised on-site for transportation purposes.

Grain size analyses were performed on the four sediment cores as well as on the samples from the seafloor surface (0-1 cm) to gain information about deposition trends. Furthermore, the total organic carbon content was determined for the seafloor surface samples (0-2 cm). For a detailed description of the analytical procedures, see

chapter 2.1.3. Analyses were performed at the Alfred Wegener Institute Helmholtz Centre for Polar and Marine Research in List/Sylt and Bremerhaven, Germany.

Tab. 4.1. Sediment core location in the soft-sediment habitat and core length.

Core	Latitude	Longitude	Water depth (mbsl)	Core length (cm)
P15	62°14.16‘S	58°41.496‘W	46	23
P22	62°13.927‘S	58°41.114‘W	48	18
P32	62°13.746‘S	58°39.641‘W	32	35
P40	62°13.484‘S	58°38.771‘W	50	40

4.1.2. Classification procedure

A fuzzy cluster analysis was applied to classify the soft-sediment habitat into marine deposition zones (see chapter 1.3.2). Three sediment variables and one geomorphic variable have been selected as input for the classification procedure, including mean grain size, mud content, organic carbon content and bathymetry (provided by G. Tosonotto, Instituto Antártico Argentino, Buenos Aires, Argentina). The single-beam bathymetric data set was chosen, since it covers also the shallow areas in Potter Cove. Artificial differences in water depth due to merging of two different data sets (in this case the single-beam and the multibeam data set) can have a negative impact on the clustering result. The software ArcGIS (10.0, ESRI) was used to transform the obtained point data into spatial information and to prepare the variables for the classification procedure (Fig. 4.2). The first step was to convert the four point data sets into four raster data sets using the geostatistical ordinary kriging interpolation method. The spatial resolution of the raster data was set to 50 m x 50 m. In order to transform the spatial variable information into vectors for the classification algorithm, a so-called fishnet of rectangular cells with the same resolution was clipped to the study area and transformed into a point data set (Fig. 4.1). The information of every variable was subsequently assigned to its associated fishnet point and transformed into variable vectors, as a requirement for the fuzzy cluster analysis calculation. The output of the analysis, i.e. the classification and the confusion index in vector format,

were subsequently assigned to the original fishnet point data set that was transformed back into raster data.

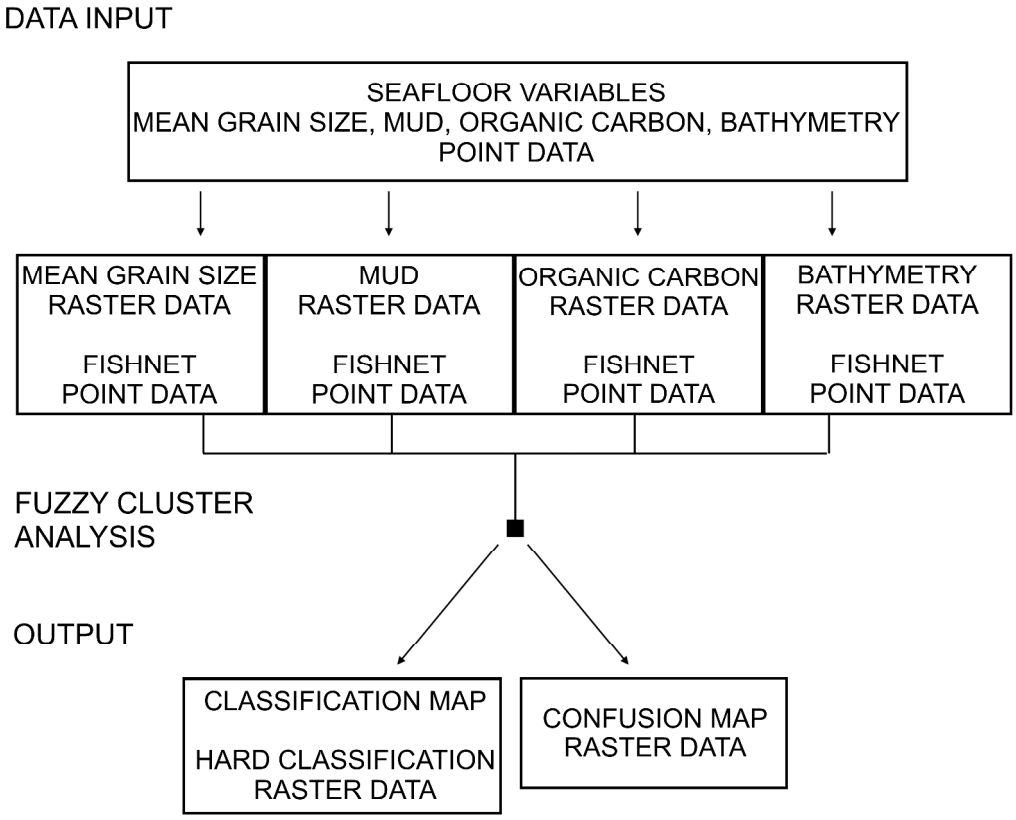

Fig. 4.2. Workflow diagram showing the performance of the fuzzy cluster analysis, including data input, data transformation and data output.

Before performing the fuzzy cluster algorithm, Pearson's Correlation Coefficients between the variables were calculated and evaluated, since correlating variables would negatively influence the clustering result. The results reveal no strong correlations between the variables, thus all variables were valid to be integrated into the analysis. A linear stretch algorithm was applied on the data, to achieve the same extent (0-1000) for all variables and, therefore, ensure that they are equally weighted. The XB index was calculated as a cluster validity measure to determine the optimal amount of clusters in the data set (Xie and Beni, 1991). The fuzzy exponent, determining the overlap at cluster boundaries was set to a value of 2, which is commonly used (Burrough and MacDonnell, 1998). All computations were performed using the software R (version 2.15.1, package e1071).

4.2. Results

4.2.1. Seafloor variables

The mean grain size distribution ranges from fine silt to coarse sand within the soft-sediment habitat in Potter Cove (Fig. 4.3A). The coarsest sediments occur close to the meltwater outlets that are located on Potter Peninsula. A small area near the recent glacier front reveals the smallest sediment fractions. Generally, a coarsening trend is recognised downfjord and towards the stone habitat.

Mud contents are found between 3 and 100 vol.% (Fig. 4.3B). High mud contents are mainly deposited below the 25 m isobath in the central basins of the cove. Further, high contents occur close to the recent glacier front, including the area, where the smallest mean grain sizes are found. Contents gradually decrease towards the rim of the cove and towards Maxwell Bay. Lowest contents are found near the outlet of the meltwater streams and south of Mirounga Point in accordance with the grain size variable.

Organic carbon contents lie within the range of 0.05 to 0.52 wt.%. The lowest contents occur near the glacier terminus and near the meltwater outlets (Fig. 4.3C). The central deeper parts further downfjord reveal the highest contents in the study area. Towards the rim and towards the entrance of Maxwell Bay, the amount of organic carbon gradually decreases again. Higher contents along the coastline are only found close to the scientific station and on the opposite side of the cove.

The seafloor in the soft-sediment habitat extends to water depths of about 50 mbsl (Fig. 4.3D). Ridges and remnants of ridges pervade through the inner part of the cove. Bathymetric depressions of varying extent are found in the central part of Potter Cove. The shallow areas nearshore are moderately inclining towards those central depressions.

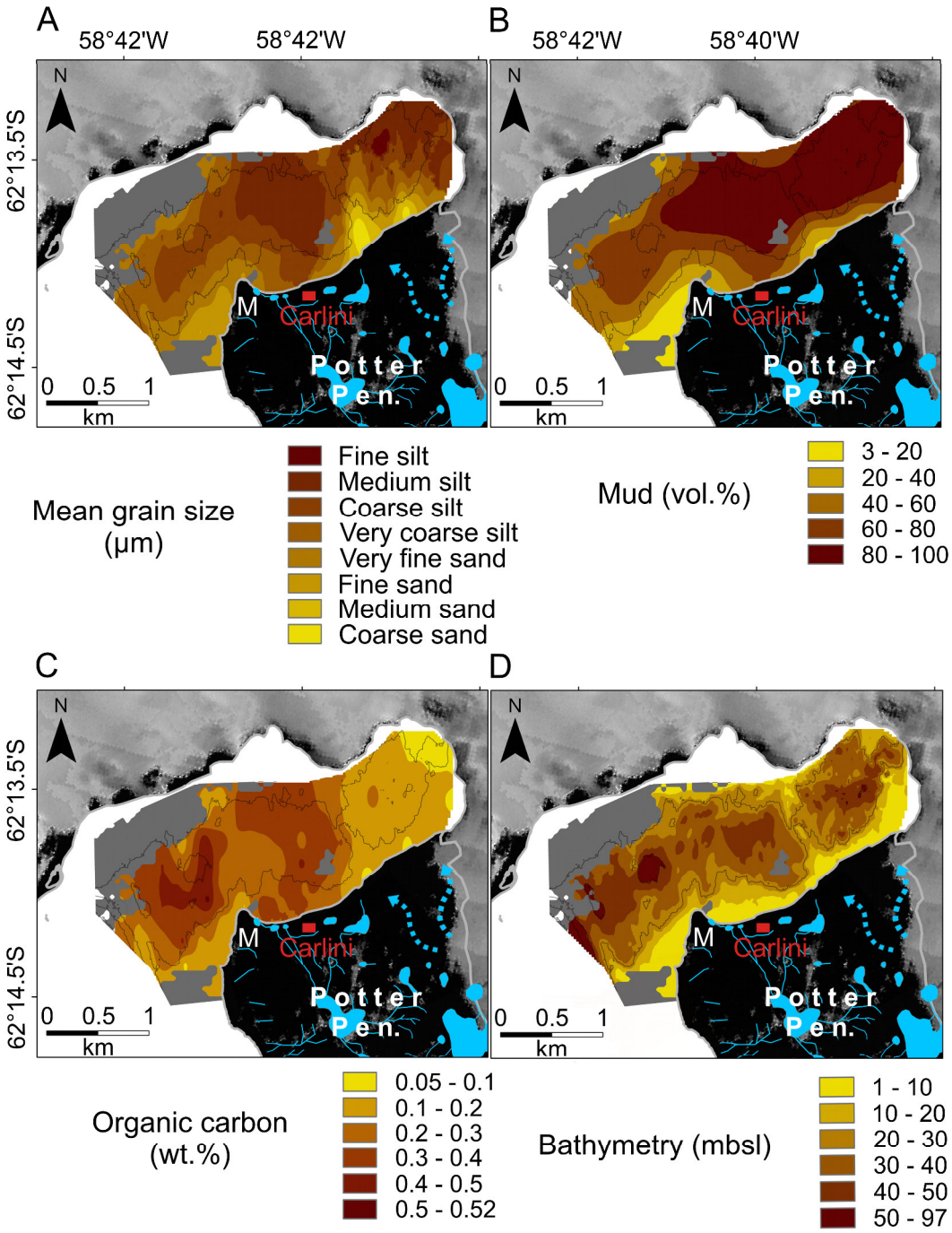

Fig. 4.3. Maps showing the spatial distributions of selected seafloor variables. A. Mean grain size, B. Mud, C. Organic carbon, D. Bathymetry. Contour lines are illustrated in 25 m intervals. The grey area represents the stone habitat. M = Mirounga Point. Landsat satellite image data are from the Antarctic Digital Database. Meltwater systems have been digitized from Kraus and del Valle (2008). Meltwater channels that developed after 2008 are indicated by dashed arrows (light blue). The coastline has been extracted from Rückamp et al. (2011).

4.2.2. Sediment cores

The four sediment cores presented in this chapter are located in a transect that runs through the central cove remote from wave and current activity. Generally, the mean grain size values in the upper part of the cores resemble the values from the surface samples that were taken independently in close vicinity to the core locations. The distributions of sand, silt and clay reveal moderate variabilities throughout the record (Fig. 4.4). Silt and sand percentages are characterised by a higher variability than the clay percentage that is rather stable throughout the record. The silt values of all cores average 72 vol.%, which makes silt the dominating grain size fraction.

The grain size distribution of the outermost core P15 in 46 mbsl is rather variable, with an increase of silt associated with a decrease of sand in the very uppermost part of the core (Fig. 4.4A). Core P22 in 48 mbsl shows a similar grain size distribution just as core P15, but with lower variations over time (Fig. 4.4B). The record of core P32 in 32 mbsl reveals highly variable sand and silt fractions in the lower part of the core. More constant conditions are found in the upper part instead, where the sand fraction drops down to a minimum, while the clay and silt fraction increases (Fig. 4.4C). The front of the Fourcade Glacier was located behind this core location sometime around 1956. The grain size distribution of core P40 in 50 mbsl at the head of the cove resembles the one from core P32, but shows a more gradual increase of silt and clay parallel to a decrease of sand towards the core top (Fig. 4.4D). Here, the core station was located at the glacier front around 1995.

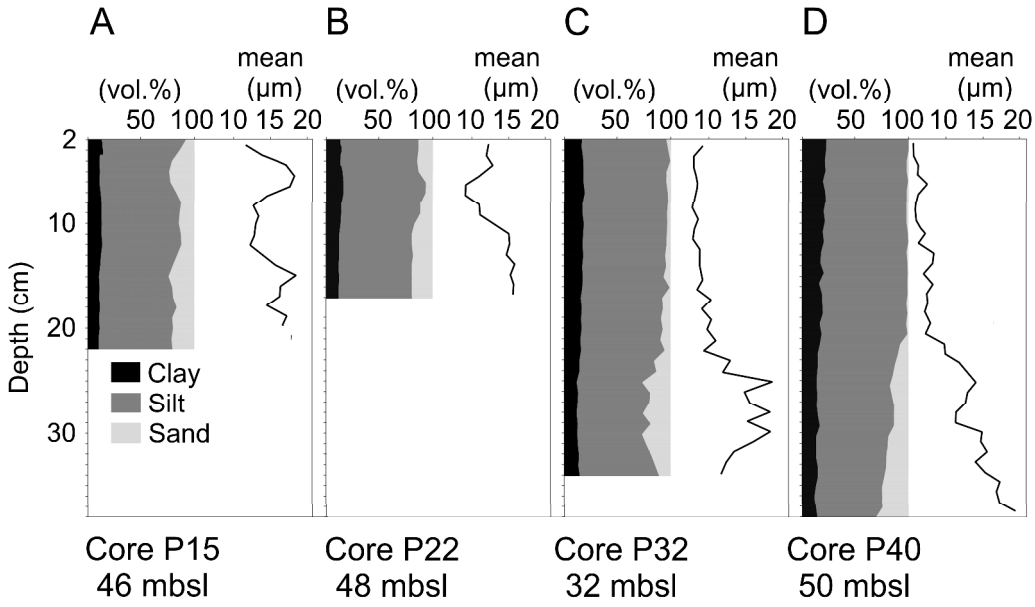

Fig. 4.4. Grain size distributions (clay-silt-sand, mean) of sediment core transect are shown. A. Core P15. B. Core P22. C. Core P32 and D. Core P40.

4.2.3. The hard classification

This subchapter presents the results of a fuzzy cluster approach that classified the four-dimensional seafloor feature space into groups according to their compactness and separation. The XB index was applied on all fuzzy cluster results between 2 and 10-cluster solutions. The results indicate that an optimal separation is achieved with 4 clusters. The map resulting from the fuzzy cluster analysis is presented in Figure 4.5A. The hard classification was achieved by assigning the cluster with the highest membership value to each raster cell. The confusion index as a measure of uncertainty in class attribution for each raster cell is shown in Figure 4.5B. Since fuzzy clustering belongs to the unsupervised classification procedures, identification of the resulting marine deposition zones was performed subsequent to the analysis. Therefore, the individual zones were characterised using boxplots (Fig. 4.6) and statistical values, such as the median (Tab. 4.2).

The first marine deposition zone (MZ_1) is mainly located in the centre of Potter Cove, except from the innermost part close to the glacier terminus (Fig. 4.5A). The distribution of the mean grain size variable reveals a median in the coarse silt fraction with compact quartiles, reflecting low variation in the data (Fig. 4.6A). Mud contents are rather high in this zone (Fig. 4.6B). The associated boxplot yields a moderate distribution range that indicates some variation of the data, but still shows a reasonable separation from the 2nd and 3rd zone. Characteristic for this zone are the highest organic carbon contents as well as the greatest water depths in the study area (Fig. 4.6C, D). The organic carbon boxplot shows also a moderate range, but a better separation from the other zones compared to the mud variable. The bathymetric distribution reveals a large range and therefore an insufficient separation against the other zones.

MZ_2 frames MZ_1 towards the north, the south and towards Maxwell Bay (Fig. 4.5A). Furthermore, MZ_2 flanks the stone habitat in the north of the cove as well as MZ_3 and parts of the shore near the scientific station in the south. The median of the mean grain size distribution in MZ_2 lies in the very coarse silt fraction (Fig. 4.6A). The variable distribution reveals slightly coarser material compared to MZ_1, also accompanied by a small range that indicates reasonable class partitioning. Mud contents are lower compared to MZ_1 (Fig. 4.6B). The moderate distribution range hardly overlaps with the other zones. Organic carbon contents are intermediate with a rather large range, reflecting higher variation in the data (Fig. 4.6C). The separation from the other zones is reasonable. The bathymetry in MZ_2 shows as in MZ_1 a large range that displays almost the full extent of variation of this variable, indicating that it did not significantly contribute to the delineation of this zone compared to the other variables (Fig. 4.6D).

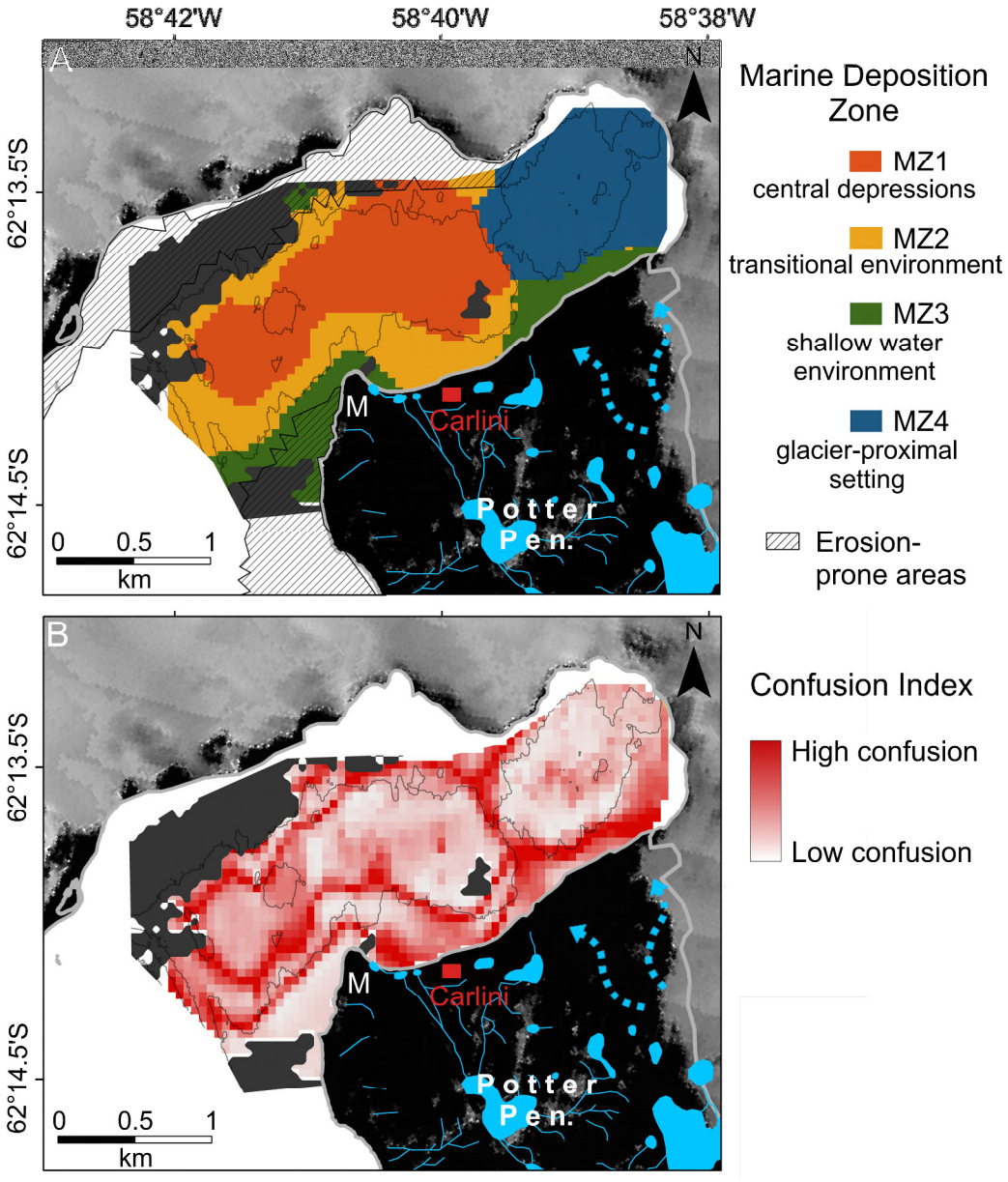

Fig. 4.5. Results of the fuzzy cluster analysis. A. Marine zonation and erosion prone areas are illustrated. B. Confusion about class attribution. The grey area represents the stone habitat. M = Mirounga Point. Contour lines in 25 m intervals. Landsat satellite image data are from the Antarctic Digital Database. Meltwater systems have been digitized from Kraus and del Valle (2008). Meltwater channels that developed after 2008 are indicated by dashed arrows (light blue). The coastline has been extracted from Rückamp et al. (2011).

The southern rim of Potter Cove is partly occupied by MZ_3 (Fig. 4.5A). This zone borders MZ_2 and the stone habitat as well as MZ_4 in the innermost part of the cove. In addition, a small isolated patch occurs in the north of the cove, partly framed by the stone habitat. The mean grain size variable reveals the coarsest sediments found in the study area with the median corresponding to fine sand (Fig. 4.6A). The associated boxplot covers almost the full data range, but the separation from the other zones is still reasonable. The 3rd and 4th quartile are larger than the other quartiles, indicating a higher variety in the coarser grain size fractions. The boxplot of the mud variable reveals the lowest values with large variation, but is still well separated from the other zones and has also a significant impact on the partitioning of this zone (Fig. 4.6B). The organic carbon variable shows low values with a small range (Fig. 4.6C). Also characteristic for MZ_3 are low water depths with a much smaller distribution range compared to the other zones (Fig. 4.6D). The associated boxplot shows compactness and a distinct separation from the other zones. The bathymetric variable provides evidence that this zone is rather found in shallow waters, even though the 1st quartile is relatively large, reflecting observations in greater water depth.

MZ_4 covers the innermost part of the cove close to the recent glacier front (Fig. 4.5A). In this zone occur the smallest mean grain sizes in the study area (Fig. 4.6A). The variable distribution reveals a compact range with the median in the coarse silt fraction similar to MZ_1. The mud content is considerably higher with low variations (Fig. 4.6B). Contents up to 100 vol.% are found in this zone. The amount of organic matter is low (Fig. 4.6C). The associated compact boxplot resembles the distribution of MZ_3, but is well separated from the first two zones. This variable significantly contributes to the separation of this zone from MZ_1. Characteristic for this zone are intermediate water depths with large variations (Fig. 4.6D).

The confusion index that assesses the classification accuracy is in some places very low, especially in the first and the fourth marine deposition zone (Fig. 4.5B). Higher indices are found along all transition zones between the zones.

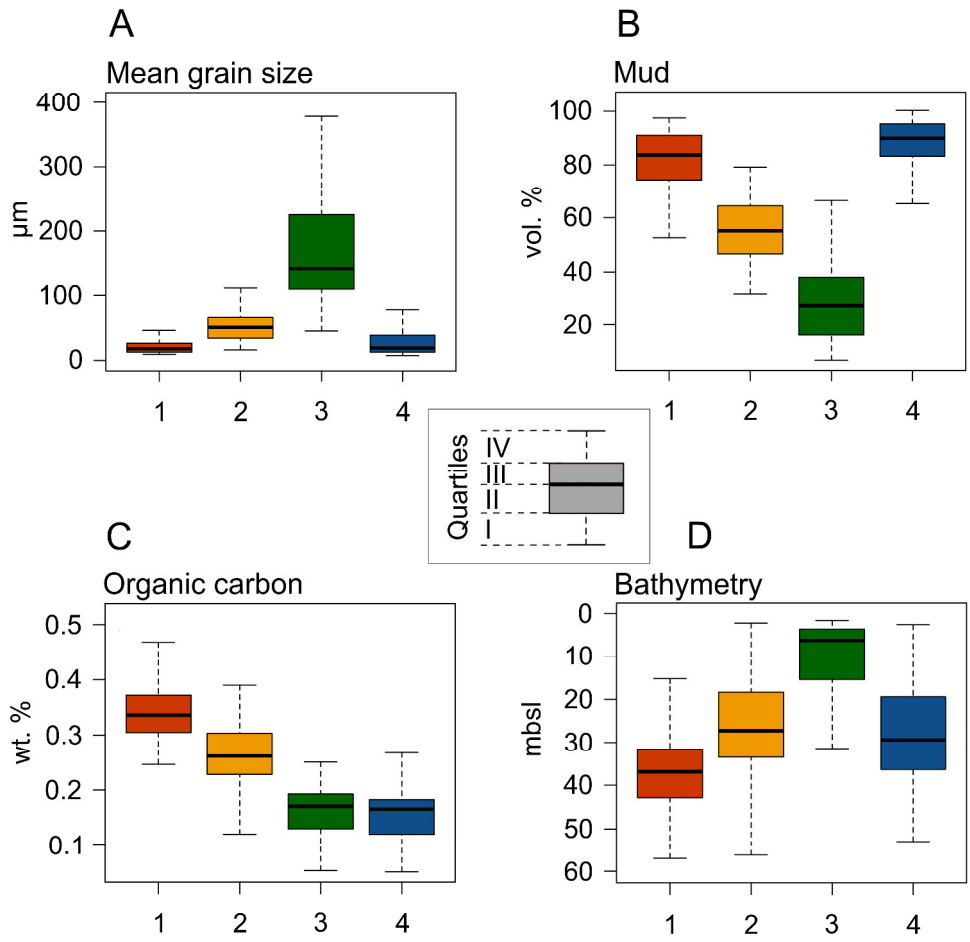

Fig. 4.6. Box-and-Whisker plots of marine deposition zones against seafloor variables. A. Mean grain size, B. Mud, C. Organic carbon, D. Bathymetry. Outliers have been removed for illustration purposes. The box can be divided into four quartiles. All four quartiles are referred to as range. The black bar represents the median.

Tab. 4.2. Median for each variable in every marine deposition zone.

	MZ_1	MZ_2	MZ_3	MZ_4
Mean grain size (µm)	17.9	50.8	143	18.9
Mud (vol.%)	83.7	55.1	27	90.8
Organic carbon (wt.%)	0.336	0.261	0.171	0.166
Bathymetry (mbsl)	-37	-27.2	-6.2	-29.4

4.3. Discussion

Seafloor variables and sediment records

Large amounts of terrigenous sediments reach the bays and fjords of the South Shetland Islands during summer months (Yoon et al., 1992). Griffith and Anderson (1989) suggested that they are mainly of glacial origin and distributed by surface meltwater plumes. Seafloor sediment distribution in the soft-sediment habitat in Potter Cove is assumed to be related to prevailing oceanographic conditions as well as to the location of sediment sources on land. Sediments are derived from the Fourcade Glacier and associated meltwater streams that are located on Potter Peninsula (Fig. 4.1). Silty sediments are deposited in low energy environments that are found at the head of the cove and in the central depressions, as illustrated by the bed shear stress results showing low or even no erosion at these locations (see chapter 3). Coarser sediments instead occur close to or within areas that are prone to sediment erosion, the transition being associated with a gradual increase in bed shear stress. Furthermore, sandy sediments are found along the southern cove that does not belong to the erosion prone areas. One reason for the occurrence of coarser sediments in areas dislocated from erosion prone areas might be the enhancement of bed shear stresses due to meltwater discharge. Since incoming streams were not included as a parameter for designating the erosion prone areas, this assumption remains speculative and cannot be completely resolved at this stage. Generally speaking, the sediments actually grade from fine silt near the head of the cove to very coarse silt at the cove mouth, which is attributed to an increase in energy conditions from the protected location at the head of the cove to the more exposed environment approaching Maxwell Bay as well as the increasing distance to the fine sediment sources. This trend stands in contrast to the study from Domack and Ishman (1993), where they found a gradual decrease of the sand content associated with an increase of the finer fractions downfjord.

The sediment cores P32 and P40 show a fining-upwards trend that is expressed by increasing mud contents and decreasing sand contents. The two outer cores in contrast (core location P15 and P22) show slightly varying, but generally stable conditions over time. In this type of environment, it is assumed that coarser material is derived by turbid subglacial meltwater from the grounding line of the glacier, since bottom currents that transport coarser grains into the system would have also winnowed the fine fractions. The presence of turbid subglacial meltwater in the ice-proximal zone has also been observed in Marian Cove, another tributary inlet to Maxwell Bay next to Potter Cove (Yoon et al., 1997). After the core locations got exposed by the retreating glacier during deglaciation, the distances to the glacier front have increased with time, while the influence of turbid meltwater has ceased

and therefore the availability of coarse material. No specific trend is recognised in the two outer cores, but the records show moderate variations of the sediment fractions, indicating recurring conditions within a certain range. This might be a result from a rather stable environment, due to the larger distance to the Fourcade Glacier and the associated meltwater streams. Variations can most likely be attributed to changing oceanographic conditions related to the proximity to Maxwell Bay. The two inner cores in contrast show high variations of the silt and sand fraction in the lower part of the core, most likely reflecting a time when the core sites were directly affected by turbid meltwater discharge along the grounding line of the glacier that was situated close to the core locations around 1956 (core location P32) and around 1995 (core location P40). It appears that the sudden changes in P32 can be ascribed to the immediate proximity to a former subglacial meltwater outlet near the grounding line. Furthermore, a clear fining upwards trend is recognised in both cores that is reflected in the increase of mud and the decrease of sand, respectively. A sediment core from the similar environment Marian Cove, King George Island also reveals a fining upwards trend that was interpreted as an indication of decreasing glacial influence (Yoon et al. 1997). However, the upper parts of the two cores show a distinct change in the records. The sand fraction drops down to a minimum and indicates a clear change concerning sediment delivery, which might not be explained by a retreating groundling line alone. In many places, the Fourcade Glacier is nowadays located at the land-sea interface which results in a shrinking extent of the tidewater front and therefore a reduced amount of potential turbid submarine meltwater outlets. As a result, a low energy environment establishes. According to this, the decrease of the sand fraction might not only be an indication of decreasing meltwater discharge events respectively increasing distance to the groundling line, but might also be ascribed to the closure of transport ways for submarine and subglacial meltwater input. Consequently, coarser material found in Potter Cove mainly originates from submarine meltwater delivery and to a lesser extent from icebergs and seasonal ice. This would be also in conjunction with the complete absence of coarse material at the seafloor near the recent glacier front and would furthermore explain the coarsening trend that is found downfjord.

Important contributors to the organic carbon content in marine sediments include macroalgae forests that occur in Potter Cove (Fischer and Wiencke, 1992; Iken et al., 1998). Phytoplankton production can also play a major role, but was found to be rather low in the study area (Schloss et al., 1997). Generally, organic matter might be derived from meltwater streams that are fed by melted glacial ice. Glaciers can receive particles through wind and snowfall or through inclusion of underlying sediments (Downes et al., 1986). Abele et al. (1999) report organic carbon input from wastewater discharge from the adjacent scientific station. Based on these findings, it can be assumed that organic carbon in the seafloor sediments from Potter Cove might reflect macroalgae growth, meltwater input and wastewater outflows, but to a

lesser degree phytoplankton productivity fluctuations. Therefore, interpretations will be made on the basis of the macroalgae distribution, the location of the meltwater outlets and the scientific station. Also other factors such as water circulation and energy zonation will be taken into consideration. The macroalgae forests are located nearshore in areas prone to sediment erosion. It can be assumed that organic carbon is derived from these assemblages, even though they occur nearshore in shallower water depths and not in the central, deeper part of the cove, where high contents occur. This can be explained by the movement of dissolved and particulate organic matter from the shallow coastal areas downslope with a subsequent deposition in the calmer conditions of the deeper basins. Likely, organic matter is transported by currents, waves or sea ice. Quartino et al. (2013) assume that macroalgae assemblages will expand into the inner part of the cove and thereby enhance the deposition of organic carbon in the bottom sediments. Sediments in the northern cove already show first indications of sub-oxic conditions (Monien et al., 2014; Pasotti, pers. comm.), which might result from an enhanced organic carbon deposition. Wastewater as a possible source for organic carbon is confirmed by the consistently higher amounts in direct vicinity to the scientific station. The low contents west of Mirounga Point reflect an environment not suitable for the deposition of organic carbon, probably due to higher energy conditions or due to the absence of an organic carbon source in those areas. The latter argument seems to be also an explanation for the low contents at the head of the cove that indicate that the amount of organic carbon derived from the glacier and associated creeks can be neglected even though, dilution of the organic carbon signal due to high glacial discharge must be taken into consideration. A study from Monien et al. (2014) also investigated organic carbon contents in seafloor sediments in Potter Cove, covering a smaller extent. The trend in the spatial carbon distribution resembles the one from this study, besides the contents are slightly higher. This deviation is attributed to the use of different sampling strategies and measuring devices as well as to different sample processing. Furthermore, the surface samples from Monien et al. (2014) were taken at 1-cm-resolution in late summer, whereas the samples from this study covered the upper 2 cm of the seafloor surface and were obtained in early summer. Especially the different sampling periods might contribute to deviating values, since macroalgae production varies throughout the year and anthropogenic wastewater discharge increases during the summer months, when the station's capacity is reached. Another investigation from the western margin of the Antarctic Peninsula and the South Shetland Islands reports similar findings as the one from this study (Domack and Ishman, 1993). They also find rather low amounts of organic carbon (0.2 – 1.6 wt.%) dominated by macroalgal detritus and a gradual increase of organic carbon downfjord in a linear fjord system (definition introduced by Syvitski et al., 1990) similar to Potter Cove. In contrast, in the more complex system of Admiralty Bay, King George Island, organic carbon is dispersed and swept out into Bransfield Strait (Domack and Ishman, 1993). It is assumed that the low organic carbon contents at

the entrance to Maxwell Bay can also be ascribed to higher energy conditions that cause export of organic carbon into Maxwell Bay and Bransfield Strait.

Clustering procedure, marine deposition zone characterisation and implications for the modern seafloor environment

The application of a fuzzy cluster algorithm has identified marine deposition zones in Potter Cove based on a set of sedimentological variables and one geomorphic variable. The fuzzy approach also quantified classification uncertainty and therefore provides indirectly a quality estimation of the clustering result. Generally, the confusion map shows higher indices between the zones, which is a common characteristic found at cluster boundaries and can be interpreted as an indication of a transition zone, rather than of classification uncertainty. The distributions of the sediment variables display moderate ranges as well as differing medians, indicating a quite equalized cluster formation by these variables. The bathymetric variable shows large variations in data distribution, which is ascribed to the nature of this variable. Its inclusion is still justified, since the classification procedure benefits from the integration of geomorphic information that designates the zones with regard to water depth.

MZ_1 – the central depressions

MZ_1 is related to the central depressions that are found in the centre of Potter Cove. This zone is characterised by coarse silt that reflects sediment input from the Fourcade Glacier and associated meltwater streams into this environment as well as conditions suitable for deposition. Furthermore, the seafloor in MZ_1 is subject to downslope movement and deposition of organic matter from macroalgae and from wastewater. The confusion index is generally low and only higher between the zones.

MZ_2 – the transitional environment

MZ_2 is referred to as the transitional environment, since it is mainly found between MZ_1 and MZ_3. The seafloor sediments (very coarse silt on average) are slightly coarser than in MZ_1, but smaller than in MZ_3. MZ_2 is furthermore characterised by intermediate organic carbon contents, even though a high availability of organic matter is assumed at least in the northern cove, since the macroalgae accumulations are located near MZ_2. The lower deposition of organic carbon compared to MZ_1 might result from higher energy conditions, such as current activity or from the sloping seafloor in this zone that impedes deposition. This might partly be true for the

locations, where MZ_2 is located close to the erosion prone areas. The confusion index in MZ_2 is low in the centre of the zone and increases towards the transition zones. Additionally, high confusion is found at the entrance towards Maxwell Bay, far from other zones. This can most likely be ascribed to a significant change in bathymetry in this area.

MZ_3 – the shallow water environment

A large part of the shallow coastal environment in the south of Potter Cove is represented by MZ_3, except in direct vicinity to the scientific station. This zone occurs on fine sand with low but slightly varying amounts of mud. Coarse material occurs sporadically that probably reached the area with icebergs or seasonal ice. Occasional higher amounts of mud are most likely deposited in bathymetric deepenings, indicating the availability of fine material in this environment. Generally, energy conditions seem to be unsuitable for deposition across the whole zone. The deposition of organic matter is also low, whereas the macroalgae accumulations are partly nearby. The low amount of fine sediments and organic carbon as well as the proximity to the erosion prone areas at some locations allow the conclusion that this zone is characterised by high energetic conditions that hinder the deposition of fine material in this environment in spite of the fact that the sources are proximal and therefore the material is available.

MZ_4 – the glacier proximal setting

MZ_4 replaces MZ_1 in direct vicinity to the glacier terminus in the innermost part of Potter Cove. This zone is characterised by coarse silt similar to MZ_1, but with slightly higher mud contents. Its location close to the glacier front confirms that fine material is derived from glacial meltwater. Low organic carbon deposition occurs just as in MZ_3. MZ_4 is spatially far off from the main organic carbon contributors, namely the macroalgae accumulations and the wastewater outlets from the scientific station. Even though dilution of the organic carbon signal due to a high meltwater discharge with higher proportion of lithogenic particles must be taken into consideration, organic matter does not seem to be transported into this environment. The clockwise water circulation partly supports this assumption (Fig. 1.1). The water masses in front of the scientific station are flowing out of the cove, whereas organic matter from the macroalgae forests in the north could potentially be transported into this zone with the inflowing waters from Maxwell Bay. The reason that organic matter does not reach the head of the cove is probably the large north-south trending ridge that is located in approximately 30 m water depth between MZ_1 and MZ_4 that most likely

inhibits water exchange. The theory of Downes et al. (1986), where glacial ice is a source of organic carbon seems not to be valid in Potter Cove, most likely due to clean ice and the absence of sedimentary rocks below. MZ_4 can be characterised as a low-energy and sheltered environment in various water depths, if not even a partly isolated basin.

4.4. Conclusions

This study presents the spatial and the temporal distribution of seafloor variables in Potter Cove. Furthermore, the variables were used to identify marine deposition zones using a fuzzy cluster approach.

Sediments in the study area range from fine silts to coarse sands with silt as the dominating grain size. The material mainly originates from the Fourcade Glacier and adjacent meltwater streams. Furthermore, a coarsening trend downfjord is recognised. Coarser material is interpreted to mainly result from submarine meltwater delivery in the past at the grounded glacier front. Two sediment cores additionally reveal high variations in their lower part, reflecting turbid subglacial meltwater discharge events that alter with calmer conditions close to the grounded glacier front. The change towards the upper part of the cores expressed by a significant decrease of the sand fraction is ascribed to the retreat of the glacier towards the land-sea interface. The retreat onto land most likely caused a reduction of turbid submarine meltwater discharge. This can be explained by a decreasing extent of the tidewater front from where sediment-laden meltwater is discharged. Nowadays, terrestrial meltwater outlets represent the main sediment source. The meltwater streams transport also coarse material through exceptional discharge events into the cove, but deposition is assumed to occur rather locally. Organic carbon deposited in the central Potter Cove is derived from the extensive macroalgae forests from the stone habitat in the shallow nearshore erosion-prone areas. Furthermore, anthropogenic wastewater input has also been confirmed as another possible source of organic carbon.

MZ_1, *the central depressions* cover the central, deeper part of the soft-sediment habitat. The sediments are supplied from the Fourcade Glacier and adjacent meltwater streams. Organic matter is derived from macroalgae accumulations and wastewater outlets through downslope movement and deposited in this rather calm seafloor environment.

MZ_2, the *transitional environment* is mainly located between MZ_1 and the shallow-water environment of MZ_3. Sediments are slightly coarser than in MZ_1, whereas deposition of organic matter is lower. These changes are attributed to higher energy conditions upon approaching the coast that winnow the fine material found in MZ_1 or even impede deposition in the first place.

MZ_3, *the shallow water environment* is characterised by a high energy seafloor environment proximal to the coast. The seafloor is covered by coarse sediments with low mud and organic carbon contents. Wave and current activity as well as turbulences at meltwater outlets hinder deposition of fine material or act as erosion agents.

MZ_4, *the glacier proximal setting* is located in the innermost part of the cove and might even be described as a partly isolated basin, where conditions are favourable for deposition. The seafloor is rather heterogeneous in intermediate water depths. High amounts of sediment-laden glacial meltwater is derived from the Fourcade Glacier and meltwater streams and partly deposited in this environment. Almost no organic carbon is deposited, what disproves the assumption that glacial ice is a source of organic matter in Potter Cove.

5. SUMMARY AND OVERALL CONCLUSIONS

THE POTTER COVE - A MARINE SYSTEM EXPERIENCING CLIMATE-INDUCED GLACIAL RETREAT

Coastal environments along the Antarctic Peninsula have been and are still increasingly pressurized by climate change. Well-studied areas in front of rapidly retreating tidewater glaciers like Potter Cove are representative for similar settings and therefore shed light on environmental change not only on a local, but also on a regional scale. In the frame of the IMCOAST Project, seafloor characteristics of Potter Cove have been revealed in great detail evidenced by hydroacoustic data, sediment samples and video recordings, allowing the reconstruction of past, the investigation of present and assumptions about future environments in Potter Cove.

The modern Potter Cove

Erosion-prone areas designated by critical bed shear stress appear to control the distribution of soft-sediment and stone habitats in modern Potter Cove. Moreover, bed shear stress can be a reliable predictor variable of habitat distribution on a local up to a regional scale. Erosion prone areas in Potter Cove occur all along the northern coast except for the innermost part, whereas they are restricted to the shallow waters in the south-east of the cove. This results most likely from Mirounga Point that shelters the southern coast on its lee side.
Most of the soft-sediment habitat lies outside the erosion prone areas. An overlap is only found southwest of Mirounga Point and along the eastern limit of the stone habitat in the northern cove. Different marine organisms colonize the benthic zone in this habitat. The seafloor is pervaded by moraine ridges of different shapes and sizes. Fine sediments drape till deposits, originating from meltwater plumes that were brought by glacial runoff and glacifluvial streams into the system. The thinning of the sediment drape towards the head of the cove is attributed to a decreasing time span since the seafloor has been uncovered by the retreating glacier. In addition to that, a coarsening trend downfjord is recognised, which is explained by the recent retreat of the Fourcade Glacier onto the land-sea interface. This retreat resulted in a reduced

ice-ocean interaction and therefore the closure of transport ways for subglacial meltwater discharge at the grounding line that transported coarse material into the cove. As a consequence, meltwater plumes became the main sediment source and blanketed the former trend. It must also be considered that meltwater plumes have additionally increased in size and frequency. The soft-sediment habitat can be further divided into four marine deposition zones. MZ_1, *the central depressions* are found in the centre of Potter Cove and can be described as a calm seafloor environment with conditions favourable for deposition. Bottom currents or wave activity that might lead to sediment erosion do not occur in this area. The seafloor is characterised by fine sediments (coarse silt on average) that are derived from sediment-laden meltwater plumes. Relatively high amounts of organic matter from macroalgae accumulations and wastewater outlets reach this zone via downslope transport. MZ_2, the *transitional environment* represents the transition between MZ_1 and MZ_3. Coarser sediments and lower organic carbon contents compared to MZ_1 characterise this zone, which is attributed to a gradual energy increase towards the rim of the cove. MZ_3, *the shallow water environment*, located in direct vicinity to the erosion prone areas, is covered by fine sand with rather low organic carbon contents. Relatively higher energy conditions are characteristic for this zone, where deposition of fine material is impeded. This zone partly overlaps with the erosion prone areas except near the meltwater outlets that have not been included as a parameter in the bed shear stress calculations. It is, however, assumed that turbulent meltwater discharge also enhances bed shear stress on a small scale. It is noteworthy to mention that two independent scientific approaches, including the designation of erosion prone areas as well as the marine zonation lead to a similar outcome, in particular the detection of a high-energy and therefore non-depositional environment in the soft-sediment habitat. Furthermore, conditions are suitable for the establishment of the stone habitat in this zone. MZ_4, *the glacier proximal setting* is located near the Fourcade Glacier front in intermediate water depth and characterised by coarse silt. The fine lithogenic particles are derived from meltwater plumes and subsequently deposited in this sheltered environment. Organic matter is barely found in sediments from this zone, which excludes glacial ice as a source of organic carbon. Small amounts of coarse material most likely originate from exceptional meltwater discharges from the creeks located on Potter Peninsula. In sum, this zone is carefully described as a sheltered environment or even a partly isolated basin due to the moraine complex that currently separates this environment from the rest of the cove.

The stone habitat is found along the northern and southeastern coast of Potter Cove. It mainly overlaps with the erosion prone areas, but extends further into deeper waters and did not advance into the easternmost erosion prone areas so far. The seafloor consists of stones and boulders that are derived from adjacent cliffs on land or represent remnants of moraines deposited by the Fourcade Glacier. Further, bedrock outcrops and patches with fine sediments occur in between. The critical bed shear stresses in the erosion prone areas hinder sedimentation and enable thereby

the establishment of macroalgae in clear waters. Stone habitats that are located beside the erosion prone areas lead to the conclusion that conditions for the establishment of this habitat are also suitable in deeper waters where bed shear stress gradually decreases.

The outer Potter Cove is characterised by a steep slope that connects the inner cove with Maxwell Bay. The seafloor surface is intersected by iceberg plough marks on the upper slope, indicating ice disturbance in this area. This process is probably enhanced by trapped icebergs that are unable to enter the inner cove due to the outermost moraine ridge. Another type of depressions, interpreted as pockmarks, occur at the bottom of the slope in approximately 100 to 200 m water depth. Their formation can either be attributed to seepage of thermogenic gases or to pore water migration. The latter might be associated with an enhanced sediment load on the slope, either through gravity flows or through sediment input via the observed channel structures that run perpendicular to the outer cove axis. They most likely result from sediment-laden meltwater erosion in combination with turbidity currents underneath ice or close to a former ice margin. One distinct structure represents the submarine extension of the observed braided drainage system on Potter Peninsula. The timing of their formation is not known.

The palaeoenvironmental history of Potter Cove

This study provides insights into the complex and so far incomplete deglaciation history of Potter Cove. The submarine landforms and sub-bottom characteristics enable the reconstruction of glacial dynamics during the Late Holocene. The seafloor in Potter Cove reveals a terminal moraine complex between the inner and the outer cove. It marks the maximum extent of the Fourcade Glacier grounding line during the neoglacial advance between 2.6 and 1.7 cal kyr BP. By that time, the seafloor in the outer cove was already subject to gravity flows that were triggered at the grounding line. The formation of pockmarks might have also initiated during this time. As the Fourcade Glacier retreated, two other large moraine complexes were deposited between the terminal moraine complex and the innermost moraine complex, reflecting major stillstands or readvances. Their formation is attributed to cooling events that occurred after 1.7 cal kyr BP, including the LIA. The innermost moraine might have developed sometime around the 1950s and is assumed to be related to the local topography, rather than to a cooling event. Afterwards, the glacier uncovered the basin at the head of the cove within only 50 years. Small moraines are also present throughout the whole inner cove, reflecting events on a minor scale. Outlets incised into the moraine complexes indicate high-energy subglacial meltwater activity and were formed during or shortly after the deposition of the associated complex. Also sediment-laden meltwater input from terrestrial streams of varying scale and complexity into the cove is revealed. It is assumed that soft-sediment

habitats established in the newly ice free areas following the retreating glacier. It remains speculative, when exactly critical bed shear stresses enabled the formation of the stone habitat in the shallow areas of the cove. It is only known so far that macroalgae accumulations have already been observed in 1996 inside the inner Potter Cove.

Future scenarios for Potter Cove, delineated in conjunction with assessment reports of the IPCC

The 5th Assessment Report (AR5) of the Intergovernmental Panel on Climate Change (IPCC) assesses scientific and socio-economic aspects of climate change as well as mitigation strategies (IPCC, 2013). AR5 reports a warming of the ocean and the atmosphere, a reduction of ice and snow as well as global mean sea level rise. Combined land and ocean surface temperatures show a warming of 0.85°C between 1880 and 2012. Additionally, the period from 1983 to 2012 has been the warmest 30-year period in the northern hemisphere since the last 800 years. Ice mass loss from the Antarctic Ice Sheet was greatest in the northern Antarctic Peninsula region and in the Amundsen Sea. Future climate scenarios with one exception predict that the increase in global surface temperatures will exceed at least 1.5°C by the end of the 21st century relative to pre-industrial times (1850-1900 AD). The "worst case" scenario even reports an increase of 4.8°C. As a consequence, sea ice and snow cover will mainly decrease in the northern hemisphere, while glacier volume will decrease worldwide. Strongest ocean surface warming is predicted for the northern hemisphere, whereas the Southern Ocean will experience strongest warming at greater depth. An assessment of Antarctic climate change over the 21st century was given by Bracegirdle et al. (2008) based on data from the 4th Assessment Report (AR4) of the IPCC (IPCC, 2007). The results show a projected warming of 0.34°C per decade, an increase in precipitation intensities especially in coastal regions and a decrease in sea-ice extent. They also report an increase in south-westerly winds around Antarctica. This trend has already been observed by Thompson and Solomon (2002).

In polar and subpolar coastal settings such as Potter Cove, all of these changes will have serious impacts on the marine environment. Based on the assessment of the climate change impact worldwide and in Antarctica, the following generalized predictions for the future of Potter Cove can be made: On the basis of the predicted temperature trend, ice mass loss is assumed to continue. As a consequence terrestrial discharge will increase, additionally amplified through enhanced precipitation rates. Stronger wind intensities might lead to unpredictable changes in the water circulation system and to redistribution of coastal sediments. Furthermore, single marine species as well as the functionality of marine ecosystems will be significantly affected.

A closer look on the predictions suggests a shift from a glacier-proximal to a glacier-distal environment in Potter Cove, where glacimarine processes will influence the area to a lesser extent than in the past. Today, parts of the Fourcade Glacier front are located at the land-sea interface. Continued glacial mass loss will sooner or later lead to a complete retreat on land and expose new seafloor at the head of the cove. The deposition of further moraine ridges during the retreat is unlikely, due to predicted fast retreat rates that have already been observed in the very recent past. Submarine meltwater outlets located at the glacier front that act as transport ways for sediments will disappear and turbulent discharge events will be replaced by calm seafloor conditions. Instead, new terrestrial meltwater pathways will establish and continuously transport fine material into the cove. Coarse material will only reach the cove through sea ice and icebergs and exceptional discharge events, as it happens nowadays in the southern inner cove. But since the topography beneath the Fourcade Glacier is not known in detail, it cannot be assessed at the recent status of investigation where new meltwater pathways will form. Enhanced calving of ice shelves and glaciers will increase the number of drifting icebergs that will retain iceberg ploughing as a substantial process on the upper slope of the outer Potter Cove. This in turn will most likely trigger further gravity flows and thereby favour the formation of pockmarks that result from the load of water-saturated sediments. Large quantities of sediment-laden meltwater from the adjacent peninsulas might also reach the outer cove through the submarine channels, contributing together with the gravity flows to a sediment overload.

The future development of the habitats in Potter Cove remains speculative, but an eastward advance of the stone habitat into all erosion prone areas is conceivable. It can be assumed that continued erosion will uncover the stone and boulder deposits that lie underneath the fine sediment drape, thus enabling the settlement of macroalgae. Nevertheless, if meltwater pathways will establish in direct proximity, macroalgae growth can be inhibited due to increased turbidity in the water column caused by high-energy meltwater discharge. Furthermore, a poleward strengthening of south-westerly winds can lead to energy changes applied to the cove environment. This could extend the erosion prone areas into deeper waters, which would favour the establishment of the stone habitat in these areas. Further consequences of stronger winds could also include a change in the circulation system in the cove that might lead a relocation of the erosion prone areas with an effect on the habitat and the sediment distribution in the cove. Generally, an expansion of the stone habitat is very likely and would lead to a greater macroalgae coverage with long-term effects on the benthic communities in the cove, for instance under the aspect of organic carbon supply. But also enhanced anthropogenic activity will increase wastewater input, if no countermeasures will be initiated.

The marine zonation of the soft-sediment habitat is also prone to shifts in size and spatial distribution. MZ_1, referred to as *the central depressions* might reduce in size, due to an advance of the stone habitat and the associated replacement of the contiguous marine deposition zones. MZ_1 would mainly be affected by higher sedimentation rates and an enhanced organic carbon supply that can lead to anoxic conditions in seafloor sediments with various consequences for the marine ecosystem. However, an advance of MZ_1 into *the glacier proximal setting* MZ_4 is also considered as possible. This depends on whether water masses from the northern cove will penetrate into the sheltered environment of MZ_4 or if the moraine complex will still shield this location, despite predicted higher energy conditions. If water overcomes the morainal barrier, macroalgal carbon from the northern cove could be transported into MZ_4. Since low organic matter mainly contributed to the separation of MZ_4 from MZ_1, enhanced contents would favour the establishment of MZ_1 at the head of the cove. An advance of the stone habitat into the shallow areas instead is questionable, but not excluded. Preconditions would be high energy conditions exposing stone and boulder deposits combined with only local sediment-laden meltwater discharge that do not impede permanent macroalgae growth on a larger scale. Here it will be determining, where new meltwater outlets will establish. However, non-assessable consequences arise from the interaction of glacioisostatic uplift, tectonic uplift and eustatic sea level rise, making it impossible to say whether the head of the cove will be connected to the rest of the cove or if it will remain in its isolated position. MZ_2, the *transitional environment* will most likely shift according to distribution changes of MZ_1 and MZ_3. MZ_3, *the shallow water environment* will sooner or later be replaced by the stone habitat, considering its location in the erosion prone areas. It is assumed that this zone will follow the newly erosion prone areas that are not taken by the stone habitat, yet. Also this zone will remain near meltwater outlets and establish where new meltwater pathways will form.

6. OUTLOOK

To sum up, this PhD thesis provides valuable insights into the marine coastal system of Potter Cove that is affected by the impact of climate change. Suitable evaluation methods have been chosen to decipher the development of the cove over the last approximately 2000 cal yr BP and to investigate the present situation. The results further enabled preliminary considerations about possible future developments. However, further investigations are needed to obtain for instance a gapless deglaciation history. Considered suggestions for future research in this area are specified below.

- A more detailed picture of past and present sedimentation processes could be pursued by sediment trap measurements or age dating of the short sediment cores described in chapter 4. Knowledge of past sedimentation rates could for instance shed light on the timing of seafloor exposure after the glacier retreated.

- The origin of organic carbon in marine sediments has been identified in this thesis. Still, the weightings of the individual sources could not be assessed in detail. A geochemical approach could help to draw precise conclusions about this question. One particular aspect could be the amount of organic carbon derived from wastewater that would furthermore assess the not insignificant human impact on this sensitive coastal environment.

- A continuous monitoring approach on a yearly basis (e.g. monitoring of the habitat distribution by hydroacoustic means) would assess the impact of climate change in great detail and allow future predictions on a sound basis.

- The statistical classification approach could be applied as a standard method in fjords and coves on King George Island and along the Antarctic Peninsula, enabling an objective comparison between Potter Cove and other environments.

- The outcome of the classification proves the cluster analysis to be an appropriate method to objectively group an area into marine zones. The marine zones could be the basis for estimating species distributions, as long as distribution patterns are known. The classification approach from this study could further be complemented through the integration of biotic variables.

7. REFERENCES

Abele, D., Ferreyra, G.A., Schloss, I., 1999. H_2O_2 accumulation from photochemical production and atmospheric wet deposition in Antarctic coastal and off-shore waters of Potter Cove, King George Island, South Shetland Islands. Antarctic Science, 11(2), 131-139.

Aller, J.Y., 1989. Quantifying sediment disturbance by bottom currents and its effect on benthic communities in a deep-sea western boundary zone. Deep-Sea Research I, 36, 901-934.

Bartholomä, A., 2006. Acoustic bottom detection and seabed classification in the German Bight, southern North Sea. Geo-Marine Letters, 26, 177-184.

Bentley, M.J., Fogwill, C.J., Le Brocq, A.M., Hubbard, A.L., Sugden, D.E., Dunai, T.J., Freeman, S.P.H.T., 2010. Deglacial history of the West Antarctic Ice Sheet in the Weddell Sea embayment: constraints on past ice volume change. Geology, 38, 411-414.

Berkman, P.A., Forman, S.L., 1996. Pre-bomb radiocarbon and the reservoir correction for calcareous marine species in the Southern Ocean. Geophysical Research Letters, 23, 363-366.

Bertler, N.A.N., Mayewski, P.A., Carter, L., 2011. Cold conditions in Antarctica during the Little Ice Age - Implications for abrupt climate change mechanisms. Earth and Planetary Science Letters, 308, 41-51.

Bezdek, J.C., Ehrlich, R., Full, W., 1984. FCM: The fuzzy c-means clustering algorithm. Computers and Geosciences, 10, 191-203.

Blindow, N., Suckro, S., Rückamp, M., Braun, M., Schindler, M., Breuer, B., Saurer, H., Simões, J., Lange, M., 2010. Geometry and thermal regime of the King George Island ice cap, Antarctica, from GPR and GPS. Annals of Glaciology, 51(55), 103-109.

Blott, S.J., Pye, K., 2001. Gradistat: a grain size distribution and statistics package for the analysis of unconsolidated sediments. Earth Surface Processes and Landforms, 26(11), 1237-1248.

Booij, N., Ris, R.C., Holthuijsen, L.H., 1999. A third-generation wave model for coastal regions. 1. Model description and validation. Journal of Geophysical Research, 104(C4), 7649-7666.

Bracegirdle, T.J., Connolley, W.M., Turner, J., 2008. Antarctic climate change over the twenty first century. Journal of Geophysical Research, 113, D03103.

Braun, M., Simões, J.C., Vogt, S., Bremer, U.F., Blindow, N., Pfender, M., Saurer, H., Aquino, F.E., Ferro, F.A., 2001. An improved topographic database for King George Island: compilation, application and outlook. Antarctic Science, 13, 41-52.

Brown, C.J., Mitchell, A., Limpenny, D.S., Robertson, M.R., Service, M., Golding, N., 2005. Mapping seabed habitats in the Firth of Lorn off the west coast of Scotland: evaluation and comparison of habitat maps produced using the acoustic ground-discrimination system RoxAnn, and sidescan sonar. ICES Journal of Marine Science, 62(4), 790-802.

Burns, D.R., Queen, C.B., Sisk, H., Mullarkey, W., Chivers, R.C., 1989. Rapid and convenient acoustic seabed discrimination. Proceedings of the Institute of Acoustics, 11, 169-178.

Burrough, P.A., McDonnell, R.A., 1998. Principles of geographical information systems. Oxford University Press, Oxford, USA, 193 pp.

Burrough, P.A., van Gaans, P.F.M., Hootsmans, R.J., 1997. Continuous classification in soil survey: spatial correlation, confusion and boundaries. Geoderma, 77, 115-135.

Carrasco, J.F., 2013. Decadal changes in the near-surface air temperature in the western side of the Antarctic Peninsula. Atmospheric and Climate Sciences, 3, 275-281.

Chen, C., Liu, H., Beardsley, R.C., 2003. An unstructured grid, finite-volume, three-dimensional, primitive equations ocean model: application to coastal ocean and estuaries. Journal of Atmospheric and Oceanic Technology, 20(1), 159-186.

Chivers, R.C., Emerson, N.C., Burns, D., 1990. New acoustic processing for underway surveying. The Hydrographic Journal, 56, 9-17.

Cholwek, G., Bonde, J., Li, X., Richards, C., Yin, K., 2000. Processing RoxAnn sonar data to improve its categorization of lake bed surficial substrates. Marine Geophysical Researches, 21, 409-421.

Christoffersen, P., Piotrowski, J.A., Larsen, N.K., 2005. Basal processes beneath an Arctic glacier and their geomorphic imprint after a surge, Elisebreen, Svalbard. Quaternary Research, 64, 125-137.

Cowan, E.A., Hillenbrand, C.-D., Hassler, L.E., Ake, M.T., 2008. Coarse-grained terrigenous sediment deposition on continental rise drifts: A record of PlioPleistocene glaciation on the Antarctic Peninsula. Palaeogeography, Palaeoclimatology, Palaeoecology, 265, 275-291.

Cook, A.J., Fox, A.J., Vaughan, D.G., Ferrigno, J.G., 2005. Retreating glacier fronts on the Antarctic Peninsula over the past half-century. Science, 308, 541-544.

Das, S.B., Alley, R.B., 2008. Rise in frequency of surface melting at Siple Dome through the Holocene: Evidence for increasing marine influence on the climate of West Antarctica. Journal of Geophysical Research, 113, D02112.

Davies, B.J., Hambrey, M.J., Smellie, J.L., Carrivick, J.L., Glasser, N.F., 2012. Antarctic Peninsula Ice Sheet evolution during the Cenozoic Era. Quaternary Science Reviews, 31, 30-66.

Domack, E.W., Ishman, S.E., 1993. Oceanographic and physiographic controls on modern sedimentation within Antarctic fjords. Geological Society of America Bulletin, 105, 1175-1189.

Dowdeswell, J.A., Fugelli, E.M.G., 2012. The seismic architecture and geometry of grounding-zone wedges formed at the marine margins of past ice sheets. Geological Society of America Bulletin, 124, 1750-1761.

Dowdeswell, J.A., Vásquez, M., 2013. Submarine landforms in the fjords of southern Chile: implications for glacimarine processes and sedimentation in a mild glacier-influenced environment. Quaternary Science Reviews, 64, 1-19.

Downes, M.T., Howard-Williams, C., Vincent, W.F., 1986. Sources of organic nitrogen, phosphorus and carbon in antarctic streams. Hydrobiologia, 134, 215-225.

Ferron F.A., Simões J.C., Aquino F.E., Setzer A.W., 2004. Air temperature series for King George Island, Antarctica. Pesquisa Antártica Brasileira (Brazilian Antarctic Research), 4, 155-169.

Fischer, G., Wiencke, C., 1992. Stable carbon isotope composition, depth distribution and fate of macroalgae from the Antarctic Peninsula Region. Polar Biology, 12(3-4), 341-348.

Folk, R.L., Ward, W.C., 1957. Brazos River bar: a study in the significance of grain-size parameters. Journal of Sedimentary Petrology, 27(1), 3-26.

Forwick, M., Baeten, N.J., Vorren, T.O., 2009. Pockmarks in Spitsbergen fjords. Norwegian Journal of Geology, 89, 65-77.

Foster-Smith, R.L., Sotheran, I.S., 2003. Mapping marine benthic biotopes using acoustic ground-discrimination systems. International Journal of Remote Sensing, 24(13), 2761-2784.

Gohl, K., 2007. The expedition ANTARKTIS-XXIII/4 of the research vessel Polarstern in 2006. Reports on Polar and Marine Research, Bremerhaven, Germany, Alfred Wegener Institute for Polar and Marine Research, 557, 166 pp.

Greenstreet, S.P.R., Tuck, I.D., Grewar, G.N., Armstrong, E., Reid, D.G., Wright, P.J., 1997. An assessment of the acoustic survey technique, RoxAnn, as a means of mapping seabed habitat. ICES Journal of Marine Science, 54, 939-959.

Greenstreet, S.P.R., Holland, G.J., Guirey, E.J., Armstrong, E., Fraser, H.M., Gibb, I.M. 2010. Combining hydroacoustic seabed survey and grab sampling techniques to assess “local” sandeel population abundance. ICES Journal of Marine Science, 67(5), 971-984.

Griffith, T.W., Anderson, J.B., 1989. Climatic controls of sedimentation in bays and fjords of the northern Antarctic Peninsula. Marine Geology, 85(2-4), 181-204.

Hair, J.F., Anderson, R.E., Tatham, R.L., Black, W.C., 2009. Multivariate data analysis. Prentice Hall, New Jersey, USA, 816 pp.

Hamilton, L.J., Mulhearn, P.J., Poeckert, R., 1999. Comparison of RoxAnn and QTC-View acoustic bottom classification system performance for the Cairns area, Great Barrier Reef, Australia. Continental Shelf Research, 19(12), 1577-1597.

Hardie, R.J., 2008. Sonavision, Operation and Installation Manual. Sonavision Limited, Aberdeen, Scotland, 30 pp.

Hass, H.C., Kuhn, G., Monien, P., Brumsack, H.-J., Forwick, M., 2010. Climate fluctuations during the past two millennia as recorded in sediments from Maxwell Bay, South Shetland Islands, West Antarctica. In: Howe, J.A., Austin, W.E.N., Forwick, M., Paetzel, M., (eds.). Fjord Systems and Archives. Geological Society, London, UK, Special Publications, 344, pp. 243-260.

Hemer, M.A., 2006. The magnitude and frequency of combined flow bed shear stress as a measure of exposure on the Australian continental shelf. Continental Shelf Research, 26(11), 1258-1280.

Heroy, D.C., Anderson, J.B., 2005. Ice-sheet extent of the Antarctic Peninsula region during the Last Glacial Maximum (LGM) - Insights from glacial geomorphology. Geological Society of America Bulletin, 117, 1497-1512.

Heroy, D.C., Sjunneskog, C., Anderson, J.B., 2008. Holocene climate change in the Bransfield Basin, Antarctic Peninsula: evidence from sediment and diatom analysis. Antarctic Science, 20, 69-87 M3-M10.

Hobbs, C.A., 1985. Side-scan sonar as a tool for mapping spatial variations in sediment type. Geo-Marine Letters, 5, 241-245.

Humborstad, O.-B., Nøttestad, L., Løkkeborg, S., Rapp, H.T., 2004. RoxAnn bottom classification system, side-scan sonar and video-sledge: spatial resolution and their use in assessing trawling impacts. ICES Journal of Marine Science, 61, 53-63.

Ierodiaconou, D., Monk, J., Rattray, A., Laurenson, L., Versace, V.L., 2011. Comparison of automated classification techniques for predicting biological communities using hydroacoustics and video observations. Continental Shelf Research, 31, 28-38.

Ingólfsson, Ó., Hjort, C., Berkman, P., Björck, S., Colhoun, E., Goodwin, I.D., Hall, B., Hirakawa, K., Melles, M., Möller, P., Prentice, M., 1998. Antarctic glacial history since the Last Glacial Maximum: An overview of the record on land. Antarctic Science, 10, 326-344.

Iken, K., Quartino, M.L., Barrera-Oro, E., Palermo, J., Wiencke, C., Brey, T., 1998. Trophic relations between macroalgae and herbivores in Potter Cove (King George Island, Antarctica). In: Wiencke, C., Ferreyra, G.A., Arntz, W., Rinaldi, C., (eds.). The Potter Cove coastal ecosystem, Antarctica. Reports on Polar and Marine Research, Bremerhaven, Germany, Alfred Wegener Institute for Polar and Marine Research, 299, pp. 258-262.

IPCC, 2007: Climate Change 2007: The Physical Science Basis. Contribution of Working Group I to the Fourth Assessment Report of the Intergovernmental Panel on Climate Change. Solomon, S., Qin, D., Manning, M., Chen, Z., Marquis, M., Averyt, K.B., Tignor, M., Miller, H.L. (eds.). Cambridge University Press, Cambridge, United Kingdom and New York, NY, USA, 996 pp.

IPCC, 2013: Climate Change 2013: The Physical Science Basis. Contribution of Working Group I to the Fifth Assessment Report of the Intergovernmental Panel on Climate Change. Stoker, T.F., Qin, D., Plattner, G.-K., Tignor, M., Allen, S.K., Boschung, J., Nauels, A., Xia, Y., Bex, V., Midgley, P.M. (eds.). Cambridge University Press, Cambridge, United Kingdom and New York, NY, USA, 1535 pp.

Jakobsson, M., Anderson, J.B., Nitsche, F.O., Dowdeswell, J.A., Gyllencreutz, R., Kirchner, N., Mohammad, R., O'Reagan, M., Alley, R.B., Anandakrishnan, S., Eriksson, B., Kirshner, A., Fernandez, R., Stolldorf, T., Minzoni, R., Majewski, W., 2011. Geological record of ice shelf break-up and grounding line retreat, Pine Island Bay, West Antarctica. Geology, 39, 691-694.

Jerosch, K., Schlüter, M., Foucher, J.-P., Allais, A.-G., Klages, M., Edy, C., 2007. Spatial distribution of mud flows, chemoautotrophic communities and biogeochemical habitats at Håkon Mosby Mud Volcano. Marine Geology, 243, 1-17.

John, B.S., Sudgen, D.E., 1971. Raised marine features and phases of glaciation in the South Shetland Islands. British Antarctic Survey Bulletin, 24, 45-111.

Kenny, A.J., Cato, I., Desprez, M., Fader, G., Schüttenhelm, R.T.E., Side, J., 2003. An overview of seabed-mapping technologies in the context of marine habitat classification. ICES Journal of Marine Science, 60(2), 411-418.

Khim, B.K., Yoon, H.I., 2003. Postglacial marine environmental changes in Maxwell Bay, King George Island, West Antarctica. Polar Research, 22(2), 341-353.

Khim, B.K., Shim, J., Yoon, H.I., Kang, Y.C., Jang, Y.H., 2007. Lithogenic and biogenic particle deposition in an Antarctic coastal environment (Marian Cove, King George Island): Seasonal patterns from a sediment trap study. Estuarine, Coastal and Shelf Science, 73(1-2), 111-122.

Klöser, H., Ferreyra, G., Schloss, I., Mercuri, G., Laturnus, F., Curtosi, A., 1994. Hydrography of Potter Cove, a small fjord-like inlet on King George Island (South Shetlands). Estuarine, Coastal and Shelf Science, 38(5), 523-537.

Klöser, H., Quartino, M.L., Wiencke, C., 1996. Distribution of macroalgae and macroalgal communities in gradients of physical conditions in Potter Cove, King George Island, Antarctica. Hydrobiologia, 333(1), 1-17.

Kloser, R.J., Bax, N.J., Ryan, T., Williams, A., Baker, B.A., 2001. Remote sensing of seabed types in the Australian South East Fishery - development and application of normal incident acoustic techniques and associated “ground truthing”. Journal of Marine and Freshwater Research, 552, 475-489.

Kostylev, V.E., Todd, B.J., Fader, G.B.J., Courtney, R.C., Cameron, G.D.M., Pickrill, R.A., 2001. Benthic habitat mapping on the Scotian Shelf based on multibeam bathymetry, surficial geology and seafloor photographs. Marine Ecology-Progress Series, 219, 121-137.

Kraus, S., 2005. Magmatic dyke systems of the South Shetland Islands volcanic arc (West Antarctica): reflections of the geodynamic history. PhD thesis, Ludwig-Maximilians-Universität, München, Germany, 130 pp.

Kraus, S., del Valle, R., 2008. Geological map of Potter Peninsula (King George Island, South Shetland Islands, Antarctic Peninsula). Instituto Antártico Chileno, Punta Arenas and Instituto Antártico Argentino, Buenos Aires, Argentina, doi:10.1594/PANGAEA.667386.

Kruss, A., Tęgowski, J., Wiktor, J., Tatarek, A., 2006. Acoustic estimation of macrophytes in the Hornsund fjord (the Svalbard Archipelago). Hydroacoustics, 9, 89-96.

Kruss, A., Blondel, P., Tęgowski, J., Wiktor, J., Tatarek, A., 2008. Estimation of macrophytes using single-beam and multibeam echosounding for environmental monitoring of arctic fjords (Kongsfjord, West Svalbard Island). Proceedings of the 7th European Conference on Noise Control/EURONOISE, 28 June - 03 July 2008, Paris, France, 1743-1748.

Lee, Y.I., Lim, H.S., Yoon, H.I., 2004. Geochemistry of soils of King George Island, South Shetland Islands, West Antarctica: implications for pedogenesis in cold polar regions. Geochimica et Cosmochimica Acta, 68, 4319-4333.

Lee, J.I., Bak, Y.-S., Yoo, K.-C., Hyoun, S.L., Ho, I.Y., Suk, H.Y., 2010. Climate changes in the South Orkney Plateau during the last 8600 years. The Holocene, 20, 395-404.

Lim, C.H. 2014. Modelling waves and currents in Potter Cove, King George Island, Antarctica. PhD thesis, Carl von Ossietzky University, Oldenburg, Germany, 112 pp.

Lim, C.H., Lettmann, K., Wolff, J.-O., 2013. Numerical study on wave dynamics and wave-induced bed erosion characteristics in Potter Cove, Antarctica. Ocean Dynamics, 63(11-12), 1151-1174.

Lindhorst, S., Schutter, I., 2014. Polar gravel beach-ridge systems: Sedimentary architecture, genesis, and implications for climate reconstructions (South Shetland Islands/Western Antarctic Peninsula). Geomorphology, 221, 187-203.

López-Martínez, J., Serrano, E., Schmid, T., Mink, S., Linés, C., 2012. Periglacial processes and landforms in the South Shetland Islands (northern Antarctic Peninsula region). Geomorphology, 155-156, 62-79.

Lowe, A.L., Anderson, J.B., 2003. Evidence for abundant subglacial meltwater beneath the paleo-ice sheet in Pine Island Bay, Antarctica. Journal of Glaciology, 49, 125-138.

Lucieer, V., 2005. Applying discriminate analysis to characterise shallow rocky reef habitat. Proceedings of the Symposium on Spatial-temporal Modeling, Spatial Reasoning, Analysis, Data Mining and Data Fusion, 27 - 29 August 2005, Beijing, China, 215-219.

Lucieer, V., Lucieer, A., 2009. Fuzzy clustering for seafloor classification. Marine Geology, 264(3-4), 230-241.

MacQueen, J., 1967. Some methods for classification and analysis of multivariate observations. Proceedings of the Fifth Berkeley Symposium on Mathematical Statistics and Probability, 21 June - 18 July 1965 and 27 December 1965 - 7 January 1966, Berkeley, USA, 1, 281-297.

Magorrian, B.H., Service, M., Clarke, W., 1995. An acoustic bottom-classification survey of Strangford Lough, Northern Ireland. Journal of the Marine Biological Association of the United Kingdom, 75, 987-992.

Majewski, W., Wellner, J.S., Szczuciński, W., Anderson, J.B., 2012. Holocene oceanographic and glacial changes recorded in Maxwell Bay, West Antarctica. Marine Geology, 326-328, 67-79.

Martinson, D.G., Stammerjohn, S.E., Iannuzzi, R.A., Smith, R.C., Vernet, M., 2008. Western Antarctic Peninsula physical oceanography and spatio-temporal variability. Deep-Sea Research Part II - Topical Studies in Oceanography, 55(18-19), 1964-1987.

Masiokas, M., Rivera, A., Espizua, L.E., Villalba, R., Delgado, S., Aravena, J.C., 2009. Glacier fluctuations in extratropical South America during the past 1000 years. Palaeogeography, Palaeoclimatology, Palaeoecology, 281, 242-268.

McRea Jr, J.E., Greene, H.G., O'Connell, V.M., Wakefield, W.W., 1999. Mapping marine habitats with high resolution sidescan sonar. Oceanologica Acta, 22, 679-686.

Mercer, J.H., 1978. West Antarctic ice sheet and CO_2 greenhouse effect: a threat of disaster. Nature, 271, 321-325.

Mielck, F., Bartsch, I., Hass, H.C., Wölfl, A.-C., Bürk, D., Betzler, C., 2014. Predicting spatial kelp abundance in shallow coastal waters using the acoustic ground discrimination system RoxAnn. Estuarine, Coastal and Shelf Science, 143, 1-11.

Milliken, K.T., Anderson, J.B., Wellner, J.S., Bohaty, S.M., Manley, P.L., 2009. High-resolution Holocene climate record from Maxwell Bay, South Shetland Islands, Antarctica. Geological Society of America Bulletin, 121(11-12), 1711-1725.

Moline, M.A., Karnovsky, N.J., Brown, Z., Divoky, G.J., Frazer, T.K., Jacoby, C.A., Torres. J.J., Fraser, W., 2008. High latitude changes in ice dynamics and their impact on polar marine ecosystems. Annals of the New York Academy of Science, 1134, 267-319.

Moll, A., Braun, M., 2006. Determination of glacier velocities on King George Island (Antarctica) by DInSAR. Proceedings of the Geoscience and Remote Sensing Symposium/IGARSS, 31 July - 4 August 2006, Denver, USA, 1228-1232.

Monien, P., Schnetger, B., Brumsack, H.-J., Hass, H.C., Kuhn, G., 2011. A geochemical record of late Holocene palaeoenvironmental changes at King George Island (maritime Antarctica). Antarctic Science, 23(3), 255-267.

Monien, P., Lettmann, K., Monien, D., Asendorf, S., Wölfl, A.-C., Lim, C.H., Thal, J., Schnetger, B., Brumsack, H.-G., 2014. Redox conditions and trace metal cycling in coastal sediments from the maritime Antarctic. Geochimica et Cosmochimica Acta, 141, 26-44.

Montes-Hugo, M., Doney, S.C., Ducklow, H., Fraser, W., Martinson, D., Stammerjohn, S.E., Schofield, O., 2009. Recent changes in phytoplankton communities associated with rapid regional climate change along the Western Antarctic Peninsula. Science, 323, 1470-1473.

Mulvaney, R., Abram, N.J., Hindmarsh, R.C.A., Arrowsmith, C., Fleet, L., Triest, J., Sime, L.C., Alemany, O., Foord, S., 2012. Recent Antarctic Peninsula warming relative to Holocene climate and ice-shelf history. Nature, 489, 141-144.

Osmanoğlu, B., Braun, B., Hock, R., Navarro, F.J., 2013. Surface velocity and ice discharge of the ice cap on King George Island, Antarctica. Annals of Glaciology, 54, 111-119.

Ottesen, D., Dowdeswell, J.A., 2006. Assemblages of submarine landforms produced by tidewater glaciers in Svalbard. Journal of Geophysical Research, 111, F01016.

Ottesen, D., Dowdeswell, J.A., 2009. An inter-ice-stream glaciated margin: Submarine landforms and a geomorphic model based on marine-geophysical data from Svalbard. Geological Society of America Bulletin, 121, 1647-1665.

Ottesen, D., Dowdeswell, J.A., Benn, D.I., Kristensen, L., Christiansen, H.H., Christensen, O., Hansen, L., Lebesbye, E., Forwick, M., Vorren, T.O., 2008. Submarine landforms characteristic of glacier surges in two Spitsbergen fjords. Quaternary Science Reviews, 27, 1583-1599.

Paull, C.K., Ussler III, W., Borowski, W.S., 1999. Freshwater ice rafting: an additional mechanism for the formation of some high-latitude submarine pockmarks. Geo-Marine Letters, 19, 164-168.

Penrose, J.D., Siwabessy, P.J.W., Gavrilov, A., Parnum, I., Hamilton, L.J., Bickers, A., Brooke, B., Ryan, D.A., Kennedy, P., 2005. Acoustic techniques for seabed classification. Cooperative Research Centre for Coastal Zone, Estuary and Waterway Management, Indooroopilly, Queensland, Australia, Technical Report 32, 130 pp.

Pritchard, H.D., Ligtenberg, S.R.M., Fricker, H.A., Vaughan, D.G., Broeke, M.R., Van Den, Padman, L., 2012. Antarctic ice-sheet loss driven by basal melting of ice shelves. Nature, 484, 502-505.

Pudsey, C.J., Barker, P.F., Larter, R.D., 1994. Ice sheet retreat from the Antarctic Peninsula shelf. Continental Shelf Research, 14, 1647-1675.

Qi, J., Chen, C., Beardsley, R.C., Perrie, W., Cowles, G.W., Lai, Z., 2009. An unstructured-grid finite-volume surface wave model (FVCOM-SWAVE): Implementation, validations and applications. Ocean Modeling, 28, 153-166.

Quartino, M.L., Boraso de Zaixso, A.L., 2008. Summer macroalgal biomass in Potter Cove, South Shetland Islands, Antarctica: its production and flux to the ecosystem. Polar Biology, 31(3), 281-294.

Quartino, M.L., Zaixso, H.E., Boraso de Zaixso, A.L., 2005. Biological and environmental characterization of marine macroalgal assemblages in Potter Cove, South Shetland Islands, Antarctica. Botanica Marina, 48, 187-197.

Quartino, M.L., Deregibus, D., Campana, G.L., Latorre, G.E.J., Momo, F.R., 2013. Evidence of macroalgal colonization on newly ice-free areas following glacial retreat in Potter Cove (South Shetland Islands), Antarctica. PLoS ONE, 8(3), e58223.

Reimer, P.J., Baillie, M.G.L., Bard, E., Bayliss, A., Beck, J.W., Blackwell, P.G., Ramsey, C.B., Buck, C.E., Burr, G.S., Edwards, R.L., Friedrich, M., Grootes, P.M., Guilderson, T.P., Hajdas, I., Heaton, T.J., Hogg, A.G., Hughen, K.A., Kaiser, K.F., Kromer, B., McCormac, F.G., Manning, S.W., Reimer, R.W., Richards, D.A., Southon, J.R., Talamo, S., Turney, C.S.M., van der Plicht, J., Weyhenmeyer, C.E., 2009. IntCal09 and Marine09 radiocarbon age calibration curves, 0-50,000 years cal BP. Radiocarbon, 51(4), 1111-1150.

Roese, M., Drabble, M., 1998. Wind driven circulation in Potter Cove. In: Wiencke, C., Ferreyra, G.A., Arntz, W., Rinaldi, C., (eds.). The Potter Cove coastal ecosystem, Antarctica. Reports on Polar and Marine Research, Bremerhaven, Germany, Alfred Wegener Institute for Polar and Marine Research, 299, pp. 40-46.

Rogers, J.N., Kelley, J.T., Belknap, D.F., Gontz, A., Barnhardt, W.A., 2006. Shallow-water pockmark formation in temperate estuaries: A consideration of origins in the western gulf of Maine with special focus on Belfast Bay. Marine Geology, 225, 45-62.

Römer, M., Torres, M., Kasten, S., Kuhn, G., Graham, A.G.C., Mau, S., Little, C.T.S., Linse, K., Pape, T., Geprägs, P., Fischer, D., Wintersteller, P., Marcon, Y., Rethemeyer, J., Bohrmann, G., Shipboard scientific party ANT-XXIX/4, 2014. First evidence of widespread active methane seepage in the Southern Ocean, off the sub-Antarctic island of South Georgia. Earth and Planetary Science Letters, 403, 166-177.

Rückamp, M., Blindow, N., Suckro, S., Braun, M., Humbert, A., 2010. Dynamics of the ice cap on King George Island, Antarctica: field measurements and numerical simulations. Annals of Glaciology, 51(55), 80-90.

Rückamp, M., Braun, M., Suckro, S., Blindow, N., 2011. Observed glacial changes on the King George Island ice cap, Antarctica, in the last decade. Global Planet Change, 79, 99-109.

Sahade, R., Tatián, M., Kowalke, J., Kuehne, S., Esnal, G., 1998. Benthic faunal associations on soft substrates at Potter Cove, King George Island, Antarctica. Polar Biology, 19(2), 85-91.

Schlagintweit, G.E.O., 1993. Real-time acoustic bottom classification for hydrography: a field evaluation of RoxAnn. Canadian Hydrographic Service, Department of Fisheries and Oceans, Sidney, Canada, 16 pp.

Schloss, I.R., Ferreyra, G.A., 2002. Primary production, light and vertical mixing in Potter Cove, a shallow bay in the maritime Antarctic. Polar Biology, 25(1), 41-48.

Schloss, I.R., Klöser, H., Ferreyra, G.A., Mercuri, G., Pinola, E., 1997. Factors governing phytoplankton and particulate matter variation in Potter Cove, King George island, Antarctica. In: Battaglia, B., Valencia, J., Walton, D.W.H. (eds.). Antarctic Communities. Cambridge Univ. Press, Cambridge, UK, pp. 135-141.

Schloss, I.R., Ferreyra, G.A., Ruiz-Pino, D., 2002. Phytoplankton biomass in Antarctic Shelf Zones: A conceptual model based on Potter Cove, King George Island. Journal of Marine Systems, 36, 129-143.

Schloss, I.R., Ferreyra, G.A., González, O., Atencio, A., Fuentes, V., Tosonotto, G., Mercuri, G., Sahade, R., Tatián, M., Abele, D., 2008. Long-term hydrographic conditions and climate trends in Potter Cove. In: Wiencke, C., Ferreyra, G.A., Abele, D., Marenssi, S., (eds.). The Antarctic ecosystem of Potter Cove, King-George Island (Isla 25 de Mayo). Reports on Polar and Marine Research, Bremerhaven, Germany, Alfred Wegener Institute for Polar and Marine Research, 571, pp. 382-389.

Schloss, I.R., Abele, D., Moreau, S., Demers, S., Bers, A.V., González, O., Ferreyra, G.A., 2012. Response of phytoplankton dynamics to 19-year (1991-2009) climate trends in Potter Cove (Antarctica). Journal of Marine Systems, 92(1), 53-66.

Schöne, T., Pohl, M., Zakrajsek, A., Schenke, H., 1998. Tide gauge measurements, a contribution for the long term monitoring of sea level. In: Wiencke, C., Ferreyra, G.A., Arntz, W., Rinaldi, C., (eds.). The Potter Cove coastal ecosystem, Antarctica. Reports on Polar and Marine Research, Bremerhaven, Germany, Alfred Wegener Institute for Polar and Marine Research, 299, pp. 12-14.

Seong, Y.B., Owen, L.A., Lim, H.S., Yoon, H.I., Kim, Y., Lee, Y.I., Caffee, M.W., 2009. Rate of late Quaternary ice-cap thinning on King George Island, South Shetland Islands, West Antarctica defined by cosmogenic 36 Cl surface exposure dating. Boreas, 38, 207-213.

Shevenell, A.E., Ingalls, A.E., Domack, E.W., Kelly, C., 2011. Holocene Southern Ocean surface temperature variability west of the Antarctic Peninsula. Nature, 470, 250-254.

Simms, A.R., Milliken, K.T., Anderson, J.B., Wellner, J.S., 2011. The marine record of deglaciation of the South Shetland Islands, Antarctica since the Last Glacial Maximum. Quaternary Science Reviews, 30, 1583-1601.

Simms, A.R., Ivins, E.R., DeWitt, R., Kouremenos, P., Simkins, L.M., 2012. Timing of the most recent Neoglacial advance and retreat in the South Shetland Islands, Antarctic Peninsula: insights from raised beaches and Holocene uplift rates. Quaternary Science Reviews, 47, 41-55.

Simões, J.C., Bremer, U.F., Aquino, F.E., Ferron, F.E., 1999. Morphology and variations of glacial drainage basins in the King George Island ice field, Antarctica. Annals of Glaciology, 29, 220-224.

Somoza, L., Martínez-Frías, J., Smellie, J.L., Rey, J., Maestro, A., 2004. Evidence for hydrothermal venting and sediment volcanism discharged after recent short-lived volcanic eruptions at Deception Island, Bransfield Strait, Antarctica. Marine Geology, 203, 119-140.

Sotheran, I.S., Foster-Smith, R.L., Davies, J., 1997. Mapping of marine benthic habitats using image processing techniques within a raster based Geographic Information System. Estuarine, Coastal and Shelf Science, 44, 25-31.

Soulsby, R., 1998. Dynamics of marine sands. Thomas Telford Publications, London, UK, 249 pp.

Steig, E.J., Schneider, D.P., Rutherford, S.D., Mann, M.E., Comiso, J.C., Shindell, D.T., 2009. Warming of the Antarctic ice-sheet surface since the 1957 International Geophysical Year. Nature, 457, 459-462.

Stein, R., Grobe, H., Wahsner, M., 1994. Organic carbon, carbonate, and clay mineral distributions in eastern central Arctic Ocean surface sediments. Marine Geology, 119, 269-285.

Stewart, F.S., Stoker, M.S., 1990. Problems associated with seismic facies analysis of diamicton-dominated, shelf glacigenic sequences. Geo-Marine Letters, 10, 151-156.

Syvitski, J.P.M., William, K., LeBlanc, G., Cranston, R.E., 1990. The flux and preservation of organic carbon in Baffin Island Fjords. In: Dowdeswell, J.A., Scourse, J.D., (eds.). Glacimarine environments: Processes and sediments. Geological Society of London, Special Paper, 53, pp. 177-199.

Thompson, D.W.J., Solomon, S., 2002. Interpretation of recent southern hemisphere climate change. Science, 296, 895-899.

Vaughan, D.G., Doake, C.S.M., 1996. Recent atmospheric warming and retreat of ice shelves on the Antarctic Peninsula. Nature, 379, 328-331.

Vaughan, D.G., Marshall, G.J., Connolley, W.M., King, J.C., Mulvaney, R., 2001. Devil in the detail. Science, 293, 1777-1779.

Vaughan, D., Marshall, G., Connolley, W., Parkinson, C., Mulvaney, R., Hodgson, D., King, J., Pudsey, C., Turner, J., 2003. Recent rapid regional climate warming on the Antarctic Peninsula. Climatic Change, 60, 243-274.

Varela, L., 1998. Hydrology of Matías and Potter Creeks. In: Wiencke, C., Ferreyra, G.A., Arntz, W., Rinaldi, C., (eds.). The Potter Cove coastal ecosystem, Antarctica. Reports on Polar and Marine Research, Bremerhaven, Germany, Alfred Wegener Institute for Polar and Marine Research, 299, pp. 33-39.

Veit-Köhler, G., 1998. Meiofauna study in the Potter Cove. Sediment situation and resource availability for small crustaceans (Copepoda and Peracarida). In: Wiencke, C., Ferreyra, G.A., Arntz, W., Rinaldi, C., (eds.). The Potter Cove coastal ecosystem, Antarctica. Reports on Polar and Marine Research, Bremerhaven, Germany, Alfred Wegener Institute for Polar and Marine Research, 299, pp. 132-136.

Verfaillie, E., Degraer, S., Schelfaut, K., Willems, W., Van Lancker, V., 2009. A protocol for classifying ecologically relevant marine zones, a statistical approach. Estuarine, Coastal and Shelf Science, 83, 175-185.

Venables, W.N., Ripley, B.D., 2003. Modern Applied Statistics with S. Springer, New York, 498 pp.

Warwick, R.M., Uncles, R.J., 1980. Distribution of benthic macrofaunal associations in the Bristol Channel in relation to tidal stress. Marine Ecology-Progress Series, 3, 97-103.

Xie, L.X., Beni, G., 1991. Validity measure for fuzzy clustering. IEEE Transactions on Pattern Analysis and Machine Intelligence, 3, 841-847.

Yeo, J.P., Lee, J.I., Hur, S.D., Choi, B.G., 2004. Geochemistry of volcanic rocks in Barton and Weaver peninsulas, King George Island, Antarctica: implications for arc maturity and correlation with fossilized volcanic centers. Geosciences Journal, 8, 11-25.

Yoo, K.-C., Yoon, H.I., Kim, J.-K., Khim, B.-K., 2009. Sedimentological, geochemical and palaeontological evidence for a neoglacial cold event during the late Holocene in the continental shelf of the northern South Shetland Islands, West Antarctica. Polar Research, 28, 177-192.

Yoon, H.I., Han, M.W., Park, B.K., Han, S.J., Oh, J.K., 1992. Distribution, provenance, and dispersal pattern of clay minerals in surface sediments, Bransfield Strait, Antarctica. Geo-Marine Letters, 12(4), 223-227.

Yoon, H.I., Han, M.W., Park, B.K., Oh, J.K., Chang, S.K., 1997. Glaciomarine sedimentation and palaeo-glacial setting of Maxwell Bay and its tributary embayment, Marian Cove, South Shetland Islands, West Antarctica. Marine Geology, 140, 265-282.

Yoon H.I., Yoo, K.C., Bak, Y.S., Lim, H.S., Kim, Y., Lee, J.I., 2010. Late Holocene cyclic glaciomarine sedimentation in a subpolar fjord of the South Shetland Islands, Antarctica, and its paleoceanographic significance: Sedimentological, geochemical, and paleontological evidence. Geological Society of America Bulletin, 122, 1298-1307.

Zadeh, L.A., 1965. Fuzzy sets. Information and Control, 8(3), 338-353.

ACKNOWLEDGEMENTS

I would like to thank my supervisor Prof. Dr. Christian Betzler from the University of Hamburg for giving me the opportunity to write this PhD thesis under his supervision.

This thesis was conducted within the frame of the IMCOAST project. I am grateful to Dr. Christian Hass and Dr. Gerhard Kuhn, who were part of this research group. Both of them provided assistance when needed and were open for my ideas. Thank you Christian for letting me stay on King George Island as long as it was necessary and allowing me to make all these incredible experiences. I further thank Dr. Doris Abele and Dr. Valeria Bers for coordinating the project and for great support during the field campaigns.

I would also like to express my deepest gratitude to the people I met on King George Island during the field campaigns in 2010/2011 and 2011/2012. They have been a great help as boaters, logistic experts, mechanics, scientists and friends. I would like to mention some of them: Gastón Rihedel, Alejandro Ulrich, Dolores Deregibus, Dr. Verónica Fuentes, Alejandro Olariaga, Ilona Schutter, Prof. Dr. Caio Vinícius Gabrig Turbay, Jacek Piszczek, Konrad Jackiewicz and Adam Latusek. They all contributed to the success of this memorable adventure.

Many thanks go to Dr. Sebastian Lindhorst for moral support and for thoughtful and constructive advices during field work and thereafter.

Special thanks go to Nina Wittenberg for a wide range of unfailing assistance during the field campaigns and for the productive discussions back at the “home-office”.

I also want to thank Bulat Mavlyudov, the leader of the Russian Bellingshausen Station on King George Island for the fabulous hospitality, while I was waiting for my flight to South America.

I sincerely thank the United Kingdom Hydrographic Office for providing the multibeam data presented in this study (United Kingdom Hydrographic Office data © Crown copyright and database right). Special thanks go to the Commanding Officer, Captain Peter Sparkes RN; the Charge Surveyor, Lieutenant Commander Phil Payne RN; the Logistics Officer, Lieutenant Simon Lockley RN and the Bathymetric Data Manager Judith Thomas.

Furthermore, I would like to acknowledge Dr. Gabriela Tosonotto from the IAA (Instituto Antártico Argentino, Buenos Aires, Argentina) for providing single-beam bathymetric data.

Dr. Antonie Haas from the computer and data centre of the Alfred Wegener Institute is to be thanked for her support concerning GIS applications and for technical assistance.

Sincere thanks go to Thorsten Smit from the purchasing department of the Alfred Wegener Institute and to the Scholz Ingenieur-Büro GmbH, in particular Klaus Scholz and Jan Wommelsdorff. It is thanks to their commitment that I was able to obtain video images in Potter Cove.

I would also like to thank the Helmholtz Graduate School for Polar and Marine Research (POLMAR) for the opportunity to attend their program, in particular Dr. Claudia Hanfland, Dr. Claudia Sprengel and Dörte Rosenbaum.

A big thank you goes out to my colleagues for technical and mental support, review, scientific discussions and motivation: Thea Dammrich, Dr. Kerstin Jerosch, Dr. Finn Mielck, Dr. Patrick Monien, Dr. Donata Monien and Dr. Chai Heng Lim.

I am grateful to Prof. Dr. Symader for valuable advice along the way.

But most of all, I am grateful to my parents, Renate and Rainer Wölfl. This thesis is dedicated to them.

APPENDIX A

FURTHER PROJECT-RELATED PUBLICATIONS

A1

Redox conditions and trace metal cycling in coastal sediments from the maritime Antarctic.

Monien, P. [1], Lettmann, K. [1], Monien, D. [1], Asendorf, S. [1], Wölfl, A.-C. [2], Lim, C.H. [1], Thal, J.[3], Schnetger, B. [1], Brumsack, H.-G. [1]

[1] Institute for Chemistry and Biology of the Marine Environment (ICBM), Carl-von-Ossietzky Straße 9-11, 26129 Oldenburg, Germany

[2] Alfred Wegener Institute for Polar and Marine Research, Wadden Sea Research Station, Hafenstrasse 43, 25992 List, Germany

[3] University of Bremen, Department of Geosciences, Klagenfurter Straße, 28359 Bremen, Germany

Abstract

Redox-sensitive trace metals (Mn, Fe, U, Mo, Re), nutrients and terminal metabolic products (NO_3^-, NH_4^+, PO_4^{3-}, total alkalinity) were for the first time investigated in pore waters of Antarctic coastal sediments. The results of this study reveal a high spatial variability in redox condition in surface sediments from Potter Cove, King George Island, western Antarctic Peninsula. Particularly in the shallower areas of the bay the significant correlation between sulphate depletion and total alkalinity, the inorganic product of terminal metabolism, indicates sulphate reduction to be the major pathway of organic matter mineralisation. In contrast, dissimilatory metal oxide reduction seems to be prevailing in the newly ice-free areas and the deeper troughs, where concentrations of dissolved iron of up to 700 µM were found. We suggest that the increased accumulation of fine-grained material with high amounts of reducible metal oxides in combination with the reduced availability of metabolisable organic matter and enhanced physical and biological disturbance by bottom water currents, ice scouring and burrowing organisms favours metal oxide reduction over sulphate

reduction in these areas. Based on modelled iron fluxes we calculate an Antarctic shelf derived input of potentially bioavailable iron to the Southern Ocean of 0.35–39.5 mg m^{-2} yr^{-1}. This contribution is in the same order of magnitude as the flux provided by icebergs and significantly higher than the input by aeolian dust. For this reason suboxic shelf sediments form a key source of iron for the high nutrient-low chlorophyll (HNLC) areas of the Southern Ocean. In view of rising temperatures at the WAP accompanied by enhanced glacier retreat and the accumulation of melt water derived iron-rich material on the shelf this source may become even more important in the future.

Monien, P., Lettmann, K., Monien, D., Asendorf, S., Wölfl, A.C., Lim, C.H., Thal, J., Schnetger, B., Brumsack, H.-G., 2014. Redox conditions and trace metal cycling in coastal sediments from the maritime Antarctic. Geochimica et Cosmochimica Acta, 141, 26-44.

A2

Antarctic shallow water benthos under glacier retreat forcing

Pasotti, F.[1], Manini, E.[2], Giovannelli, D.[2,5], Wölfl, A.-C.[3], Monien, D.[4], Verleyen, E.[6], Braeckman, U.[1], Abele, D.[3], Vanreusel, A.[1]

[1] Ghent University, Marine Biology research group, Krijgslaan 281/S8, 9000 Ghent, Belgium

[2] Institute for Marine Science (ISMAR-CNR), L.go Fiera della Pesca, 60122 Ancona, Italy

[3] Alfred Wegener Institute Helmholtz Centre for Polar and Marine Research, Wadden Sea Research Station, Hafenstrasse 43, 25992 List, Germany

[4] Institute for Chemistry and Biology of the marine Environment (ICBM), Oldenburg University, Carl-von-Ossietzky Straße 9-11, 26129 Oldenburg, Germany

[5] Institute of Marine and Coastal Science (IMCS), Rutgers University, 71 Dudley Road, New Brunswick, NJ - 08901, USA

[6]Ghent University, Protistology and Aquatic Ecology, Krijgslaan 281 S8, 9000 Gent, Belgium

Abstract

The West Antarctic Peninsula is one of the fastest warming regions on the planet. Faster glacier retreat and related calving events lead to more frequent iceberg scouring, fresh water input and higher sediment loads which affect shallow water benthic marine communities in coastal areas. Ice retreat reveals new benthic substrata for colonization. We investigated the effect of climate-driven impact on three size classes of benthic biota (microbenthos, meiofauna and macrofauna) in Potter Cove (King George Island, West Antarctic Peninsula). We identified three sites

within the cove at similar water depths but experiencing different levels of glacier retreat-related disturbance. Our results document the existence of highly divergent bottom communities within a relatively small area (about 1 km^2), at the same water depth but in different positions relative to the receding glacier. In areas with frequent ice scouring and higher sediment accumulation rates, a patchy community, mainly dominated by macrobenthic scavengers (such as the polychaete *Barrukia cristata*), vagile organisms, and younger individuals of sessile species (such as the bivalve *Yoldia eightsi*) were found. Macrofauna were low in abundance and very patchily distributed in recently ice-free areas close to the glacier, whereas the nematode genus *Microlaimus* represented with high abundances a pioneer colonist of these newly exposed sites. The most diverse and abundant macrofaunal community was established in areas furthest away from recent glacier influence, contrasting with the meiofauna which showed relatively low densities. The three benthic size classes appeared to respond in different ways to the ice retreat-related disturbances, suggesting that the capacity to adapt may have a size component. We predict that, under continued deglaciation, more diverse, but less patchy, benthic assemblages will establish in such areas.

Pasotti, F., Manini, E., Giovannelli, D., Wölfl, A.C., Monien, D., Verleyen, E., Braekman, U., Abele, D., Vanreusel, A., 2014. Antarctic shallow water benthos in an area of recent rapid glacier retreat. Journal of Marine Ecology, doi: 10.1111/maec.12179.

“Wie gleichgültig geht die Natur über unsere Leistungen hinweg”

With what indifference nature ignores our achievements

- Alfred L. Wegener -